February 2019

PhD Dissertation

A Study on Advanced Localization Technique Based on Time of Arrival Trilateration

Graduate School of Chosun University

Department of Advanced Parts and Material Engineering

Sajina Pradhan

A Study on Advanced Localization Based on Time of Arrival Trilateration

February 25, 2019

Graduate School of Chosun University

Department of Advanced Parts and Material Engineering

Sajina Pradhan

A Study on Advanced Localization Based on Time of Arrival Trilateration

Advisor: Prof. Suk-seung Hwang, PhD

A dissertation submitted in partial fulfillment of the requirements for the degree of Doctor of Philosophy

October 2018

Graduate School of Chosun University
Department of Advanced Parts and Material Engineering
Sajina Pradhan

The submitted doctoral dissertation of
Sajina Pradhan is accepted

Committee Chair	Prof., Chosun University	이 충 규	(Signature)
Committee Member	Prof., Chosun University	이 동 기	(Signature)
Committee Member	Prof., Chosun University	유 영 태	(Signature)
Committee Member	Prof., Chosun University	황 석 승	(Signature)
Committee Member	Prof., Kongju National University	박 봉 석	(Signature)

December 2018

Graduate School of Chosun University

Table of Contents

List of Figures

List of Tables

Acronyms

AGPS	Assisted Global Positioning System
AOA	Angle of Arrival
BS	Base Station
E-911	Enhanced-911
FCC	Federal Communications Commission
GHz	Gigahertz
GNSS	Global Navigation Satellite System
GPRS	General Packet Radio Service
GPS	Global Positioning System
IoT	Internet of Things
LBS	Location-Based Services
LDT	Location Detection Technologies
LOS	Line of Sight
m	Meter
MHz	Megahertz
MS	Mobile Station
MSE	Mean Squared Error
NLOS	Non-Line of Sight
RF	Radio Frequency
RMSE	Root-Mean-Square Error

RSS	Received Signal Strength
TDOA	Time Difference of Arrival
TOA	Time of Arrival
UWB	Ultra-Wideband
WLAN	Wireless Local Area Network
2D	Two-Dimensional Space
3D	Three-Dimensional Space
3G	Third Generation

Abstract (English)

A Study on Advanced Localization Technique Based on Time of Arrival Trilateration

Sajina Pradhan

Advisor: Prof. Suk-seung Hwang

Department of Electronic Engineering

Graduate School of Chosun University

Location detection technology (LDT) is one of the core techniques for location-based service (LBS) in the wireless communication for improving resource management and quality of services. The location of a mobile station (MS) is estimated using the time of arrival (TOA) trilateration technique based on three circles with their centers corresponding to the coordinates of the three base stations (BSs) and their radii corresponding to distances between the MS and BSs. For accurately estimating the location of MS, three circles should meet at a point for the trilateration method, but they generally do not meet a point because the radius is increased depending on the number of time delay samples for estimating the distance between the MS and BS and the sampling rate. I classify all possible cases (four cases) where three circles do not meet at a single point. Those cases are classified based on the size of the estimated circles

and the coordinate of BSs. In order to enhance the performance of the TOA trilateration, the advanced localization algorithms suited to each case have been proposed.

In the general case (case 1), there are six intersection points of three intersecting circles based on the increased radii, the shortest distance and the line intersection algorithms are proposed. The mathematical analysis is provided to indicate the relation between the line intersection algorithm and the shortest distance algorithm. In the specific case (case 2) where there are total six intersections based on the three extended circles and a small circle has four intersections with two large circles, the comparison approach of intersection distances has been proposed. For the case 3, where there are four intersection points based on three extended circles and a small circle has two intersection points with one large circle, the small circle intersection approach has been proposed. For the case 4, there are two intersection points of two large circles and a small circle lies completely inside the overlapping area of two large circles, the closest point algorithm has been proposed. For the best performance of the location estimation, the proposed four algorithms should be employed with a hybrid form. For this purpose, I propose a mode selection algorithm to efficiently select the proper case, and a hybrid TOA trilateration algorithm based on four algorithms.

In this study, I consider all possible cases for occurring the location estimation error and verify that the proposed algorithm has a lower error comparing to the conventional TOA algorithm. This advanced hybrid TOA trilateration algorithm is expected to be mainly employed in the various fields requiring excellent location estimation performance.

Index Terms: Location detection technology, Time of arrival (TOA), Trilateration, Location estimation, Intersection of three circles

Abstract (Korean)

도래시간 삼각변 측량법 기반의 고성능 위치추정 기법에 대한 연구

사지나 프라다한

지도 교수: 황석승

전자공학과

조선대학교 대학원

위치 탐지 기술 (LDT)은 무선통신에서 자원 관리 및 서비스 품질을 향상시키기 위한 위치 기반 서비스 (LBS)의 핵심 기술 중 하나이다. 이동국(MS)의 위치는 기지국(BS)의 좌표를 중심으로 하고 이동국과 기지국들 사이의 거리를 반지름으로 갖는 3개의 원을 기반으로 하는 도래시간(TOA) 삼각변측량법으로 추정한다. 삼각변측량법을 사용하는 경우 이동국의 위치를 정확하게 추정하기 위해서는 3개의 원이 한 점에서 만나야 하지만 이동국과 기지국간의 거리를 추정하기 위한 시간 지연 샘플의 수 및 샘플링 주파수에 따라 반경이 증가하기 때문에 일반적으로 한 점에서 만나지 않는다.

본 논문에서는 3개의 원이 한 곳에서 만나지 않는 모든 가능한 경우(4가지 경우)를 분류하였다. 이러한 경우는 추정된 원의 크기와 기지국의 좌표에 따라 분류된다. 또한, TOA 삼각변측량법의 성능을 향상시키기 위한 각 경우에 적합한 향상된 위치추정 알고리즘을 제안하였다.

일반적인 경우 (Case 1)에는 증가된 반지름을 기반으로 하는 교차되는 3개의 원이 6개의

교차점을 가지는데, 이 경우에 특화된 최단거리 알고리즘과 선 교차 알고리즘을 제안한다. 또한, 선 교차 알고리즘과 최단거리 알고리즘 간의 관계를 표현하기 위한 수학적 분석이 제공된다. Case 2는 세 개의 확장된 원이 총 6 개의 교차점을 생성하고, 작은 원이 두 개의 큰 원안에 위치하며 두 개의 큰 원과 네 개의 교차점을 갖는 경우로써, 이에 특화된 교차거리 비교법을 제안한다. Case 3은 세 개의 확장된 원이 네 개의 교차점을 가지고, 작은 원이 한 개의 큰 원과 두 개의 교차점을 갖는 경우로써, 이에 특화된 작은 원 교점법을 제안한다. Case 4의 경우 두 개의 큰 원이 2개의 교차점을 갖고 한 개의 작은 원이 두 개의 큰 원의 중첩영역 내에 위치하는 경우로써, 이에 특화된 최접근점 알고리즘을 제안한다. 최적화된 위치추정 성능을 위해서는, 위에서 제시된 위치추정 기법들이 각 경우에 대해 하이브리드 형식으로 사용되어야 한다. 이를 위해, 각 경우를 효율적으로 선택할 수 있는 모드선택 알고리즘과, 모든 알고리즘을 고려한 하이브리드형 위치추정 기법을 제안한다.

본 논문에서 제안된 알고리즘은 위치추정 오차가 발생할 수 있는 모든 경우를 고려하였고, 성능평가를 통해 일반적인 TOA 삼각변측량법에 비해 작은 위치추정 오차가 발생하는 것을 확인하였다. 개선된 하이브리드형 TOA 삼각변측량법은 우수한 위치추정 성능을 필요로 하는 다양한 분야에서 주도적으로 사용될 수 있을 것으로 기대된다.

1 Introduction

1.1 Research Overview

Mobile location detection technique generates a great interest in the fields of cellular network and wireless local area network with the development of communication systems. As the wireless communication techniques are developed, we can find more and more applications related to location determination technology (LDT). The location detection of a specific user or object, including mobile humanoid robot is becoming an important issue in wireless communication environments because a lot of information related to the location of the mobile station (MS) is utilized in various communication services such as the location-based services (LBS) [1, 2]. The location information is used in a variety of fields from entertainment to emergency, which are more and more demanded. Researchers working in this field are pushing to get accurate mobile location devices with low cost, high performance, and reusability of components [3-6].

Since the mobile location has received significant attention over the past few years, some of the basic location detection methods have been described. There are a number of methods for determining the MS location, which is typically grouped into two main categories: handset-based and network-based [7-10]. The handset-based method needs a special type of handset device or network software and its representative example is a Global Positioning System (GPS) or Assisted GPS (AGPS) [11, 12]. The network-based method determines the mobile position by measuring its signal parameters received from BSs. Although the

network-based method can be easily implemented and cheaply employs existing technologies, its accuracy of the location detection performance is usually lower than that of the handset-based method. The network-based method includes received signal strength (RSS), angle of arrival (AOA), cell identification, time of arrival (TOA), time difference of arrival (TDOA), and fingerprint techniques [13-18]. In this dissertation, I mainly focus on the time of arrival (TOA) trilateration. The TOA trilateration method, which is one of representative location estimation approaches, estimates the MS location using the intersection point of three circles with their centers corresponding BS coordinates and radii corresponding the distances between MS and BSs. However, I generally estimate the distance between the MS and BS counting the number of delay samples, which is an integer. The estimated distance may be slightly increased and three circles based on the radii corresponding to the estimated distance may not intersect at a single point, resulting in location error. In order to solve this problem, I study the advanced localization technique based on TOA trilateration to estimate the location of MS.

1.2 Contributions of Dissertation

This dissertation aims at contributing to the field of localization technique. Among the different localization technique available, I mainly focus on the TOA trilateration method. The TOA trilateration may have a serious estimation error, when three circles do not meet at a single point. Thus, I classify all possible cases (four cases) where three circles do not meet at a single point as shown in Figure 1.1. The four different cases are classified based on the size of

the estimated circles and the coordinate of BSs. The number of the intersection points of three estimated circles in the four cases is given in Table 1.1 [19].

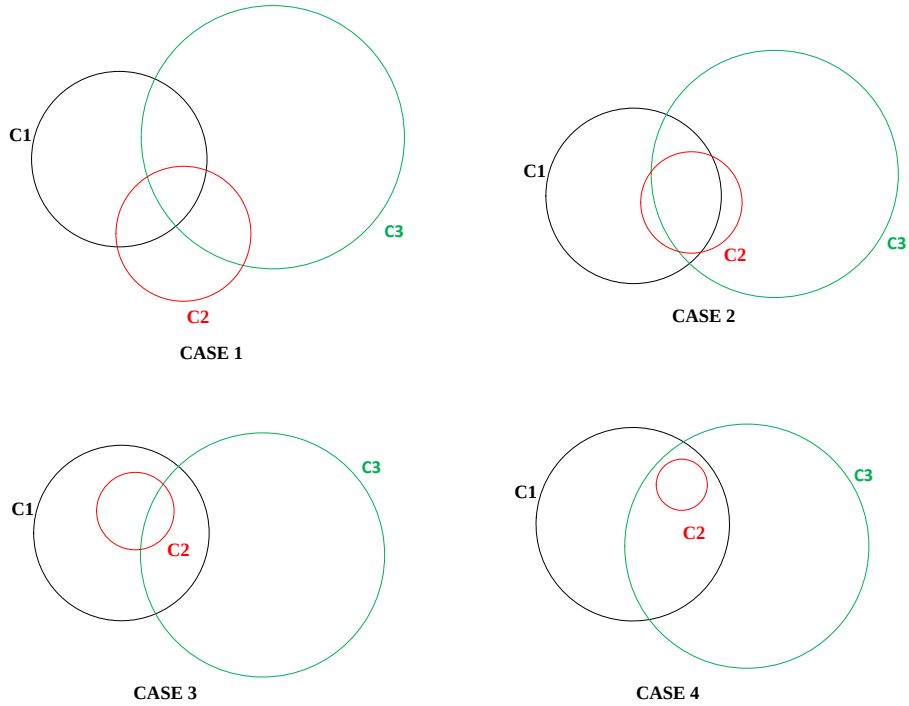

Figure 1.1 Four cases of three circles intersection

Table 1.1 The possibilities of the number of intersection points in the four cases

Number of Cases	**Number of intersection points**			**Total intersection points**
	Circles C1, C2	Circles C1, C3	Circles C2, C3	
Case 1	2	2	2	6
Case 2	2	2	2	6
Case 3	0	2	2	4
Case 4	0	2	0	2

In this dissertation, I proposed the different algorithms in four different cases to estimate the location of MS, select the proper mode cases in order to employ the proper algorithm in each case. For the best performance of estimation of MS localization, the proposed algorithm must be employed in the hybrid form.

The contributions of this dissertation are the following:

- **A TOA Shortest Distance Algorithm for Estimating Mobile Station Location**

In this paper, in order to improve the performance degradation for accurately estimating the location of MS, the shortest distance algorithm based on the selection of three interior intersection points among the entire intersection points is proposed. The proposed approach determines the averaged coordinate of three selected intersection coordinates as a location coordinate of the MS.

- **Line Intersection Algorithm for the Enhanced TOA Trilateration Technique**

TOA trilateration method estimates the distance between the BS and MS using the number of time delay, so three circles do not generally intersect at a point to give the true MS location which causes a serious problem in location detection. In order to solve this problem, a line intersection algorithm is proposed in which three lines, formed by connecting two intersection points of two specific BSs, intersect at a point to give the estimated location of MS.

- **Mathematical Analysis of Enhanced TOA Trilateration Localization Algorithm**

In this paper, the mathematic analysis is provided in order to show the relation between the shortest distance algorithm and the line intersection algorithm. In this analysis, I verify that line equations based on the intersection points obtained from the shortest distance algorithm are identical to line equations obtained from the line intersection algorithm.

- **Comparison Approach of Intersection Distances for Advanced TOA Trilateration**

The advanced TOA trilateration algorithm based on the line intersection algorithm has a good performance of estimation location of MS for the general case (case 1), but they may have serious location estimation error for the specific case (case 2), in which there are a small circle and two large circles. In the specific case, a small circle is located in an area of two large circles and a small circle meets two large circles at four intersection points. In order to solve the location estimation error problem, an efficient MS location estimation algorithm based on the comparison of the distances between two neighboring intersections is proposed, for the specific case.

- **Hybrid TOA Trilateration Algorithm Based on Line Intersection Algorithm and Comparison Approach of Intersection Distances**

A hybrid TOA trilateration algorithm is based on the idea of combining the line intersection algorithm and comparison approach of distances together to estimate the location

of MS. It combines the desired algorithms in the general case and the specific case for the best MS localization performance.

- **Mode Selection Algorithm for Advanced TOA Trilateration Techniques**

For the optimized location estimation, a proper algorithm should be effectively selected according to the proper case. Thus, the mode selection algorithm is proposed for distinguishing the four cases mode and employed the proper algorithm. The selection procedure for four cases is based on two equations that compare radii differences to center distances between the smallest circle and two large circles.

1.3 Organization of Dissertation

The structure of this dissertation is organized as follows. Chapter 2 describes the issue for TOA trilateration, when three circles do not meet at a single point. Chapter 3 describes the four cases based on the size of the estimated circles and the coordinate of BSs. Chapter 4 describes the shortest distance algorithm and the line intersection algorithm for case 1, the comparison approach of intersection distances for case 2, the small circle intersection approach for case 3 and the closest point algorithm for case 4. The performance of the proposed localization algorithms is illustrated by computer simulation results with various scenarios. The mathematical analysis is shown that the three intersecting lines based on three circles always meet at a point. Also, a mathematical analysis has been provided to show the relation between the shortest distance and line intersection algorithms. Chapter 5, I describe hybrid TOA

trilateration algorithm based on the line intersection algorithm and the comparison approach of intersection distances. I provide the performance analysis for verifying that the comparison approach of intersection distances has better performance than the line intersection algorithm, in the specific case. I, also, provide the overall selection method for distinguishing all four cases and employ the best algorithm for each individual case. Finally, chapter 6 concludes the dissertation.

2 Issue for Time of Arrival Trilateration

Location detection technology (LDT) is one of the core techniques for location-based service (LBS) in wireless communication for improving resource management and quality of services. The location of a mobile station (MS) is estimated using the time of arrival (TOA) technique based on three circles with centers corresponding to coordinates of three base stations (BSs) and radii corresponding to distances between MS and BSs. For accurately estimating the location of MS, three circles should meet at a point for the trilateration method, but they generally do not meet at a point because the radius is increased depending on the number of time delay for estimating the distance between MS and BS, and the sampling rate. The increased three circles intersect at six points and the three intersection points among them should be generally placed close to coordinate of the location for the specific MS. In this chapter, I discuss the problem of Trilateration method for TOA.

2.1 Introduction

The mobile location technique has increased the great interest in the fields of cellular and wireless local area networks with the rapid development of communication systems. New technologies and algorithms have found more and more applications in everyday human being life for the mobile location estimation. More researchers around the world are pushing forward to get high performance of the MS location with low cost, high precision, and reusability of the components.

U.S. Federal Communications Commission (FCC) mandated cellular providers to generate the MS location for Enhanced-911 services [20]. It stated that at least 95% of emergency calls, a resolution of 300 m must be achieved in a first instance and that the resolution should be increased to 150 m for improved systems. Further, in the initial stage, 67% of the calls must be located within an error of 100 m and 50 m in the improved phase. The various approaches of location detection technologies (LDT) for mobile have also been given in [8, 21-42].

Location-based services (LBS) involve the procedure to find the geographical location of the MS. It provides services based on its mobile location information. It is classified as emergency services, informational services, tracking services, and entertainment services. Emergency services include security alerts and public safety [43-45], and informational services include news, weather, sports, and stocks, etc. Tracking services include asset, fleet, logistic monitoring, and personally tracking, and entertainment services include locating a friend, dating, and gaming etc. [46, 47]. For all the location-based wireless services, the location information is an essential parameter for anyone and anywhere with high accuracy and reliability measurements [48-52]. Also, the location detection technology plays a vital role for LBS related to the modern world technique using the mobile humanoid robot.

The location of MS is determined by an intersection of three circles with the radius being the distance between MS and each BS, and the center being BS's location. Since the distance is estimated by counting the number of time delay samples, the radius of the three circles might be increased and circles usually do not intersect at a single point to give the location of MS. Instead of meeting at a point, there generally exists six intersection points from three circles. This causes the performance degradation for accurately estimating the location of MS.

2.2 Traditional Localization Technique

Geo-location, position location, and radiolocation are the commonly used terms to express the location of an object or user. Geo-location locates objects in terms of well-known global or local coordinates without employing Global Navigation Satellite System (GNSS), which has the advantage of low-cost implementation at the BS. Position location utilizes the coordinates of objects in two or three-dimensional space, which is mostly applicable in the incident detection and wireless network management. Radiolocation uses radio frequency (RF) signaling scheme to locate the objects, which has penetrating property through obstacles and propagating property for the long distance [50, 53, 54].

The localization scheme is used both in indoor and outdoor environments. In an indoor localization, the wireless local area network (WLAN) and Ultra-wideband (UWB) are well studied, but the accuracy of the indoor localization is affected by line of sight and multipath propagation [55-57]. For an outdoor localization, the Global Positioning System (GPS) is the most well-known outdoor localization techniques, which requires various high technologies to solve some problems related to the direct line-of-sight to the satellite, consuming a lot of the energy, high cost, time synchronization, and interference suppression [58]. The Internet of Things (IoT) is a novel paradigm which integrates a different kind of technologies, such as Bluetooth, Internet, Zigbee, Infrared, Wi-Fi, 3G, and General packet radio service (GPRS), and it enables those technologies to provide the location of the objects in different ways. Since various users and objects in different environments require the accurate location information in modern wireless communications, the effective location detection algorithms with high performance are dramatically developed [59-69].

In traditional localization algorithms for MS, there have been two fundamental principles used: the triangulation and trilateration method. The triangulation method determines the location of MS based on measuring the angle of the received signal from BSs. While the trilateration method estimates the location of the specific MS using at least three quadratic equations based on three circles with the center corresponding to the coordinates of BS and the radius corresponding to the distance between MS and each BS. Trilateration method is based on TOA or RSS measurements, whereas triangulation is based on AOA measurements [70-76]. Also, for accurately estimating the MS location, the triangulation requires various expensive angle measurement devices, unlike the trilateration technique. The mathematical computations for the trilateration algorithm are provided in detail in [77-85].

For a TOA method, the mobile position estimation is based on measuring parameters of radio signals that travel between the BS and MS. TOA technique measures the time from BSs to MS and it generates circles with a radius corresponding to each distance based on the measured times. The MS's position is found out by the intersections of circles from multiple TOA measurements.

2.3 Problem of Trilateration Method for Time of Arrival

For the TOA trilateration approach, the MS location is determined by solving at least three quadratic equations based on circles with radii corresponding to distances between MS and BSs and centers corresponding to coordinate of BSs [8, 22, 86-91]. In this approach, the true distance between MS and i th BS, r_i, is given by

$$r_i = \sqrt{(x - x_i)^2 + (y - y_i)^2}, \qquad i = 1,\ 2,\ 3 \tag{2.1}$$

where (x, y) and (x_i, y_i) are the coordinates of the true position of MS and the coordinates of the ith BS position, respectively. The distances between MS and BS1, BS2, and BS3 are defined as r_1, r_2, and r_3, respectively, as shown in Figure 2.1, which presents the TOA trilateration algorithm.

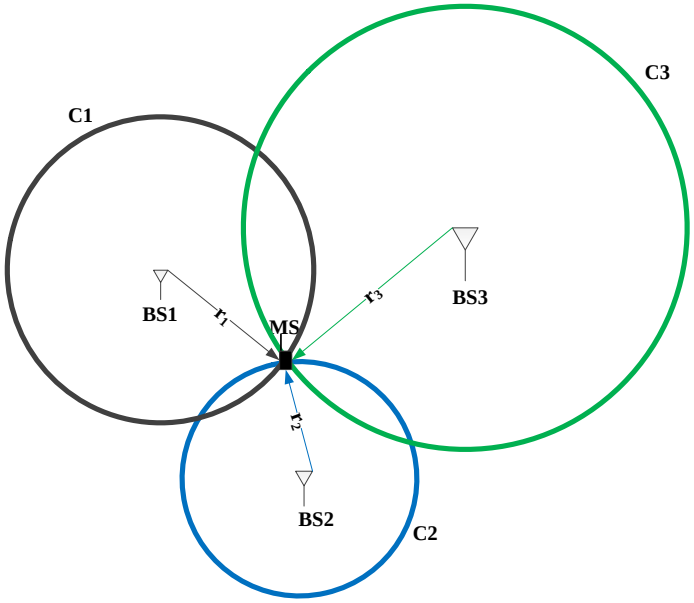

Figure 2.1 True location of mobile station at a single point using the intersection point of three circles

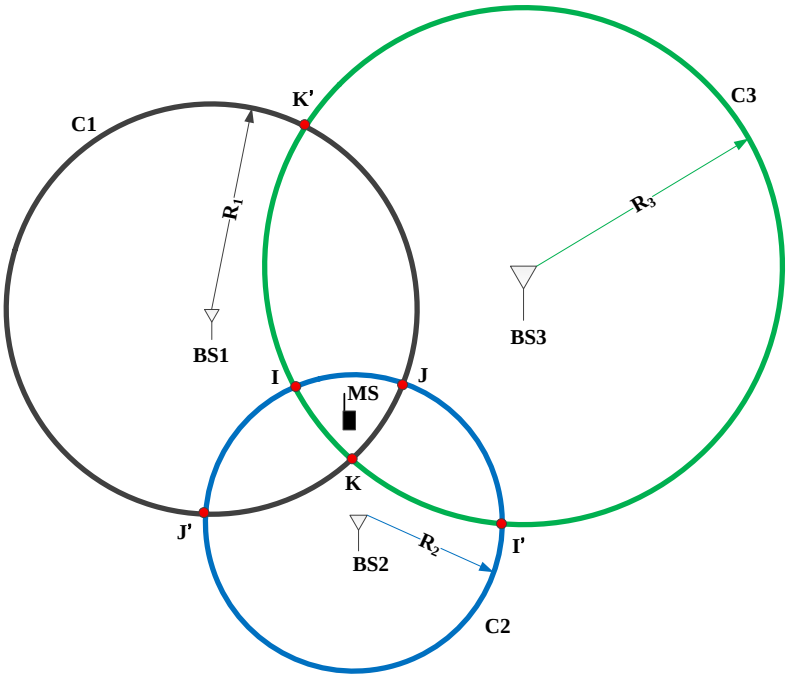

Figure 2.2 Three circles based on increased distances between mobile station and base station

The distance between MS and BS is determined by measuring the arrival time of the signal from different BSs. The transmitted signal travels at the speed of light and it arrives at MS after the certain time period known as a time delay. Since this delay depends on the distance between MS and BS, it is the same as the time delay multiplied by the velocity of the light. The number of delay samples in term of a sampling rate is calculated by

$$n_i = \text{ceil}\left(\frac{r_i}{c} \times f_s\right) \tag{2.2}$$

where n_i denotes the number of delays, c is the velocity of light $\left(c = 3 \times 10^8 \text{ m/s}\right)$ and f_s is the sampling rate. In (2.2), I employ $'ceil'$ function which defines the round up function, because the number of delays is an integer, but the right side in (2.2) may not be an integer. This integer number of delay samples results in an increment of distance between the MS and BS. Using (2.2), the distance between MS and ith BS is estimated as

$$R_i = \frac{n_i \times c}{f_s} \tag{2.3}$$

The estimated distance in (2.3) is increased from the original distance depending on the sampling rate, because the original distance is generally not a natural number, but n_i is a natural number. This increased distance results in the increased circles and three circles do not intersect at a point as shown in Figure 2.2 unlike Figure 2.1. In Figure 2.2, R_1, R_2, and R_3 are the increased distances corresponding to BS1, BS2, BS3, respectively. I, J, K, I', J', and K' are the six intersection points. Since the estimated distance by (2.3) is increased comparing to the original distance, there exists the estimation error of the MS location.

2.4 Concluding Remarks

The location of MS is determined by the intersection point of three circles whose center based on coordinates of three BSs and radius being the distances between MS and three BSs, for the TOA trilateration method. Since the distance between the MS and BS is estimated counting the number of time delay samples, those distances might be increased compared with

the original distance. The increased distances corresponding to the radii of each circle results in the error of the estimated location of MS because three circles do not meet at a single point. In this chapter, I discuss the problem formulation of trilateration for the TOA.

3 Classification of Four Possible Cases

3.1 Introduction

For a TOA method, the mobile position estimation is based on measuring parameters of radio signals that travel between BS and MS. TOA technique measures the time from BSs to MS and it generates circles with a radius corresponding to each distance based on the measured times. The MS's position is found out by the intersections of circles from multiple TOA measurements. The accurate MS location is determined based on an intersection point of three circles with the radius corresponding to the distance between each BS and MS (the center of each circle is a location of the corresponding BS). Since the TOA method determines the distance between MS and BS by counting the number of time delays, these three circles may not usually intersect at a single point, causing the serious localization error. I classify all possible cases (four cases) where three circles do not meet at a single point, for localization. Those cases are classified based on the size of the estimated circles and the coordinate of BSs.

3.2 Issue of Time of Arrival Trilateration Method

In the TOA trilateration technique, the location of MS is determined by a single intersection point of three circles with center coordinates of three BSs and radius corresponding to the distance between MS and each BS. The mathematical computations for the trilateration

algorithm are provided in detail in [70, 77-81, 92]. Assuming that there are three available BSs, the Euclidean distance between i th BS and MS is given by

$$r_i = \sqrt{(x - x_i)^2 + (y - y_i)^2}, \quad i = 1,\ 2,\ 3 \tag{3.1}$$

where (x, y) and (x_i, y_i) are the coordinates of the true MS position and ith BS position, respectively [93-96]. There are two cases (a general case and a specific case) for intersecting three original circles at a single point, shown in Figure 3.1. In the general case, three circles intersect at a point to locate MS. In the specific case, in which one small circle is located in the area of the two large circles, those three circles intersect at a point to locate MS.

The distance between the MS and BS is estimated by counting the number of delay samples or measuring the power of the received signal and is given by

$$R_i = \frac{n_i \times c}{f_s}. \tag{3.2}$$

The details of the derivation and symbol of the equation (3.2) are defined in the previous chapter 2.

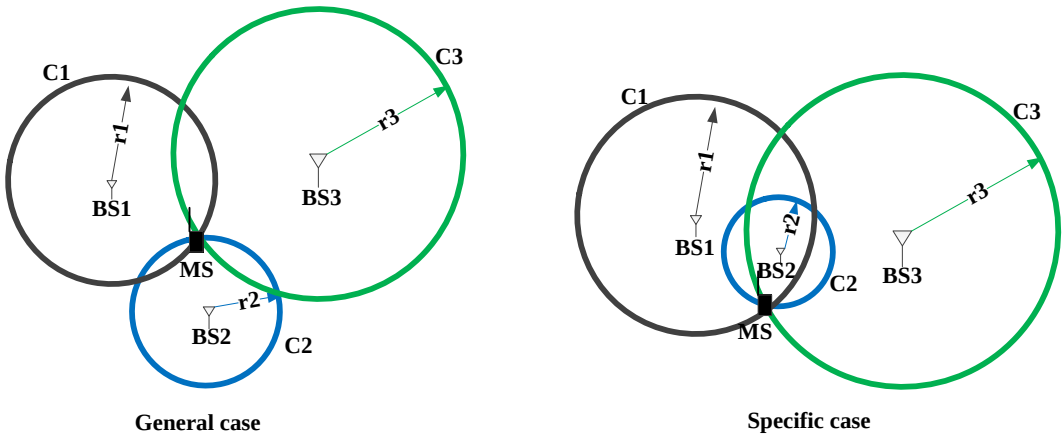

Figure 3.1 Cases for intersecting three original circles at a single point

3.3 Four Possible Cases

In the TOA method, the location of MS is determined by an intersection point of three circles formed by radius equal to the distance between individual BS and MS. Since the estimated distance (radius) is generally increased comparing to the original one, the estimated three circles may not interest at a unique point, resulting the MS localization error. This situation is classified into four cases as shown in Figure 3.2. Those cases are classified based on the size of the estimated circles and the coordinate of BSs. The detail classification of the four possible cases based on the estimated three circles is explained below.

In the case 1 (general case of three intersecting circles), there are total six intersection points (I, J, K, I', J', and K') based on the three extended circles, as shown in Figure 3.2. In this case, there exists the location estimation error, because three circles do not meet at a point. In order to provide a better location estimation of MS, the shortest distance algorithm and the line intersection algorithm have been proposed in the next chapter 4.

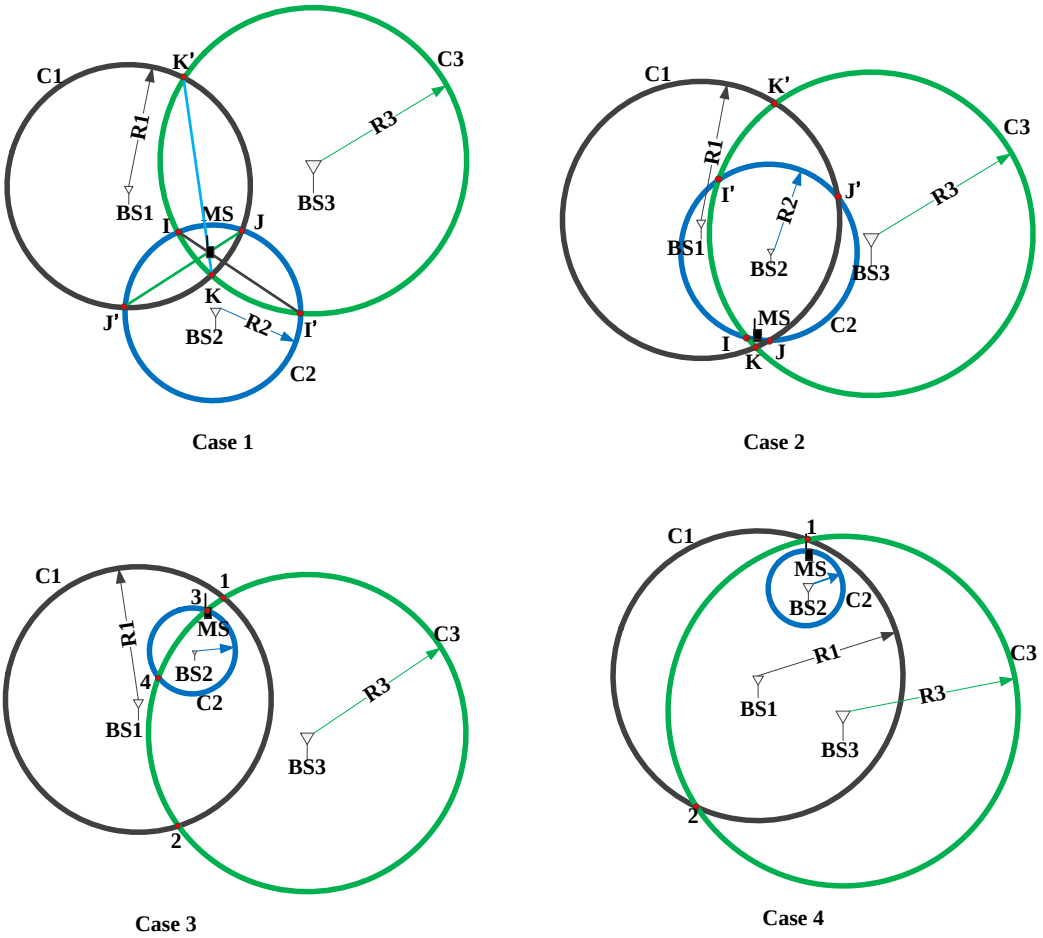

Figure 3.2 Four possible cases where three circles do not meet at a single point, for the localization environment

In the case 2 (specific case of the intersection of three circles), in which there is the small circle $C2$ is located in the area of the two large circles, $C1$ and $C3$. There are total six intersections (I, J, K, I', J', and K') based on the three extended circles and a small circle $C2$ has four intersections (I, I', J, and J') with two large circles $C1$ and $C3$, shown in Figure 3.2. In this case, there exists the location estimation error, because three

circles do not meet at a point. In order to provide a better location estimation of MS, the comparison approach of intersection distances has been proposed in the next chapter 4.

In the case 3, where there are four intersection points based on three extended circles and a small circle has two intersection points with one large circle i.e. a small circle $C2$ intersects a large circle $C3$ at point 3 and point 4, as shown in Figure 3.2. Since three extended circles do not meet at a point, there exists the location estimation error. In order to solve the MS location estimation error problem, I proposed the small circle intersection approach for the case 3, in the next chapter 4.

In the case 4, there are two intersection points of two large circles and a small circle $C2$ lies completely inside the overlapping area of two large circles $C1$ and $C3$, as shown in Figure 3.2. Since three extended circles do not meet at a point, there exists the location estimation error. In order to solve the MS location estimation error, I proposed the closest point algorithm for the case 4, in the next chapter 4.

3.4 Concluding Remarks

LDT is an important technique in a wireless communication system for LBS. In the TOA method, the location of MS is determined by an intersection point of three circles formed by a radius equal to the distance between individual BS and MS. Since the distances between MS and BSs are estimated by counting delay samples, three circles do not intersect at a point. In this chapter, I classify all possible cases (four cases) where three circles do not meet at a single point, for localization. Those cases are classified based on the size of the estimated circles and the coordinate of BSs. In order to enhance the performance of the TOA trilateration, the

advanced TOA trilateration algorithms suited to each case has been proposed in the next chapter 4.

4 Enhanced Time of Arrival Trilateration Algorithms

4.1 Introduction

The location of MS can be determined by measuring parameters of radio signals that travel between BS and MS. From the geometric approach, the TOA trilateration method forms three circles with the centers being coordinates of BSs and the radii being distances between MS and BSs, and the MS location is determined by an intersection of these three circles. Since the TOA method generally determines the distance between the MS and BS, by counting the number of time delays, the estimated distance may be slightly increased comparing to the original distance. As a result, three circles based on the estimated distances, usually may not intersect at a single point, which results in the estimation error. I classify all possible cases where the resulted circles may not meet at a single point. In order to enhance the performance of the TOA trilateration, I propose the efficient algorithms suited to each case in this chapter.

4.2 Shortest Distance Algorithm for Case 1

In the TOA trilateration technique, the distance between MS and BS is the same as the signal propagation multiplied by the speed of light [7, 8]. Since TOA estimates the distance between MS and BS by counting the number of time delays, the estimated distance between MS and BS is generally increased from the original distance. Due to the increased distance between the BS

and MS, three circles based on three available BSs do not meet at a single point and there exists six intersection points of three intersecting circles based on the estimated distances, as shown in Figure 4.1.

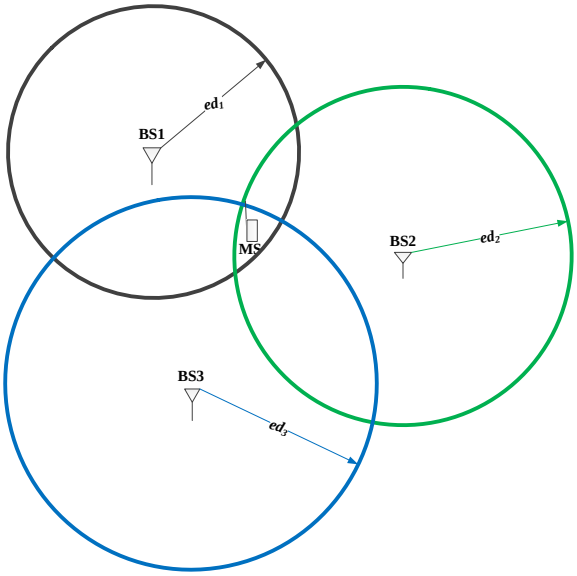

Figure 4.1 Intersection of three circles based on the estimated distances

In order to estimate the location of MS from the unmatched three circles, the selection process is performed for the three interior intersection points among six points. For the i th BS, I calculate two distances between the coordinate of the i th BS and two intersection points of two circles based on other BSs. Then, I compare the two calculated distances. In this approach, the intersection point corresponding to the shorter distance between two distances is determined to one of three interior intersection points. In order to select another two interior intersection points, this step is repeated for another two BSs. Figure 4.2 shows an example of this method. For the BS3, an assumption has been made such that the estimated distance

between MS and BS1 (ed_1) is smaller than that of the estimated distance between MS and BS2 (ed_2) in this figure. The difference of coordinates for BS1 and BS2 is defined as

$$\delta x \triangleq x_2 - x_1, \tag{4.1}$$

and

$$\delta y \triangleq y_2 - y_1, \tag{4.2}$$

and the center distance between the BS1 and BS2 is calculated by

$$\delta = \sqrt{\delta x^2 + \delta y^2}\ . \tag{4.3}$$

The distance from the BS1's center coordinate to line joining points of intersection is calculated by

$$p = \frac{\left(\delta^2 + {ed_1}^2 - {ed_2}^2\right)}{2\delta} \tag{4.4}$$

Using p in (4.4), coordinates of intersection points based on BS1 and BS2, $I\left(I_x, I_y\right)$ and $I'\left(I_x^{'}, I_y^{'}\right)$ calculated as

$$I_x = x_1 + \left(\frac{\delta x \times p}{\delta}\right) - \left(\frac{\delta y}{\delta} \times \left(\sqrt{{ed_1}^2 - p^2}\right)\right), \tag{4.5}$$

$$I_y = y_1 + \left(\frac{\delta y \times p}{\delta}\right) + \left(\frac{\delta x}{\delta} \times \left(\sqrt{ed_1^{\,2} - p^2}\right)\right), \tag{4.6}$$

and

$$I_x' = x_1 + \left(\frac{\delta x \times p}{\delta}\right) + \left(\frac{\delta y}{\delta} \times \left(\sqrt{ed_1^{\,2} - p^2}\right)\right), \tag{4.7}$$

$$I_y' = y_1 + \left(\frac{\delta y \times p}{\delta}\right) - \left(\frac{\delta x}{\delta} \times \left(\sqrt{ed_1^{\,2} - p^2}\right)\right). \tag{4.8}$$

After calculating distances between the coordinate of BS3 and, I and I', I compare two distances. Finally, I select an intersection point corresponding to the shortest distance between two distances to one of the three interior intersection points. This step is repeated for BS1 and BS2 for selecting all three intersection points among six points.

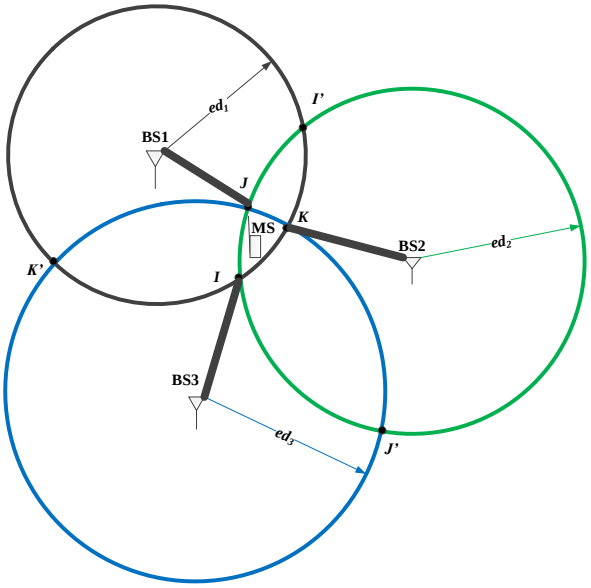

Figure 4.2 The shortest distance between intersections of circles

4.2.1 Determining Location of Mobile Station

In this section, the location of MS is estimated using the selected three interior intersection points among six entire intersection points of three circles. The location of MS is estimated using the average of the coordinates of the selected three interior intersection points among entire six intersection points. The estimated location of MS in Figure 4.2, $(\hat{x}, \hat{y})$, is given by

$$\hat{x} = \frac{I_x + J_x + K_x}{3}, \text{ and } \hat{y} = \frac{I_y + J_y + K_y}{3}. \quad (4.9)$$

The proposed algorithm for estimating the MS based on the TOA trilateration method is summarized in Table 4.1 and Figure 4.3 shows the flow chart of the proposed approach.

Table 4.1 Algorithm for estimation of mobile station position

Step 1: Initialize the circles $c1$, $c2$, and $c3$ of BSs with the radius equal to estimated distances (ed_1, ed_2, and ed_3), and coordinates of the considered BSs.

Step 2: Find all the feasible intersection points with three circles of BS.

Step 3: Calculate the distances between the center of the circle $c1\,(x_i, y_i)$ and each feasible intersection (x_j, y_j) formed by other circles of BSs $(c2 \text{ and } c3)$. For example i =1 and j =2, and 3.

$$d_{ij} = \sqrt{(x_i - x_j)^2 + (y_i - y_j)^2}, \qquad j = 1,\ 2,\ 3,\ 4,\ 5,\ 6 \qquad i = 1,\ 2,\ 3$$

Step 4: Select the intersection point corresponding to the shortest distance from step 3.

Step 5: Step 3 and step 4 are repeated for circles $c2$ and $c3$ of BSs.

Step 6: Decide the position of the object using the three selected points.

$$\hat{x} = \frac{I_x + J_x + K_x}{3}, \quad \hat{y} = \frac{I_y + J_y + K_y}{3}$$

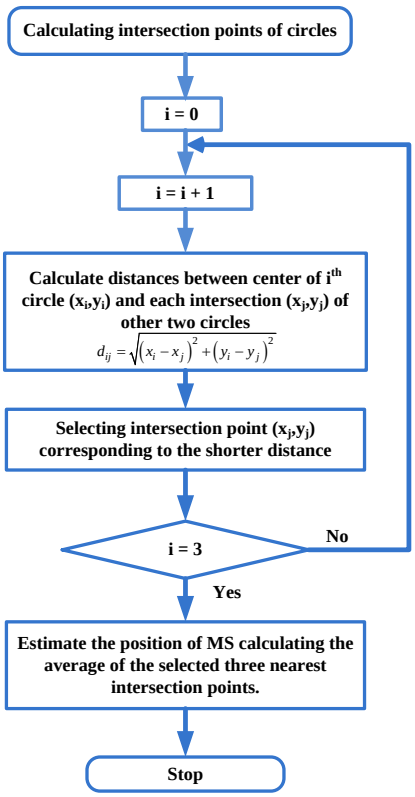

Figure 4.3 Flow chart for the proposed location estimation algorithm

4.2.2 Computer Simulations

In this section, I provide simulation results to verify the location estimation performance of the proposed algorithm. For the simulation, the location error between the original and estimated MS based on Euclidean distance is defined as

$$Error_{position} = \sqrt{(x - \hat{x})^2 + (y - \hat{y})^2} \tag{4.10}$$

and the mean squared error (MSE) of the MS location is given by

$$MSE_{position} = E\left[Error_{position}^{2} \right]. \tag{4.11}$$

Similarly, the distance error between the true distance and the estimated distance is given by

$$Error_{distance} = \sqrt{\left(d - ed_i\right)^2} \qquad i = 1,\ 2,\ 3 \tag{4.12}$$

and the mean squared error of distance is calculated as

$$MSE_{distance} = E\left[Error_{distance}^{2} \right]. \tag{4.13}$$

For the simulation scenario, I assume that there are three available base stations with fixed coordinates as follows: (-1000, 5000), (6000, -3000), (-7000, 600). The unit of coordinates used in this section is a meter (m). The various sampling rates have been selected as 10 MHz, 50 MHz, 100 MHz, 500 MHz, 1 GHz, 5 GHz, and 10 GHz. In order to calculate MSE, the simulations are performed 1,000,000 times. And the x and y coordinates of MS location are randomly chosen with ranges of -100 m ~ +100 m and -500 m ~ +500 m, for the case A and case B, respectively.

The simulation results of MSE versus various sampling rate for the estimated distance are shown in Figure 4.4 and Figure 4.5, for the case A and case B, respectively. From figures, I observe that MSE for the estimated distance is decreased, as the various sampling rate is increased. That means the MSE for the estimated location of MS will be decreased, as the sampling rate is increased. Figure 4.6 and Figure 4.7 show simulation results of MSE versus various sampling rate for the estimated location of MS in the case A and case B, respectively.

From the figures, I observe that MSE for the estimated location of MS using the shortest distance algorithm is decreased, as the sampling rate is increased. That means the performance of the MS location estimation on the higher sampling rate is better than it based on the lower sampling rate.

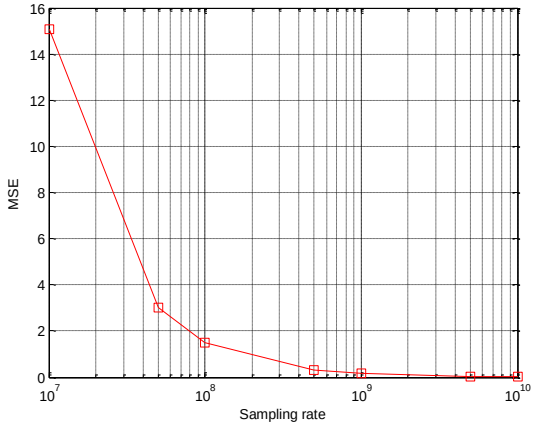

Figure 4.4 Mean squared error of the estimated distance for the case A

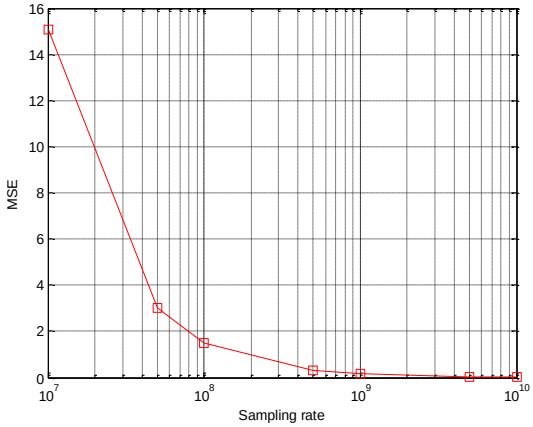

Figure 4.5 Mean squared error of the estimated distance for the case B

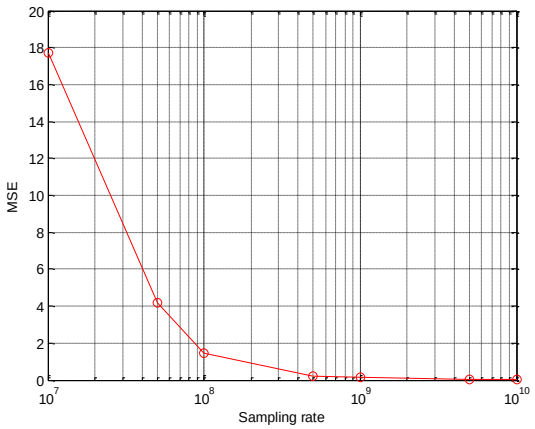

Figure 4.6 Mean squared error of position estimation for case A

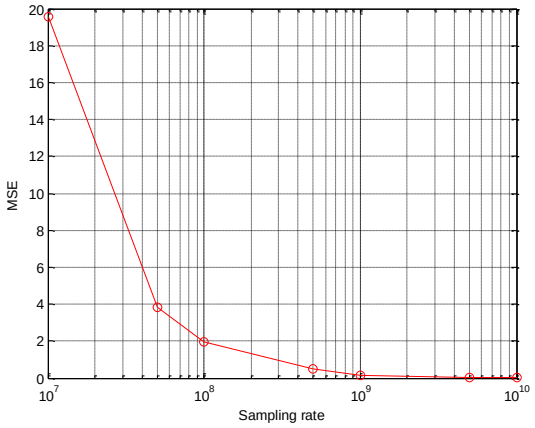

Figure 4.7 Mean squared error of position estimation for case B

4.3 Line Intersection Algorithm for Case 1

Since the TOA method measures the distance between the MS and BS by counting the number of sample delays, three circles based on the estimated distances may not meet at a point. These three circles usually generate six intersection points [92, 97-100] instead of a single

intersection point. This problem might cause a serious location detection error. In order to solve this problem, the trilateration based on the shortest distance algorithm, which selects the closest three intersection points to the locations of BSs among the entire six intersection points, was proposed [101, 102]. It determines the location of MS to the average coordinate of the selected three intersection points without considering the increased factor of each circle. This method usually has good location estimation performance, but it sometimes has a high estimation error in the extreme.

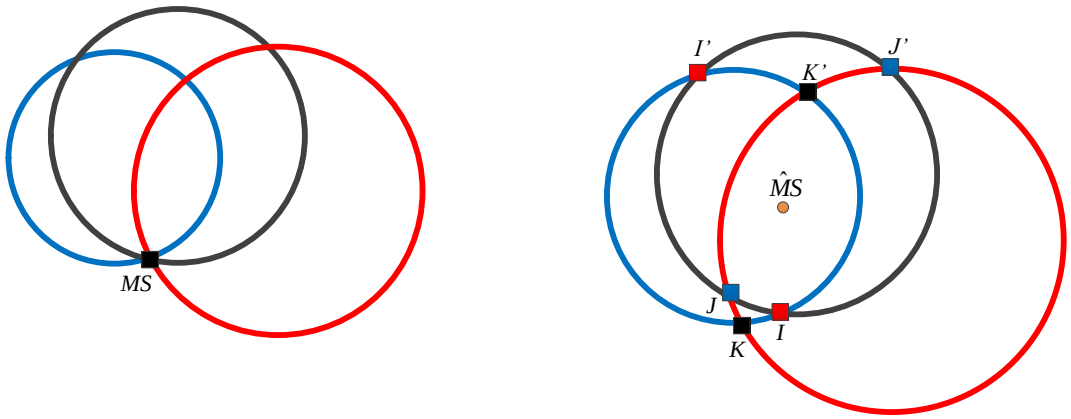

Figure 4.8 Example of the extreme case for the shortest distance algorithm (a) original location of mobile station, (b) estimated location of mobile station

Figure 4.8 shows an example of an extreme case. Figure 4.8 (a) shows the original location of MS and Figure 4.8 (b) shows the estimated location ($\hat{MS}$) of MS using shortest distance algorithm based on the averaged three interior intersection points among entire six intersection points. In this case, the estimated location is quite far away from the original location of MS, because it does not consider factors of the increased factor of each circle. In order to overcome

this problem, I propose the efficient trilateration method based on the line intersection algorithm, which does not require selecting three interior points.

From the six relevant intersection points, there are three straight lines which connect two intersection points for specific two circles. These lines must meet at a point shown in Figure 4.9, and I determine the location of MS to this line intersection point. After I measure the distances between MS and BSs, three circle equations corresponding to each BS is given by

$$x^2 + y^2 + \alpha_1 x + \beta_1 y + \gamma_1 = 0, \tag{4.14}$$

$$x^2 + y^2 + \alpha_2 x + \beta_2 y + \gamma_2 = 0, \tag{4.15}$$

$$x^2 + y^2 + \alpha_3 x + \beta_3 y + \gamma_3 = 0 \tag{4.16}$$

where $\alpha_i = -2x_i$, $\beta_i = -2y_i$, and $\gamma_i = x_i^2 + y_i^2 - ed_i^2$. Next, I solve three simultaneous equations of (4.14) and (4.15), (4.15) and (4.16), and, (4.16) and (4.14) to generate three line equations, yielding

$$(\alpha_1 - \alpha_2)x + (\beta_1 - \beta_2)y + (\gamma_1 - \gamma_2) = 0, \tag{4.17}$$

$$(\alpha_2 - \alpha_3)x + (\beta_2 - \beta_3)y + (\gamma_2 - \gamma_3) = 0, \tag{4.18}$$

$$(\alpha_3 - \alpha_1)x + (\beta_3 - \beta_1)y + (\gamma_3 - \gamma_1) = 0. \tag{4.19}$$

(4.17), (4.18), and (4.19) are intersection line equations of two circles based on BS1 and BS2, BS2 and BS3, and BS3 and BS1, respectively. Finally, I determine the MS location solving two equations among three intersection line equations. Considering (4.17) and (4.18), two equations form a matrix to get a solution, yielding

$$\begin{bmatrix} (\alpha_1 - \alpha_2) & (\beta_1 - \beta_2) \\ (\alpha_2 - \alpha_3) & (\beta_2 - \beta_3) \end{bmatrix} \begin{bmatrix} x \\ y \end{bmatrix} = \begin{bmatrix} (\gamma_2 - \gamma_1) \\ (\gamma_3 - \gamma_2) \end{bmatrix}, \tag{4.20}$$

and the estimated location of MS, $(\hat{x}, \hat{y})$, is given by

$$\hat{x} = \frac{(\gamma_2 - \gamma_1)(\beta_2 - \beta_3) - (\gamma_3 - \gamma_2)(\beta_1 - \beta_2)}{(\alpha_1 - \alpha_2)(\beta_2 - \beta_3) - (\alpha_2 - \alpha_3)(\beta_1 - \beta_2)}, \tag{4.21}$$

$$\hat{y} = \frac{(\alpha_1 - \alpha_2)(\gamma_3 - \gamma_2) - (\gamma_2 - \gamma_1)(\alpha_2 - \alpha_3)}{(\alpha_1 - \alpha_2)(\beta_2 - \beta_3) - (\alpha_2 - \alpha_3)(\beta_1 - \beta_2)}. \tag{4.22}$$

where $(\hat{x}, \hat{y})$ is the coordinate of the estimated MS location. Since this algorithm does not need to select three interior intersection points and does not affect in the extreme case, it is more efficient and accurate than the shortest distance algorithm. The steps to estimate the position of MS using the proposed algorithm is summarized in Table 4.2.

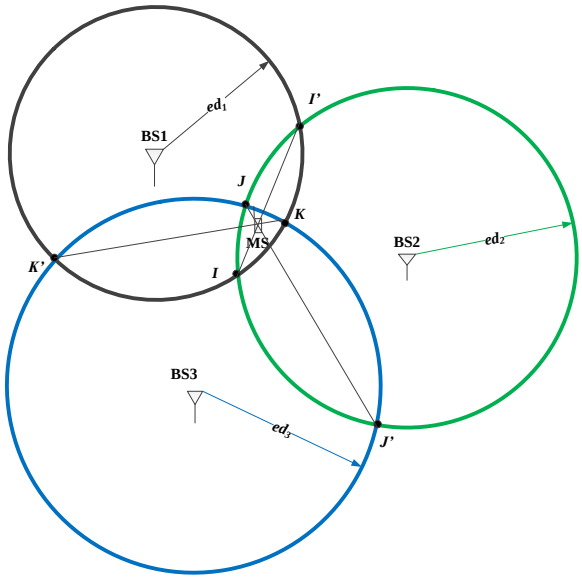

Figure 4.9 Line intersection algorithm

Table 4.2 An algorithm for estimation of mobile station position using line intersection

1. Estimate three distances between three BSs and MS using

$$ed_i = \frac{n_i \times c}{f_s}, \quad i=1, 2, 3.$$

2. Generate three circle equations using

$$x^2 + y^2 + \alpha_i x + \beta_i y + \gamma_i = 0$$

where $\alpha_i = -2x_i$, $\beta_i = -2y_i$, and $\gamma_i = x_i^2 + y_i^2 - ed_i^2$.

3. Determine the location of MS, $(\hat{x}, \hat{y})$, using

$$\hat{x} = \frac{(\gamma_2 - \gamma_1)(\beta_2 - \beta_3) - (\gamma_3 - \gamma_2)(\beta_1 - \beta_2)}{(\alpha_1 - \alpha_2)(\beta_2 - \beta_3) - (\alpha_2 - \alpha_3)(\beta_1 - \beta_2)},$$

$$\hat{y} = \frac{(\alpha_1 - \alpha_2)(\gamma_3 - \gamma_2) - (\gamma_2 - \gamma_1)(\alpha_2 - \alpha_3)}{(\alpha_1 - \alpha_2)(\beta_2 - \beta_3) - (\alpha_2 - \alpha_3)(\beta_1 - \beta_2)}.$$

4.3.1 Mathematical Analysis of Enhanced Time of Arrival Trilateration Algorithms

In this section, I easily show that three straight lines considered in the line intersection algorithm, which connect two intersection points of specific two circles among entire three circles, always meet at a single point [103]. In addition, the detailed analytic mathematic relation between the shortest distance algorithm and the line intersection algorithm is presented [104, 105].

4.3.1.1 Mathematical Verification for Line Intersection Algorithm

The line intersection algorithm has the excellent performance for estimating the location of MS and it is efficient comparing to the shortest distance algorithm. However, it must assume that three lines, which connect two intersection points of two specific circles, meet at a single point. In this subsection, I mathematically show that three lines always meet at a single point and the above assumption is not required.

The solutions of the estimated MS location provided in (4.21) and (4.22) are the results from (4.17) and (4.18) based on BS1 and BS2, and BS2 and BS3. Therefore, if the estimated location coordinate, $(\hat{x}, \hat{y})$, in (4.21) and (4.22) is satisfied to (4.19), three intersection lines should meet at a single point. In order to show this, I substitute (4.21) and (4.22) into the left side of (4.19) as follows:

$$
\begin{aligned}
&(\alpha_3-\alpha_1)\left[\frac{(\gamma_2-\gamma_1)(\beta_2-\beta_3)-(\gamma_3-\gamma_2)(\beta_1-\beta_2)}{(\alpha_1-\alpha_2)(\beta_2-\beta_3)-(\alpha_2-\alpha_3)(\beta_1-\beta_2)}\right]\\
&+(\beta_3-\beta_1)\left[\frac{(\alpha_1-\alpha_2)(\gamma_3-\gamma_2)-(\gamma_2-\gamma_1)(\alpha_2-\alpha_3)}{(\alpha_1-\alpha_2)(\beta_2-\beta_3)-(\alpha_2-\alpha_3)(\beta_1-\beta_2)}\right]+(\gamma_3-\gamma_1)\\
&=\frac{(\alpha_3-\alpha_1)(\gamma_2-\gamma_1)(\beta_2-\beta_3)}{(\alpha_1-\alpha_2)(\beta_2-\beta_3)-(\alpha_2-\alpha_3)(\beta_1-\beta_2)}-\frac{(\alpha_3-\alpha_1)(\gamma_3-\gamma_2)(\beta_1-\beta_2)}{(\alpha_1-\alpha_2)(\beta_2-\beta_3)-(\alpha_2-\alpha_3)(\beta_1-\beta_2)}\\
&+\frac{(\beta_3-\beta_1)(\alpha_1-\alpha_2)(\gamma_3-\gamma_2)}{(\alpha_1-\alpha_2)(\beta_2-\beta_3)-(\alpha_2-\alpha_3)(\beta_1-\beta_2)}-\frac{(\beta_3-\beta_1)(\gamma_2-\gamma_1)(\alpha_2-\alpha_3)}{(\alpha_1-\alpha_2)(\beta_2-\beta_3)-(\alpha_2-\alpha_3)(\beta_1-\beta_2)}\\
&+\frac{(\gamma_3-\gamma_1)\left[(\alpha_1-\alpha_2)(\beta_2-\beta_3)-(\alpha_2-\alpha_3)(\beta_1-\beta_2)\right]}{(\alpha_1-\alpha_2)(\beta_2-\beta_3)-(\alpha_2-\alpha_3)(\beta_1-\beta_2)}
\end{aligned}
\tag{4.23}
$$

Since the numerator of (4.23) is calculated to

$$
\begin{aligned}
&(\alpha_3-\alpha_1)(\gamma_2-\gamma_1)(\beta_2-\beta_3)-(\alpha_3-\alpha_1)(\gamma_3-\gamma_2)(\beta_1-\beta_2)\\
&+(\beta_3-\beta_1)(\alpha_1-\alpha_2)(\gamma_3-\gamma_2)-(\beta_3-\beta_1)(\gamma_2-\gamma_1)(\alpha_2-\alpha_3)\\
&+(\gamma_3-\gamma_1)(\alpha_1-\alpha_2)(\beta_2-\beta_3)-(\gamma_3-\gamma_1)(\alpha_2-\alpha_3)(\beta_1-\beta_2)\\
&=0.
\end{aligned}
\tag{4.24}
$$

Equation (4.19) is satisfied, when I substitute the estimated location coordinate, $(\hat{x}, \hat{y})$, into (4.19). From this result, I easily show that three intersection lines, which connect two intersection points of two specific circles among three circles based on three BSs, meet at a single point. Therefore, the line intersection algorithm operates well for all cases to estimate the location of MS, unlike the shortest distance algorithm.

4.3.1.2 Mathematical Relations between Two Algorithms

In this subsection, I provide a mathematical analysis to show the relation between the shortest distance and line intersection algorithms. The line equation based on two intersection points of two circles obtained from the shortest distance algorithm is given by

$$y - I_y = \frac{I_y' - I_y}{I_x' - I_x}(x - I_x). \tag{4.25}$$

From the shortest distance algorithm, I find two coordinates of two circle intersection points from (4.5) to (4.8). From these equations, I get,

$$\begin{aligned} I_y' - I_y &= y_1 + \left(\frac{\delta y \times p}{\delta}\right) - \left(\frac{\delta x}{\delta} \times \left(\sqrt{ed_1^2 - p^2}\right)\right) - \left[y_1 + \left(\frac{\delta y \times p}{\delta}\right) + \left(\frac{\delta x}{\delta} \times \left(\sqrt{ed_1^2 - p^2}\right)\right)\right], \\ &= -2 \times \left(\frac{\delta x}{\delta} \times \left(\sqrt{ed_1^2 - p^2}\right)\right) \end{aligned} \tag{4.26}$$

$$\begin{aligned} I_x' - I_x &= x_1 + \left(\frac{\delta x \times p}{\delta}\right) + \left(\frac{\delta y}{\delta} \times \left(\sqrt{ed_1^2 - p^2}\right)\right) - \left[x_1 + \left(\frac{\delta x \times p}{\delta}\right) - \left(\frac{\delta y}{\delta} \times \left(\sqrt{ed_1^2 - p^2}\right)\right)\right], \\ &= 2 \times \left(\frac{\delta y}{\delta} \times \left(\sqrt{ed_1^2 - p^2}\right)\right) \end{aligned} \tag{4.27}$$

and

$$y - I_y = y - y_1 - \left(\frac{\delta y \times p}{\delta}\right) - \left(\frac{\delta x}{\delta} \times \left(\sqrt{ed_1^2 - p^2}\right)\right), \tag{4.28}$$

$$x - I_x = x - x_1 - \left(\frac{\delta x \times p}{\delta}\right) + \left(\frac{\delta y}{\delta} \times \left(\sqrt{ed_1^2 - p^2}\right)\right). \tag{4.29}$$

Substituting and rearranging (4.26), (4.27), (4.28), and (4.29) in (4.25), it can be rewritten as

$$y - y_1 - \left(\frac{\delta y \times p}{\delta}\right) - \left(\frac{\delta x}{\delta} \times \left(\sqrt{ed_1^{\,2} - p^2}\right)\right) = \frac{-2 \times \left(\frac{\delta x}{\delta} \times \left(\sqrt{ed_1^{\,2} - p^2}\right)\right)}{2 \times \left(\frac{\delta y}{\delta} \times \left(\sqrt{ed_1^{\,2} - p^2}\right)\right)} \times \left[x - x_1 - \left(\frac{\delta x \times p}{\delta}\right) + \left(\frac{\delta y}{\delta} \times \left(\sqrt{ed_1^{\,2} - p^2}\right)\right)\right]. \quad (4.30)$$

By solving (4.30), I obtain

$$\left[(\delta \times \delta y) \times y\right] + \left[(\delta \times \delta x) \times x\right] + \left[-(y_1 \times \delta \times \delta y) - (x_1 \times \delta \times \delta x) - (\delta x^2 + \delta y^2) \times p\right] = 0. \quad (4.31)$$

Substituting (4.1), (4.2), (4.3) and (4.4) in (4.31), I get

$$\left[\left(\sqrt{(x_2 - x_1)^2 + (y_2 - y_1)^2} \times (y_2 - y_1)\right) \times y\right] + \left[\left(\sqrt{(x_2 - x_1)^2 + (y_2 - y_1)^2} \times (x_2 - x_1)\right) \times x\right] + \begin{bmatrix} -\left(y_1 \times \sqrt{(x_2 - x_1)^2 + (y_2 - y_1)^2} \times (y_2 - y_1)\right) \\ -\left(x_1 \times \sqrt{(x_2 - x_1)^2 + (y_2 - y_1)^2} \times (x_2 - x_1)\right) \\ -\frac{\left((x_2 - x_1)^2 + (y_2 - y_1)^2\right) \times \left((x_2 - x_1)^2 + (y_2 - y_1)^2 + ed_1^{\,2} - ed_2^{\,2}\right)}{2 \times \sqrt{(x_2 - x_1)^2 + (y_2 - y_1)^2}} \end{bmatrix} = 0. \quad (4.32)$$

From (4.32), I also obtain

$$\begin{aligned}&(2y_2-2y_1)\times y+(2x_2-2x_1)\times x\\&+\left[-(2y_1\times(y_2-y_1))-(2x_1\times(x_2-x_1))-\left((x_2-x_1)^2+(y_2-y_1)^2+ed_1^{\,2}-ed_2^{\,2}\right)\right]=0,\end{aligned} \tag{4.33}$$

and (4.33) is finally simplified to

$$(2y_2-2y_1)\times y+(2x_2-2x_1)\times x+y_1^{\,2}+x_1^{\,2}-x_2^{\,2}-y_2^{\,2}-ed_1^{\,2}+ed_2^{\,2}=0\,. \tag{4.34}$$

Note that (4.34) is identical to the line equation connecting two intersections of two circles obtained from the line intersection algorithm, in (4.17). From this process, I observe that line equation based on the intersection points obtained from the shortest distance algorithm is identical to the line equation obtained from the line intersection algorithm.

4.3.2 Computer Simulation

In this section, the computer simulation results are provided to compare the location estimation performances for the shortest distance algorithm and the line intersection algorithm. For the simulation, I assume that three fixed BSs are located at coordinates (-1000, 5000), (6000, -4000), and (-7000, 500), respectively. The unit of each BS's coordinate is in meter (m), and I consider the different sampling rates of 10 MHz, 50 MHz, 100 MHz, 500 MHz, 1 GHz, 5 GHz, and 10 GHz. The MS location coordinates are randomly chosen with ranges from -100 m to +100 m, from -600 m to +600 m, and from -1000 m to +1000 m, for the case A, the case B, and the case C, respectively.

4.3.2.1 Error Model

The performance of the localization algorithm is generally evaluated by the mean squared error (MSE) [106-109]. The error of the estimated distance between the MS and BS is defined as

$$Error_{\text{dist}} \triangleq \sqrt{\left(d_i - ed_i\right)^2}, \quad \text{i=1, 2, 3,} \tag{4.35}$$

and the mean squared error (MSE) of the distance is calculated as

$$MSE_{\text{dist}} = E\left[Error_{\text{dist}}^2 \right], \tag{4.36}$$

where $E[\ ]$ is an expectation operator. Similarly, the error between the true position of MS and the estimated position of MS is defined as

$$Error_{\text{pos}} \triangleq \sqrt{\left(x - \hat{x}\right)^2 + \left(y - \hat{y}\right)^2}, \tag{4.37}$$

where this error is represented in the Euclidean distance. In addition, MSE for estimating the MS position is given by

$$MSE_{\text{pos}} = E\left[Error_{\text{pos}}^2 \right]. \tag{4.38}$$

In order to accurately calculate MSE, the simulations are performed 100,000 times for each sampling rate.

4.3.2.2 Simulation Results

The simulation results for the distance MSE versus various sampling rates are shown in Figure 4.10, Figure 4.11, and Figure 4.12, for the case A, case B, and case C, respectively. From figures, I observe that MSEs for estimating the distances between MS and BS are decreased as the sampling rates are increased. Also, I show simulation results to observe the MSE performances versus various sampling rates for estimating the MS location and to compare them, for the shortest distance and the line intersection algorithms, in Figure 4.13, Figure 4.14, and Figure 4.15 for the case A, case B, and case C, respectively. From these results, I observe that the MSE curves of the line intersection algorithm are lower than them of the shortest distance algorithm for all cases. For a close-by look at differences of MSE between both algorithms, I enlarge the plot in the sampling rate range from 10^9 Hz to 10^{10} Hz, in Figure 4.16, Figure 4.17, and Figure 4.18, for the case A, case B, and case C, respectively. From these figures, I see slightly distinct variations between both algorithms in that range, though they seem to be closely overlapped in Figure 4.13, Figure 4.14, and Figure 4.15.

MSE of both algorithms decreases as the sampling rate increases, which means the performance of the estimated location of MS based on the higher sampling rate is better than that of the lower sampling rate. Since the carrier frequency is generally proportional to the sampling rate but inversely proportional to the time period, the resolution for estimating the distance between MS and BS is improved for the higher sampling rate, expecting the higher

localization accuracy. Consequently, I verify that the location estimation performance of the line intersection algorithm is better, and it is more efficient than that of the shortest distance algorithm because the line intersection algorithm does not need to select three interior intersection points among entire six intersection points, unlike the shortest distance algorithm. Also, the line intersection algorithm does not require to the assumption that three intersection lines, which connect two intersection points of two circles among three entire circles, must meet at a single point because I easily showed that they are always met at a single point.

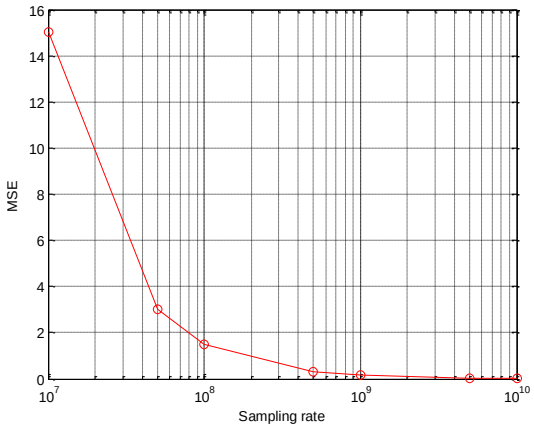

Figure 4.10 Mean squared error of distances between mobile station and base station for the case A

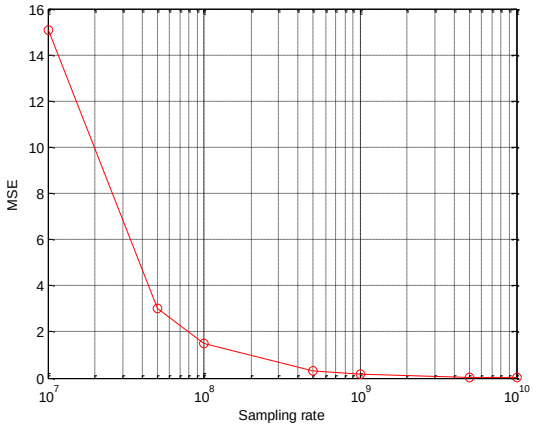

Figure 4.11 Mean squared error of distances between mobile station and base station for the case B

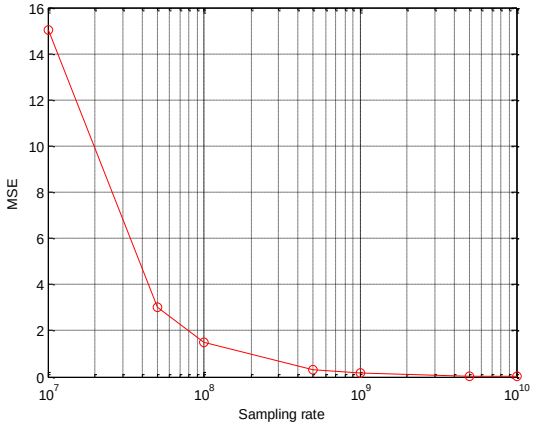

Figure 4.12 Mean squared error of distances between mobile station and base station for the case C

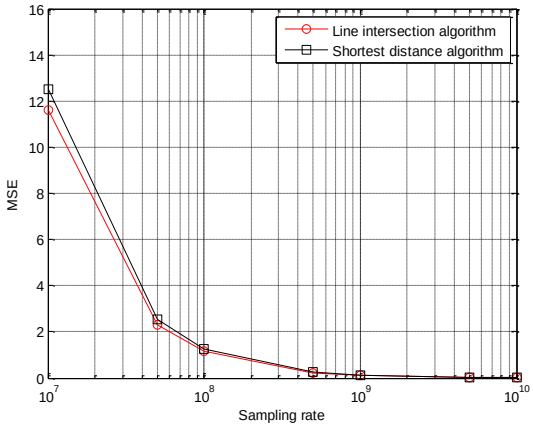

Figure 4.13 Mean squared error of mobile station position estimation using the shortest distance and the line intersection algorithms for the case A

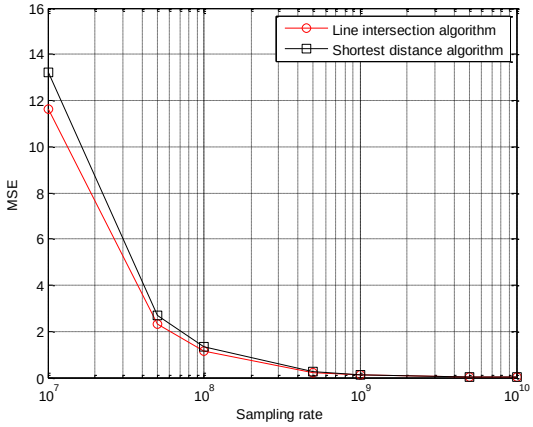

Figure 4.14 Mean squared error of mobile station position estimation using the shortest distance and the line intersection algorithms for the case B

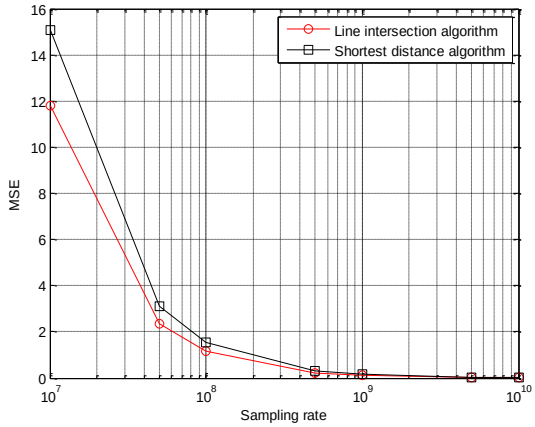

Figure 4.15 Mean squared error of mobile station position estimation using the shortest distance and the line intersection algorithms for the case C

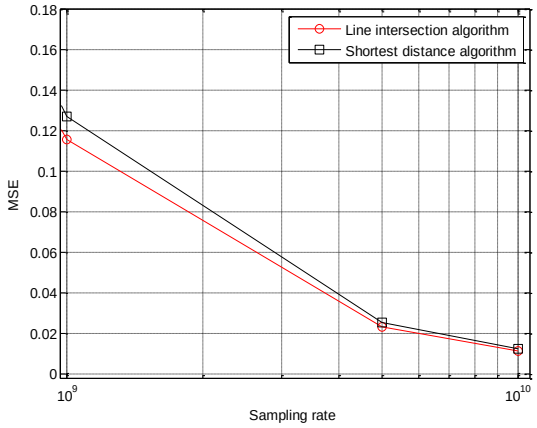

Figure 4.16 The enlarged mean squared error curves of the mobile station position estimation for the case A

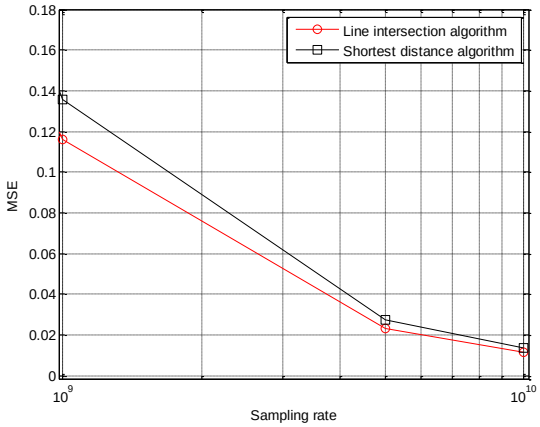

Figure 4.17 The enlarged mean squared error curves of the mobile station position estimation for the case B

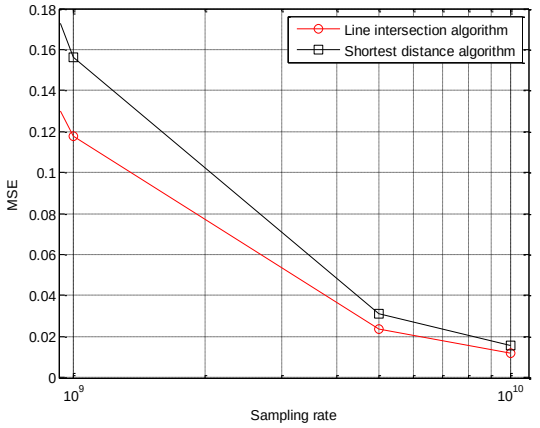

Figure 4.18 The enlarged mean squared error curves of the mobile station position estimation for the case C

4.4 Comparison Approach of Intersection Distances for Case 2

The time of arrival (TOA) trilateration method is one of the representative algorithms for the location detection technology (LDT), which estimates the location of mobile station (MS) at a unique intersection point of three circles with radii corresponding to distances between MS

and base stations (BS) and centers corresponding to coordinates of BSs. However, there may be serious estimation errors, when they do not meet at a point because the estimated radii of them are increased. The solutions for reducing the estimation position error in the general case of meeting three circles with the extended radius have been recently provided as the shortest distance algorithm [101, 102] and the line intersection algorithm [110, 111]. Although these algorithms have good performance for estimating the location of MS in the general case of three circles, but they may have a high estimation error in the specific case (case 2), which has two large circles and one small circle located in the area of two large circles. In order to solve the high estimation error problem, the efficient location estimation algorithm is proposed for the specific case (case 2). In this case, there are total six intersections based on the three extended circles and a small circle has four intersections with two large circles. The proposed approach compares distances based on four neighboring intersections and selects the shortest one. Finally, it determines the averaged coordinate of two intersections corresponding to the shortest distance, as the location of MS [112]. The location estimating the performance of the proposed algorithm is illustrated by the computer simulation example.

In this section, I consider the specific case (case 2) for the intersection of three circles, in which there is the small circle $C3$ is located in the area of the two large circles, $C1$ and $C2$, shown in Figure 4.19. In the figure, MS is located at the point marked by a red triangle. The extended circles, due to the increased radii $\left(\hat{d}_i\right)$, meet at a six points $\left(I, J, K, I', J', \text{and } K'\right)$, trilateration, such as the shortest distance and the line intersection algorithms, do not consider this type of the particular specific case and there may have serious location estimation error in this specific case, in this paper, I propose an efficient location estimation algorithm specialized in this case.

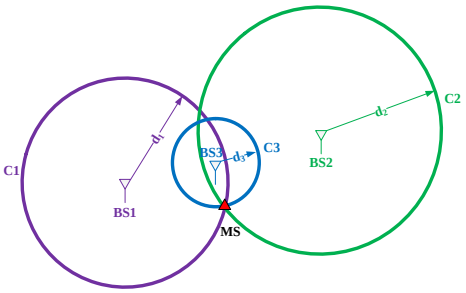

Figure 4.19 The true location using an intersection point of three circles

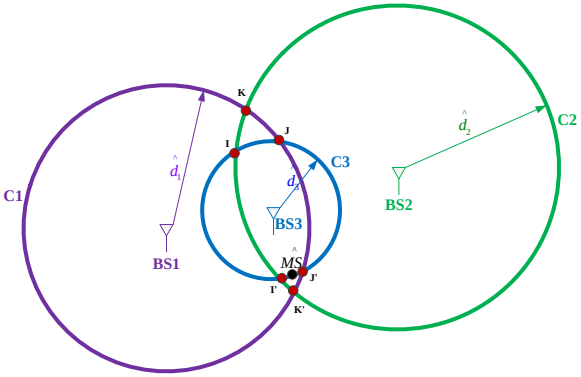

Figure 4.20 In the considered specific case, three intersecting circles with the increased radii, due to the integer number of delay samples.

First of all, the proposed algorithm finds the coordinates of all six intersection points. Among entire six intersection points, I only consider four intersections formed by a small circle $(C3)$ with two large circles $(C1 \text{ and } C2)$, (Note that I use I, J, I', and J', in Figure 4.20 and I arrange $I=1$, $J=2$, $I'=3$, and $J'=4$, for an efficient explanation of the proposed algorithm). Based on the calculated coordinates, I calculate the distance between the two intersection points of I and J, and the distance between the two intersection points of I' and J'. The distances between two neighboring intersection points can be given by

$$d_{j\,j+1} = \sqrt{\left(x_j - x_{j+1}\right)^2 + \left(y_j - y_{j+1}\right)^2} \qquad j = 1,\ 3, \tag{4.39}$$

where $d_{12} = d_{IJ}$ and $d_{34} = d_{I'J'}$ are distances between I and J, and between I' and J', respectively, and $\left(x_j, j_j\right)$ is a coordinate of the j th intersection point among the four considered points. After calculating two distances, I compare both and select the shorter distance. Finally, the proposed approach determines the average of two coordinates corresponding to the selected shorter distance, as the estimated location of MS. In Figure 4.20, the estimated location of the MS, $\left(\hat{x}, \hat{y}\right)$, is given by

$$\hat{x} = \frac{I_x' + J_x'}{2} \quad , \quad \hat{y} = \frac{I_y' + J_y'}{2} \tag{4.40}$$

The true position of MS in Figure 4.19 is formed by an intersection point of three circles, but it is located above the line connecting I' and J', which it might be close to that line, Figure 4.20 based on the increased distances. In the case of the line intersection algorithm, the estimated MS position should be located below circles, which it might be quite far away from the true location, in Figure 4.20, in the specific case. Therefore, considering that all radii of the three circles are increased, I determine the averaged coordinate of I' and J' in Figure 4.20, as the estimated MS location. Although it is not the optimum estimated position of MS, it is very close to the true position comparing to the estimated result of the conventional estimation technique like the line intersection algorithm, in the specific case, which a relatively small circle is located in the area of the two large circles.

The proposed comparison approach of intersection distances is summarized in Table 4.3, and its flow chart is shown in Figure 4.21.

Table 4.3 Comparison approach of intersection distances

1.	Initialize the circles $C1$, $C2$, and $C3$, based on centers of BSs and radii equal to estimated distances.
2.	Find the entire six intersections coordinate points $(I, J, K, I', J', \text{and } K')$ of the intersection of three circles.
3.	Determine two intersection points (I', J') of a small circle $C3$ with two large circles $C1$ and $C2$, and calculate the distance between both points (distance between I' and J').
4.	Repeat step 3 for other intersection points (I, J).
5.	Compare two distances ((distance between I' and J') and (distance between I and J).
6.	Select the shorter distance between two distances.
7.	Determine two intersection points corresponding to the selected shorter distance.
8.	Calculate the averaged coordinate of two intersection points and determine it as the estimated MS location, given by $\hat{x} = \frac{I_x' + J_x'}{2}$, and $\hat{y} = \frac{I_y' + J_y'}{2}$.

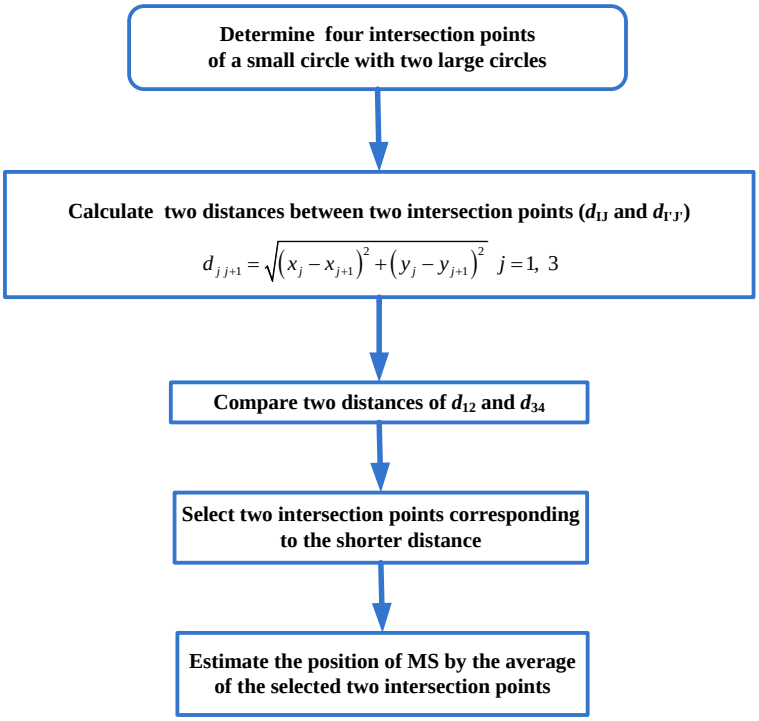

Figure 4.21 Flow chart for comparison approach of intersection distances

4.4.1 Computer Simulation

In this section, the MS location estimation performance of the comparison approach of intersection distances is presented by the computer simulation example. I consider the specific case, which a small circle is located in the area of the two large circles, in this simulation.

4.4.1.1 Simulation Scenario

For the simulation, I assume that there are three fixed BSs. The simulation is performed in two sets of the coordinates for three BSs to observe and to analyze the difference between the

proposed algorithm and the conventional algorithm like the line intersection algorithm, in the considered specific case. The coordinates of the three fixed BSs for two sets are provided as follows:

(i) First set: (-3000, 5000), (1500, 3000), and (7000, 600)

(ii) Second set: (-1000, 3000), (1000, 1000), and (5000, 500)

The unit of each coordinate is in meter (m) and the various sampling rates are 10 MHz, 50 MHz, 100 MHz, 500 MHz, 1 GHz, 5 GHz, and 10 GHz. In the simulation scenario, I have randomly chosen x and y coordinates of MS, for both sets. The case A selects coordinates of the MS range in between -100 m and +100 m and the case B selects coordinate of the MS range in between -500 m and +500 m.

4.4.1.2 Error Model for Simulation

The performance of the comparison approach of intersection distances is shown by mean squared errors (MSE) of the estimated MS location and all results are performed 1,000,000 times for each sampling rate to calculate the accurate MSE. The distance error between the true distance and the estimated distance is given by

$$Error_{distance} = \sqrt{\left(d - \hat{d}\right)^2}, \tag{4.41}$$

and MSE of distance is given by

$$MSE_{distance} = E\left[Error_{distance}^2 \right], \tag{4.42}$$

where $E[\ ]$ denotes the expectation operator. Similarly, the error between the true and the estimated position of MS is calculated by

$$Error_{position} = \sqrt{(x-\hat{x})^2 + (y-\hat{y})^2}, \tag{4.43}$$

and MSE about the MS position is given by

$$MSE_{position} = E\left[Error_{position}^2 \right]. \tag{4.44}$$

4.4.1.3 Simulation Results

4.4.1.3.1 Simulation Results for the First Set

Based on the first set of BSs, the simulation results of the distance MSE versus various sampling rates are shown in Figure 4.22 and Figure 4.23, for the case A and case B, respectively. From figures, I observe that the distance MSE is decreased as the sampling rate is increased because the high sampling rate means the high resolution. Since the sampling rate is the inverse of the time period, at the higher sampling rate, the time period is shorter and the resolution for estimating the distance between BS and MS is improved. Therefore, the

performance for estimating the distance is better and the distance MSE is lower, for the higher sampling rate. In general, higher sampling rates lead to higher localization accuracy. The comparisons of MSEs for the estimated locations based on the comparison approach of intersection distances and the line intersection algorithm are shown in Figure 4.24 and Figure 4.25 for the case A and case B, respectively. From figures, I observe that the MSE curves of the comparison approach of intersection distances are lower than that of the line intersection algorithm and the location MSE is decreased as the sampling rate is increased in both cases. Figure 4.26 and Figure 4.27 show the enlarged versions of Figure 4.24 and Figure 4.25, respectively, in the range from 1 GHz to 10 GHz, to clearly compare the performance of both algorithms in the specific case in the environment of the high sampling rate.

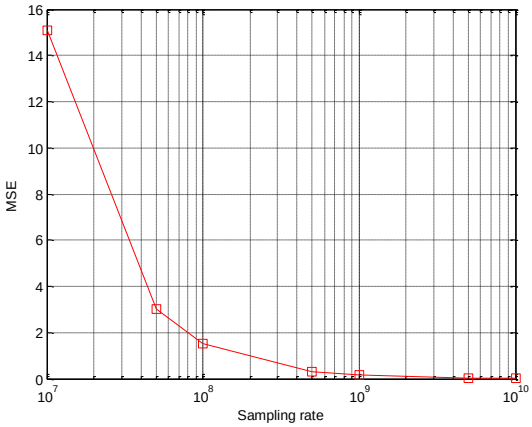

Figure 4.22 For the first set: mean squared error curve of the distance for the case A

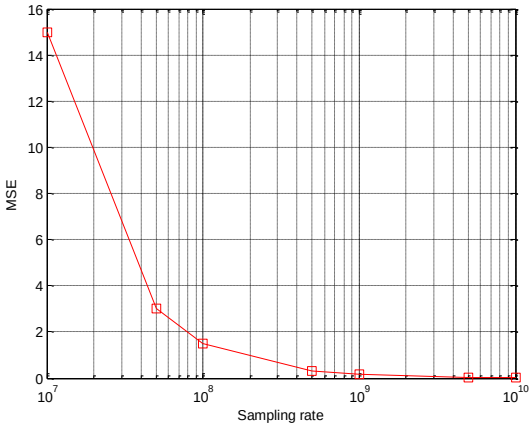

Figure 4.23 For the first set: mean squared error curve of the distance for the case B

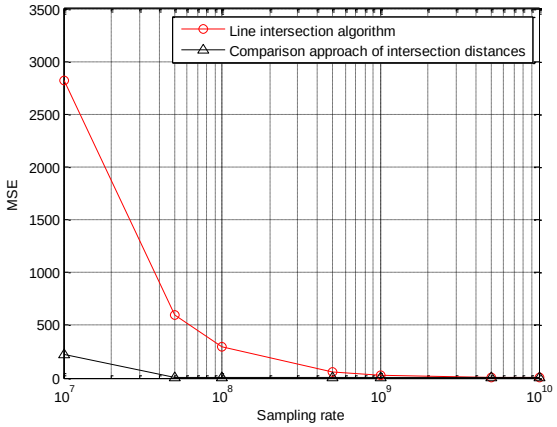

Figure 4.24 For the first set: mean squared error curves of the estimated mobile station position based on the comparison approach of intersection distances and the line intersection algorithm for the case A

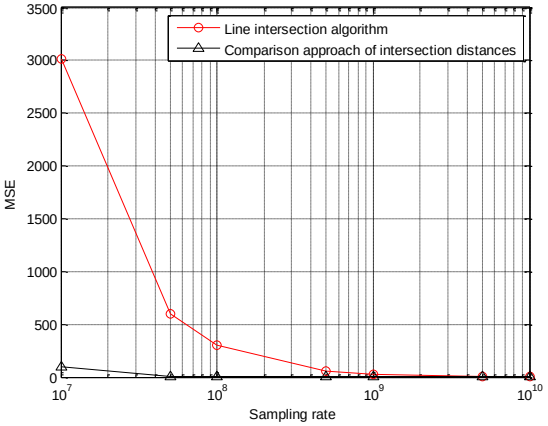

Figure 4.25 For the first set: mean squared error curves of the estimated mobile station position based on the comparison approach of intersection distances and the line intersection algorithm for the case B

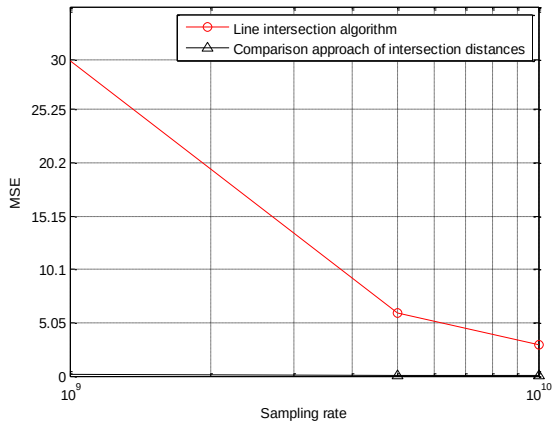

Figure 4.26 For the first set: the enlarged version of mean squared error curves of the estimated mobile station position based on the comparison approach of intersection distances and the line intersection algorithm for the case A, in the sampling rate of 1 GHz to 10 GHz

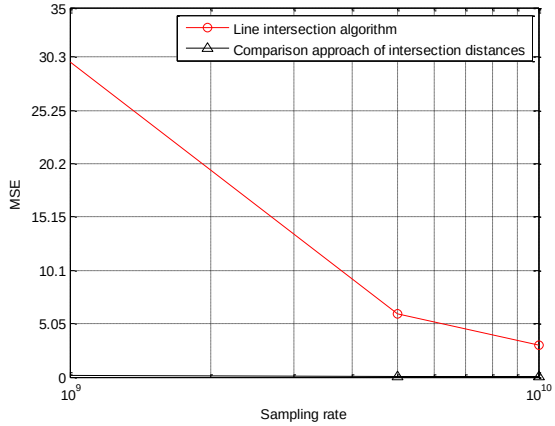

Figure 4.27 For the first set: the enlarged version of mean squared error curves of the estimated mobile station position based on the comparison approach of intersection distances and the line intersection algorithm for the case B, in the sampling rate from 1 GHz to 10 GHz

4.4.1.3.2 Simulation Results for the Second Set

Based on the second set of BSs, the simulation results of the distance MSE versus various sampling rates are shown in Figure 4.28 and Figure 4.29, for the case A and case B,

respectively. From figures, I observe that the distance MSE is decreased like the results of the first set, as the sampling rate is increased. Similar to the first set, the comparisons of MSEs for the estimated locations, based on the comparison approach of intersection distances and the line intersection algorithm is presented in Figure 4.30 and Figure 4.31 for the case A and case B, respectively. From figures, I observe that the MSE curves of the comparison approach of intersection distances are lower than that of the line intersection algorithm and the location MSE is decreased as the sampling rate is increased in both cases. Figure 4.32 and Figure 4.33 show the enlarged versions of Figure 4.30 and Figure 4.31, respectively, in the range from 1 GHz to 10 GHz. These results are similar to them of the first set.

Through the simulation results, I observe that the comparison approach of intersection distances has better performance for the location estimation of MS than that of the line intersection algorithm for this specific case of that a small circle is located in two large circles, for all cases.

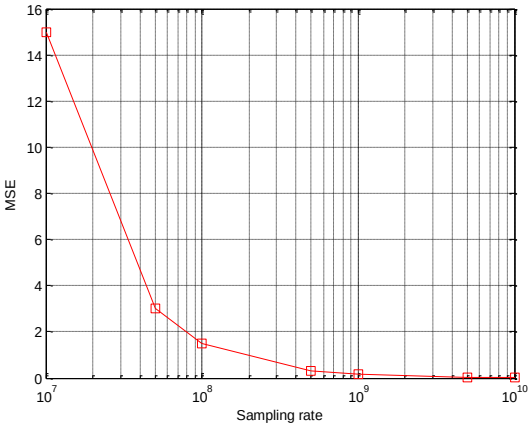

Figure 4.28 For the second set: mean squared error curve of the distance for the case A

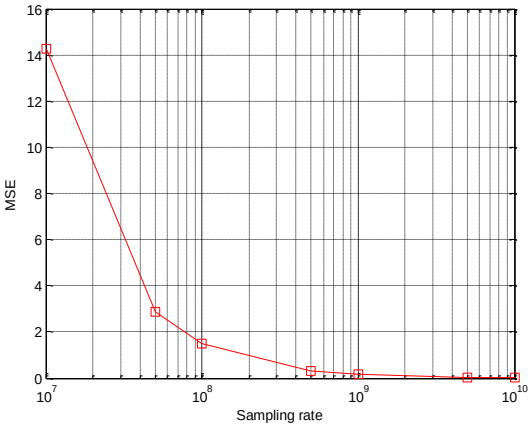

Figure 4.29 For the second set: mean squared error curve of the distance for the case B

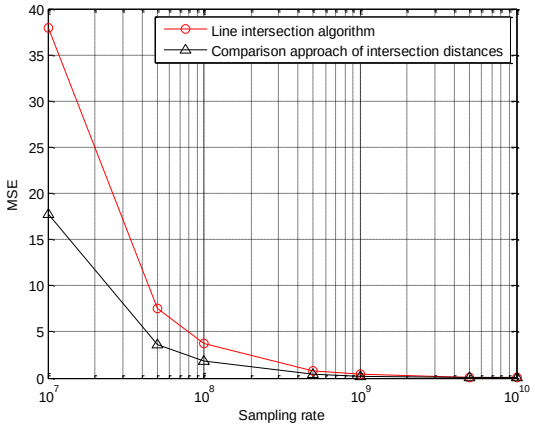

Figure 4.30 For the second set: mean squared error curves of the estimated mobile station position based on the comparison approach of intersection distances and the line intersection algorithm for the case A

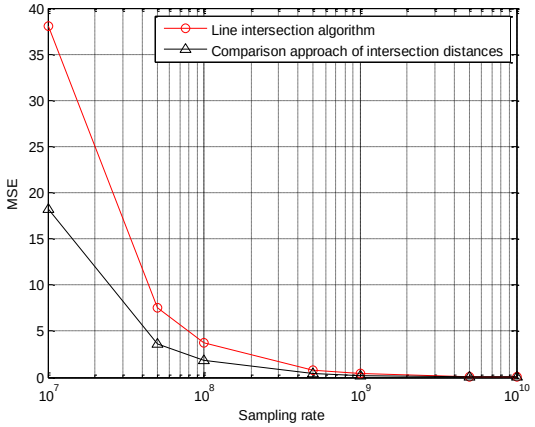

Figure 4.31 For the second set: mean squared error curves of the estimated mobile station position based on the comparison approach of intersection distances and the line intersection algorithm for the case B

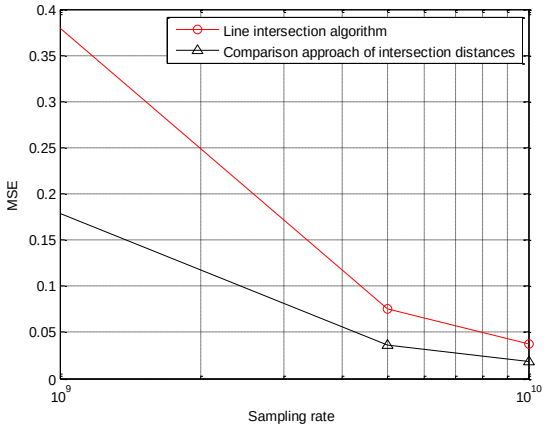

Figure 4.32 For the second set: the enlarged version of mean squared error curves of the estimated mobile station position based on the comparison approach of intersection distances and the line intersection algorithm for the case A, in the sampling rate of 1 GHz to 10 GHz

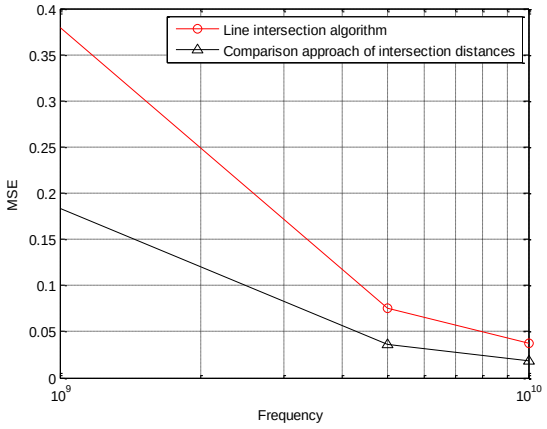

Figure 4.33 For the second set: the enlarged version of mean squared error curves of the estimated mean squared error position based on the comparison approach of intersection distances and the line intersection algorithm for the case B, in the sampling rate from 1 GHz to 10 GHz

4.5 Small Circle Intersection Approach for Case 3

For Case 3, where there are four intersection points based on three extended circles and a small circle has two intersection points with one large circle, I propose the small circle intersection approach. This algorithm calculates four distances between two intersection points for a small circle and two intersection points with two large circles, and determines a point to the small circle intersection point corresponding the shortest distances among four distances.

In detail, a small circle $C2$ intersects a large circle $C3$ at point 3 and point 4 in Figure 4.34. Also, the two large circles $C1$ and $C3$ intersect at point 1 and point 2. I calculate four distances, between four intersection points of circles, and the distance equation is given by

$$d_{lk} = \sqrt{(x_l - \alpha_k)^2 + (y_l - \beta_k)^2}, \quad \text{for } l = 1,\ 2, \text{ and } k = 1,\ 2 \tag{4.45}$$

where (x_l, y_l) is the coordinate of the intersection point of a small circle $(C2)$ with one of the large circles and (α_k, β_k) is the coordinate of the intersection point of the two large circles $(C1, \text{ and } C3)$. I compare these four distances, determine shortest distance and select an intersection point to the small circle intersection point (x_l, y_l) corresponding to the selected shorter distance as the estimated MS location. This approach is summarized in Table 4.4.

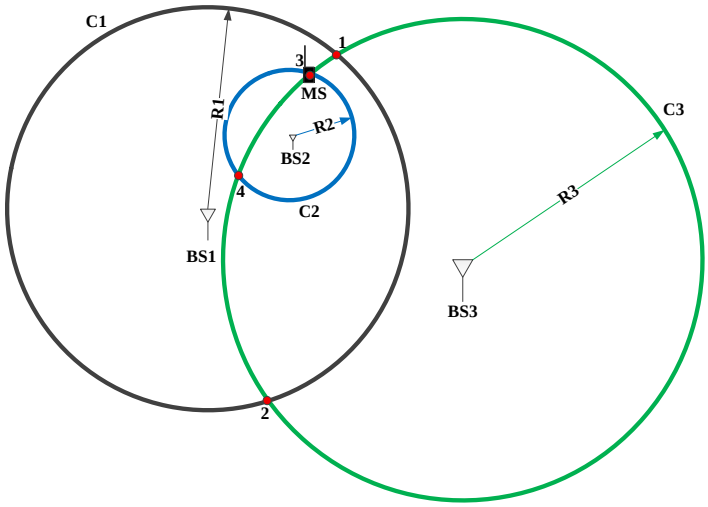

Figure 4.34 Case 3 where three circles do not meet at a single point, for the localization environment

Table 4.4 Small circle intersection approach

1. Calculate four distances,

$$d_{lk} = \sqrt{\left(x_l - \alpha_k\right)^2 + \left(y_l - \beta_k\right)^2}, \quad \text{for } l = 1,\ 2, \text{ and } k = 1,\ 2,$$

where (x_l, y_l) is the coordinate of the intersection point of a small circle $(C2)$ with one of the large circles and (α_k, β_k) is the coordinate of the intersection point of the two large circles $(C1, \text{ and } C3)$.

2. Compare four distances, and select the shortest distance.
3. Determine an intersection point (x_l, y_l) of the small circle $(C2)$ corresponding to the shortest distance as the estimated MS location.

4.6 Closest Point Algorithm for Case 4

For Case 4, there are two intersection points of two large circles and a small circle lies completely inside the overlapping area of two large circles, as shown in Figure 4.35. The closest point algorithm determines the MS location as the closest point on the small circle circumference to the intersection point corresponding to the shorter distance between the center of a small circle and two intersection points of the two large circles.

In this algorithm, I determine two intersection points of the two large circles, $C1$ and $C3$. First, I calculate the distances between the center of the small circle $(C2)$ and two intersection points of the two large circles, $C1$, and $C3$. These distances are given by $d_{2i1} = \sqrt{(x_2 - x_{i1})^2 + (y_2 - y_{i1})^2}$, and $d_{2i2} = \sqrt{(x_2 - x_{i2})^2 + (y_2 - y_{i2})^2}$. I compare these two distances. I select the intersection point $\left[(x_{iK}, y_{iK}); \text{ for } K = 1 \text{ or } 2\right]$ corresponding to the shorter distance. Thus, this algorithm determines the estimated MS location as the closest point $(\hat{x}_C, \hat{y}_C)$ on the small circle $C2$ edge from the selected intersection points, which is calculated by

$$\hat{x}_C = x_2 + R_2 \frac{(x_{iK} - x_2)}{\sqrt{(x_{iK} - x_2)^2 + (y_{iK} - y_2)^2}}, \quad \text{and} \quad \hat{y}_C = y_2 + R_2 \frac{(y_{iK} - y_2)}{\sqrt{(x_{iK} - x_2)^2 + (y_{iK} - y_2)^2}}. \tag{4.46}$$

This algorithm is summarized in Table 4.5. The flow chart for the closest point algorithm is shown in Figure 4.36.

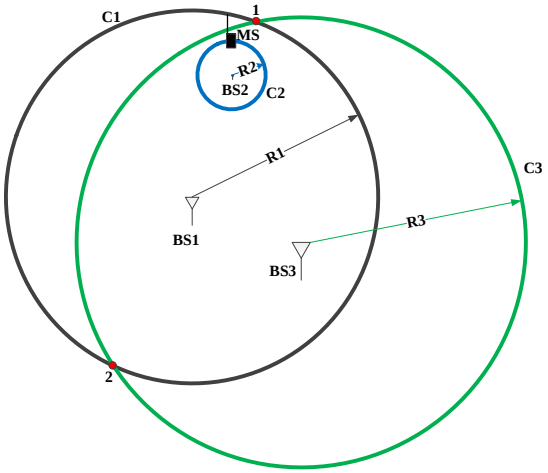

Figure 4.35 Case 4 where three circles do not meet at a single point, for the localization environment

Table 4.5 Closest point algorithm

1. Calculate distances between the center of the small circle $C2$ and the intersection point of large circles, $C1$ and $C3$

$$d_{2i1} = \sqrt{(x_2 - x_{i1})^2 + (y_2 - y_{i1})^2} \text{ , and } d_{2i2} = \sqrt{(x_2 - x_{i2})^2 + (y_2 - y_{i2})^2} \text{ .}$$

2. Compare two distances $(d_{2i1}, \text{and } d_{2i2})$ and select the intersection point $\left[(x_{iK}, y_{iK}); \text{ for } K = 1 \text{ or } 2\right]$ corresponding to the shorter distance.

3. The estimated MS location as the closest point $(\hat{x}_C, \hat{y}_C)$ on the small circle $(C2)$ is given by

$$\hat{x}_C = x_2 + R_2 \frac{(x_{iK} - x_2)}{\sqrt{(x_{iK} - x_2)^2 + (y_{iK} - y_2)^2}}, \text{ and } \hat{y}_C = y_2 + R_2 \frac{(y_{iK} - y_2)}{\sqrt{(x_{iK} - x_2)^2 + (y_{iK} - y_2)^2}} \text{ .}$$

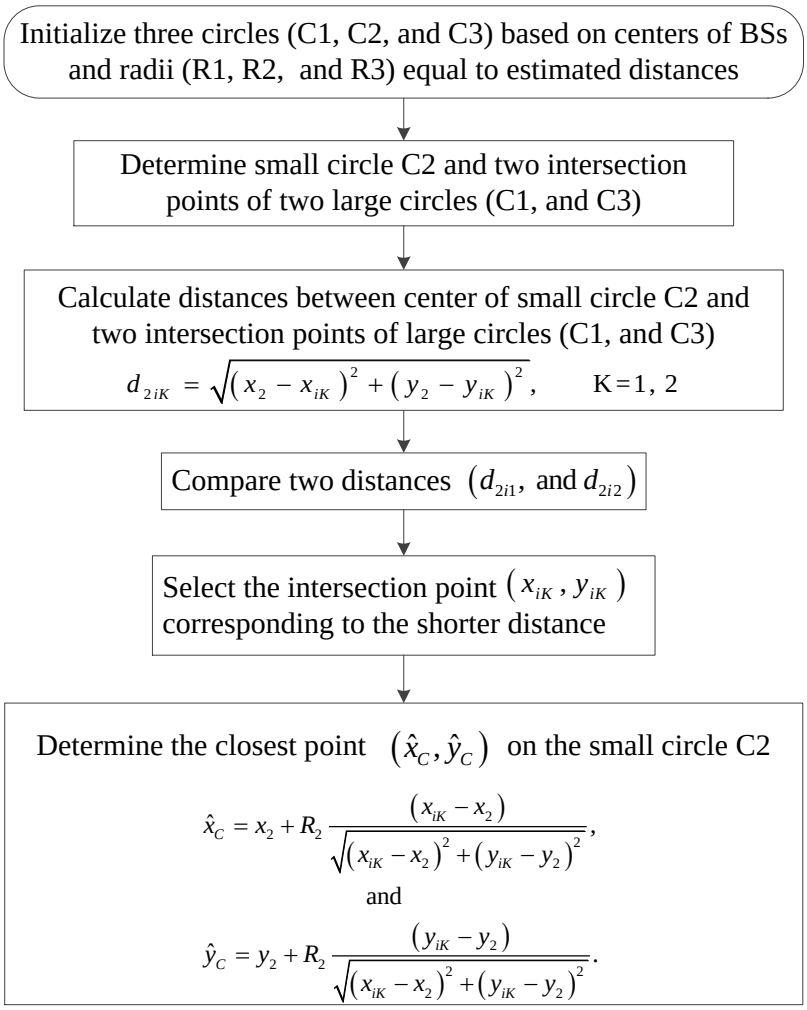

Figure 4.36 Flow chart for closest point algorithm

4.7 Concluding Remarks

The TOA trilateration method for estimating the MS location is determined by an intersection point of three circles based on centers corresponding to coordinates of three BSs and radii corresponding to distances between MS and three BSs. There may exist a serious estimation error for the MS location when the estimated radii of circles are increased and they do not meet at a point. In order to solve the MS location error, the advanced TOA trilateration algorithms are proposed. They are the shortest distance algorithm and the line intersection algorithm in case 1, the comparison approach of intersection distances in the case 2, the small circle intersection approach in the case 3, and the closest point algorithm in case 3, respectively.

5 Hybrid and Mode Selection Time of Arrival Trilateration Algorithms

5.1 Introduction

The time-of-arrival (TOA) trilateration estimates the location of the mobile station (MS) using an intersection point of three circles based on distances (radii) between MS and at least three base stations (BS) and coordinates (centers) of BSs [80, 113]. Since the distance between MS and BS is generally estimated by the number of delay samples and it is an integer number, the radius of the circle is usually increased and three circles may not meet at a point, which results in the serious estimation error. In order to overcome this problem, the shortest distance and the line intersection algorithms for the general case and the comparison approach of intersection distances for the specific case have been recently proposed. In this chapter, I provide the selection methodology between these two cases for using the line intersection algorithm or the comparison approach of intersection distances, for the MS location estimation. The selection procedure for both cases is based on comparing the radii of the two large circles to distances between four intersection points of a small circle with others and center coordinates of corresponding large circles [114]. Also, for the best performance of the location estimation, the proposed algorithms should be employed with a hybrid form that is the hybrid approach based on the line intersection algorithm for the general case and the comparison approach of intersection distances for the specific case.

In addition, I provide the mode selection for distinguishing four cases. The selection procedure for four cases is based on comparing radii difference between the smallest circle and two large circles to center distances between the smallest circle and the two large circles. I should select the best algorithm according to four different cases for the optimized performance. In this chapter, I also proposed the overall selection mode between four different cases based on comparing radii difference between the small circle and two large circles with that of center distances between small circle and two large circles. For the proposed method, I calculate the distance between the center of the small circle and one of the large circles and also, calculate the radius difference between the small circle and one of the large circles. I repeat the center distance and radius difference calculations for another large circle. This algorithm compares two center distances to the two radii difference. Either center distance is greater than radii difference between the small circle and one of the large circles or center distance is greater than radii differences between the small circle and another large circle. If this condition is satisfied, it selects the mode selection algorithm between case 1 and case 2 and distinguishes between the general case and specific case. It applies the line intersection algorithm in case 1 and comparison approach of intersection distances in case 2. If both two center distances are less than two radii differences between small circle and the large circles, it selects case 4 and identifies that small circle completely lies inside the overlapping area of the two large circles. If the center distance is greater than radii differences between small circle and one of the large circles and other center distance is less than radii differences between small circle and another large circle, it selects case 3. It identifies that small circle lies inside the one of the large circle, but not completely lie inside another large circle, and implements the closest point algorithm.

5.2 Advanced Time of Arrival Trilateration Algorithms

In this section, I present the advanced TOA trilateration algorithms in four cases to solve the problem for the MS location estimation, caused by the unmatched intersection point of three circles.

5.2.1 Line Intersection Algorithm for Case 1

In the general case, the true location of MS, based on the ideal TOA trilateration approach, is shown in Figure 5.1. Since the estimated distance between MS and BS is generally increased compared to the original distance, three circles based on the estimated distances may not meet at a single point, causing the serious estimation error for the MS location. In order to solve this problem, I consider the line intersection algorithm [111] for the enhanced TOA trilateration, which estimates the MS location using the intersection point of three intersection lines connecting two intersection points of specific two circles. Three intersection lines must meet at a point and this single intersection point becomes the estimated location of MS as shown in Figure 5.2. In the general case (case 1), the line intersection algorithm has the excellent estimation performance for the MS location comparing to the shortest distance algorithm, because it considers the increasing factor of the estimated circles.

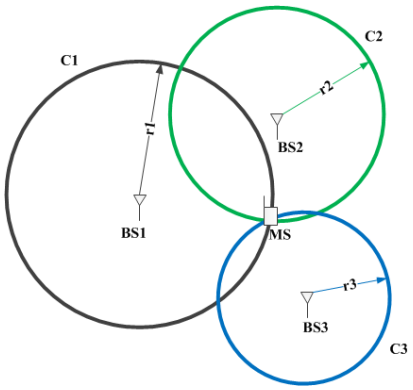

Figure 5.1 The mobile station location estimation based on the ideal time of arrival trilateration in the general case

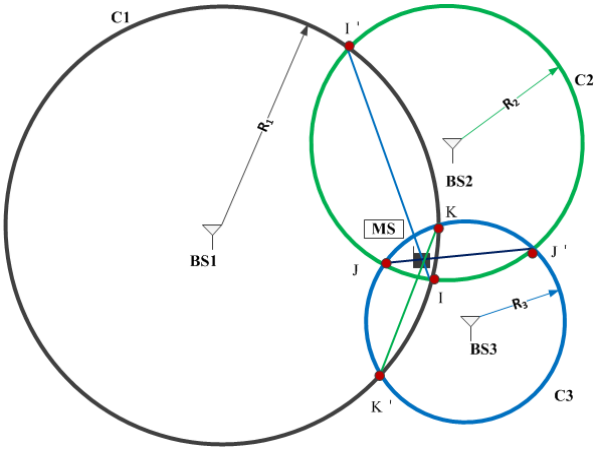

Figure 5.2 Concept of the line intersection algorithm

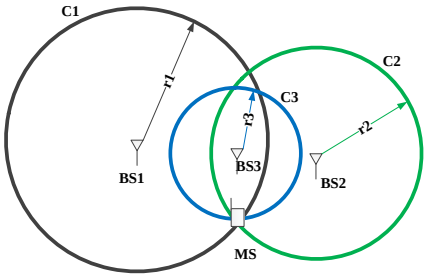

Figure 5.3 The mobile station location based on the ideal time of arrival trilateration in the specific case

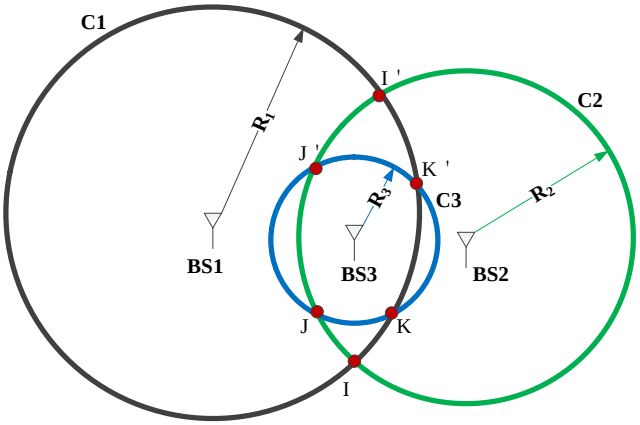

Figure 5.4 Concept of the comparison approach of intersection distances in the specific case

5.2.2 Comparison Approach of Intersection Distances for Case 2

As I mentioned earlier, in the specific case, a small circle is located inside the area of two large circles, as shown in Figure 5.3. Although the line intersection algorithm has the excellent performance in the case 1 (general case), it does not have the good estimation performance in the case 2 (specific case) for estimating the MS location. In order to improve the estimation performance for the MS location in the specific case, I employ the comparison approach of intersection distances [115]. This algorithm focuses on comparing distances between two neighboring points of four interior intersections related to a small circle, among six entire intersection points, shown in Figure 5.4. Two distances are calculated from two intersecting points of the small circle with one large circle to the neighboring intersection points of the small circle with another large circle. After calculating two distances, I compare them and select the shorter distance. Finally, this approach determines the averaged coordinate of two intersection points corresponding to the shorter distance as the estimated MS location. Although the comparison approach of intersection distances does not have the good

performance for estimating the MS location in the general case, it has the good estimation performance comparing to the line intersection algorithm in the specific case.

5.2.3 Small Circle Intersection Approach for Case 3

For Case 3, where there are four intersection points based on three extended circles and a small circle has two intersection points with one large circle, I propose the small circle intersection approach. It calculates four distances between two intersection points for a small circle and two intersection points with two large circles, and determines MS location to a point to the small circle intersection point corresponding the shortest distances among four distances.

5.2.4 Closest Point Algorithm for Case 4

For Case 4, there are two intersection points of two large circles and a small circle lies completely inside the overlapping area of two large circles. The closest point algorithm determines the MS location as the closest point on the small circle circumference to the intersection point corresponding to the shorter distance between the center of a small circle and two intersection points of the two large circles.

5.3 Performance Analysis between Two Advanced TOA Trilateration Algorithms

In the general case, it is clear that the location estimation performance of the line intersection algorithm is better than that of the comparison approach of intersection distances, observed from Figure 5.2 and Figure 5.4. In this section, I show that the comparison approach of intersection distances has better estimation performance than the line intersection algorithm, in the specific case.

Based on true distances between MS and BSs, three circles meet at a single point, and results of the line intersection algorithm and the comparison approach of intersection distances should be the same as the single intersection point. Also, the considered two intersection points in Figure 5.2 and Figure 5.4, J and K, meet at the same single point. However, as the estimated distances are increased from original distances, the true position of MS, the estimated results of both algorithms, and two intersection points, J and K, do not meet at the same point. Two intersection points, J and K, and the estimated MS position of the line intersection algorithm form a triangle as shown in Figure 5.5, instead of meeting at the same point. The estimated MS position based on the comparison approach of intersection distances is located in the center of a line connecting J and K, as shown in Figure 5.6. From the figure, I observe that the distance between the true position of MS and the estimated position based on the line intersection algorithm is much longer than the distance between the true position of MS and the estimated position based on the comparison approach of intersection distances. In other words, the performance for estimating the MS location of the comparison approach of intersection distances is better than that of the line intersection algorithm, in the specific case where a small circle is located in the area of the two large circles.

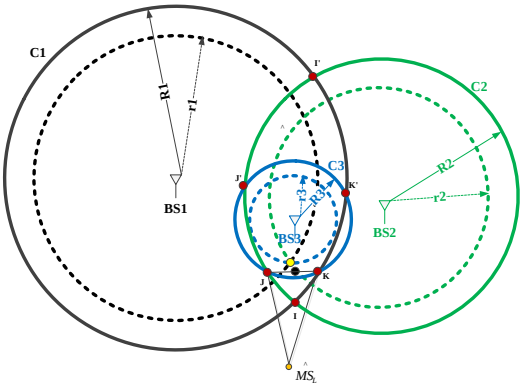

Figure 5.5 Comparison of the original circles and the extended circles

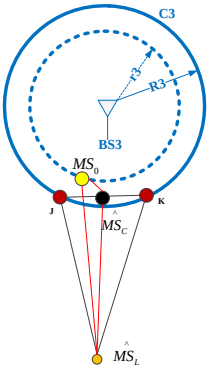

Figure 5.6 Enlarged version focusing on the small circle

Figure 5.7 Triangle formed by the three points of the original mobile station location and the estimated two locations of the advanced time of arrival trilateration algorithms

The comparison approach of intersection distances selects the coordinates of intersection points, J and K, corresponding to the shorter distance. In Figure 5.5, two lines connecting two intersection points, J and J', and connecting two intersection points, K and K', obtained from the line intersection algorithm must pass the intersection points J and K, respectively, selected by the comparison approach of intersection distances.

The line equation formed by connecting the original MS location, (x_0, y_0), and the estimated MS location, $(\hat{x}_L, \hat{y}_L)$, of the line intersection algorithm is given by

$$(y - y_0)(\hat{x}_L - x_0) - (x - x_0)(\hat{y}_L - y_0) = 0 \tag{5.1}$$

In order to compare the performances of both algorithms, I need to consider two cases:

Case 1: three points based on the original MS location and the MS locations estimated by two algorithms are placed in a line.

Case 2: three points of them are not placed in a line.

For the Case 1, it is easy to show that the performance of the comparison approach of intersection distances is better than that of the line intersection algorithm, in the specific case, because the distance between the original MS location and the estimated MS location by the comparison approach of intersection distances is much shorter than the distance between the original MS location and the estimated MS location by the line intersection algorithm (Note that the $(\hat{x}_C, \hat{y}_C)$ is located between (x_0, y_0) and $(\hat{x}_L, \hat{y}_L)$ in a line). For the Case 2, substituting $(\hat{x}_C, \hat{y}_C)$ into variables in the left side of (5.1), I get

$$(\hat{y}_C - y_0)(\hat{x}_L - x_0) - (\hat{y}_L - y_0)(\hat{x}_C - x_0) \neq 0, \tag{5.2}$$

because $(\hat{x}_C, \hat{y}_C)$ is not located in the line connecting the original MS location and the estimated MS location based on the line intersection algorithm. Therefore, three points of (x_0, y_0), $(\hat{x}_C, \hat{y}_C)$ and $(\hat{x}_L, \hat{y}_L)$ form a triangle in Case 2, as shown in Figure 5.6. In Figure 5.7, I set (x_0, y_0), $(\hat{x}_L, \hat{y}_L)$ and $(\hat{x}_C, \hat{y}_C)$ to O, L, and C, respectively, and consider an auxiliary point, M, where the length between O and M is the same as the length between O and C. In general, the length of OM is shorter than OL, because it is included in the line of OL. From this result, the length of OC is generally shorter than the length of OL. In other words, the performance of the comparison approach of intersection distances is better than that for the line intersection algorithm for Case 2 [116].

5.3.1 Computer Simulations

In this section, I provide computer simulation scenarios with the simulation results to illustrate the MS location estimation performance.

5.3.1.1 Simulation Scenario Parameters

In this section, the performances of estimating the MS location for the advanced TOA trilateration algorithms such as the line intersection algorithm and the comparison approach of intersection distances are provided and compared in the specific case, through computer

simulation examples. For the simulation scenario, I assume that there are three fixed BSs with coordinates of (-1000, 4000), (1000, 2000), and (5000, 700), respectively. The unit of the coordinate is in meter (m), and various sampling rates are considered such as 10 MHz, 50 MHz, 100 MHz, 500 MHz, 1 GHz, 5 GHz, and 10 GHz. I also assume that coordinates of the MS location are randomly chosen within ranges from -100 m to +100 m and from -1000 m to +1000 m for the case A and the case B, respectively.

5.3.1.2 Simulation Results

The simulation results for estimating the MS location for the case A and case B are shown in Figure 5.8 and Figure 5.9, respectively. From the figures, I observe that the comparison approach of intersection distances has lower MSEs comparing to MSEs for the line intersection algorithm, in the specific case. Therefore, the location estimation performance of the comparison approach of intersection distances is better than that of the line intersection algorithm, in the specific case, although the performance of the line intersection algorithm is better than that of the comparison approach of intersection distances, in the general case. I, also, observe that the MSE curves for both algorithms are decreased as the sampling rates are increased for both cases.

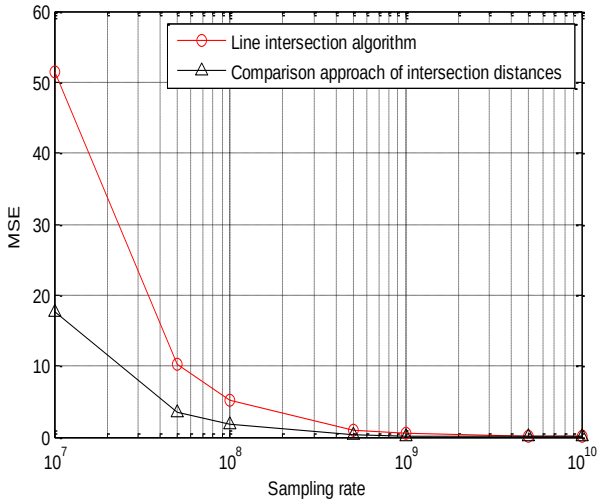

Figure 5.8 Mean squared error curves of the mobile station location estimation for the case A, in the specific case

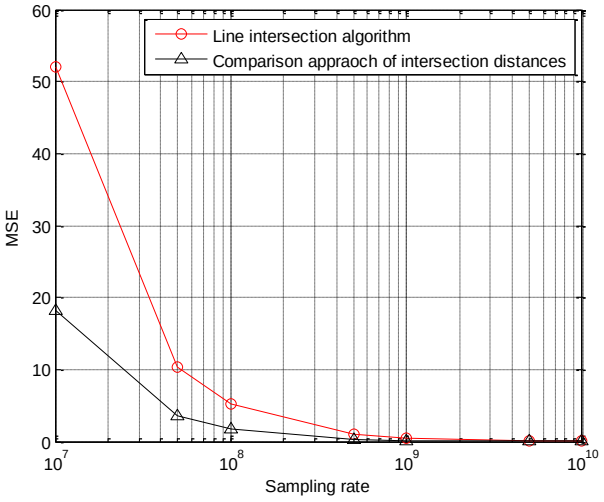

Figure 5.9 Mean squared error curves of the mobile location estimation for the case B, in the specific case

5.4 Mode Selection Algorithm for Case 1 and Case 2

For the optimized location estimation, I must select an algorithm between the line intersection algorithm and the comparison approach of intersection distances, according to the proper case. In this section, I propose the mode selection algorithm for distinguishing the general case and the specific case. If the algorithm selects the general case, the hybrid algorithm is operated to the mode for the line intersection algorithm. However, if it selects the specific case, the hybrid algorithm is operated to the mode for the comparison approach of intersection distances.

In order to correctly select the proper case, the proposed mode selection algorithm calculates four distances related to the centers of the two large circles and four intersection points of a small circle with two large circles. Each distance is calculated from the center of each large circle to the intersection of the small circle with another large circle, defined as

$$d_{lk} = \sqrt{(x_l - \alpha_k)^2 + (y_l - \beta_k)^2}, \quad \text{for } l = 1,\ 2, \text{ and } k = 1,\ 2 \tag{5.3}$$

where (x_l, y_l) is the coordinates of the center of the l th large circle and (α_k, β_k) is the coordinates of the k th intersection point of the small circle with another large circle. Next, the distances related to the l th large circle are compared to the radius of the l th large circle; d_{11} and d_{12} are compared to R_1, and d_{21} and d_{22} are compared to R_2. If all distances related to the l th large circle are shorter than the radius of the l th large circle (d_{11} and d_{12} are

shorter than R_1, and d_{21} and d_{22} are shorter than R_2), it selects the specific case mode and the hybrid algorithm is operated to the comparison approach of intersection distances. Otherwise, it selects the general case mode and the hybrid algorithm is operated to the line intersection algorithm.

Figure 5.10 shows the flow chart of the mode selection algorithm and Table 5.1 summarizes the detail steps of the mode selection algorithm. Using the proposed mode selection algorithm, I can alternatively employ both advanced TOA trilateration algorithms, according to the proper case between the general case and the specific case, with the optimized performance for estimating the MS location.

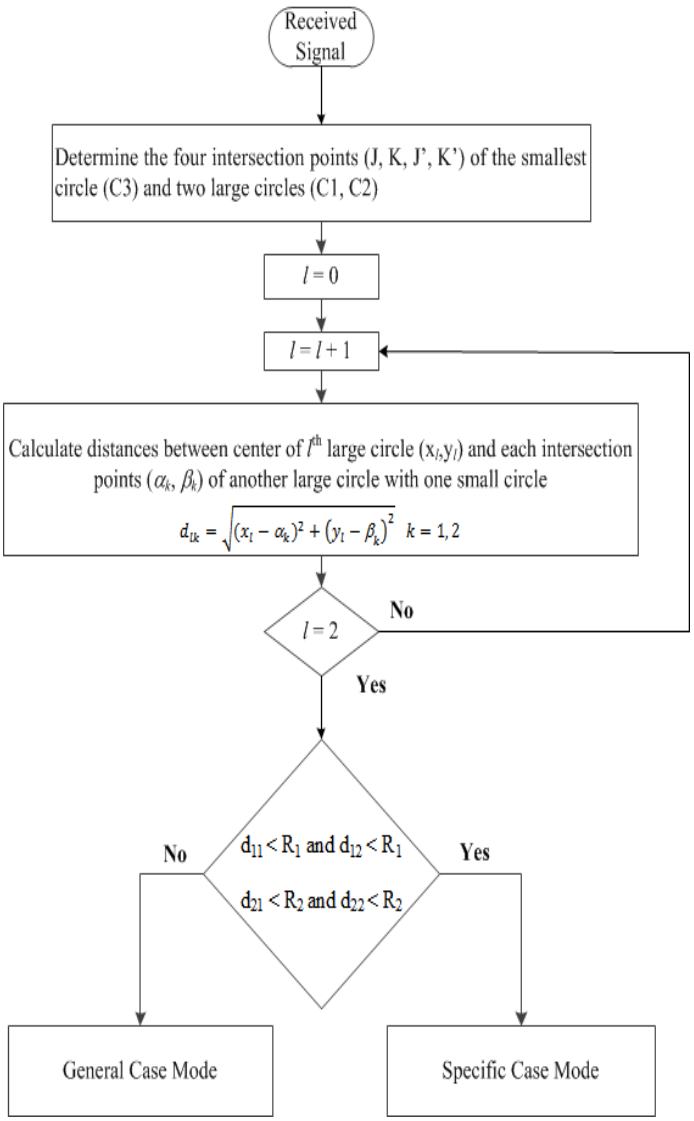

Figure 5.10 Flow chart of the mode selection algorithm between case 1 and case 2

Table 5.1 Mode selection algorithm between case 1 and case 2

1. Find the two intersection points (J, J') formed by the small circle $C3$ intersected with the large circle $C2$.
2. Calculate the distances from the center of the large circle $C1$ (x_1, y_1) to the two intersection points (J, J'), given by

$$d_{1k} = \sqrt{(x_1 - \alpha_k)^2 + (y_1 - \beta_k)^2}, \quad \text{for } k = 1, 2.$$

3. Find the two intersection points (K, K') formed by the small circle $C3$ intersected with the large circle $C1$.
4. Calculate the distances from the center of the large circle $C2$ (x_2, y_2) to the two intersection points (K, K'), given by

$$d_{2k} = \sqrt{(x_2 - \alpha_k)^2 + (y_2 - \beta_k)^2}, \quad \text{for } k = 1, 2.$$

5. Compare the increased radius of $C1$, R_1, to d_{11} and d_{12}.
6. Compare the increased radius of $C2$, R_2, to d_{21} and d_{22}.
7. a. $d_{11} < R_1$ and $d_{12} < R_1$, and $d_{21} < R_2$ and $d_{22} < R_2$

   ☞ Specific mode (employing comparison approach of intersection distances)

   b. Otherwise

   ☞ General mode (employing line intersection algorithm).

5.4.1 Computer Simulations

In this section, I provide computer simulation scenarios with the simulation results to illustrate the MS location estimation performance for the mode selection algorithm.

5.4.1.1 Simulation Scenario Parameters for Mode Selection Algorithm

For the simulation, I consider three fixed BSs and two cases for coordinates of BSs and MS for distinguishing between the general case and the specific case:

1. General case: three BSs with coordinates of (-1000, 5000), (6000, -3000), and (-7000, 600).
2. Specific case: three BSs with coordinates of (-3000, 5000), (1500, 3000), and (7000, 600).

The unit of the coordinate is a meter (m) and I consider the different sampling rate of 50 MHz, 100 MHz, 500 MHz, 1 GHz, 5 GHz, and 10 GHz. Also, I consider two scenarios for the occurrence possibility of the general case and the specific case:

1. First scenario: 90% general case and 10% specific case.
2. Second scenario: 95% general case and 5% specific case.

I assume that the MS location coordinate is randomly chosen with ranges from -100 to +100 and from -500 to +500 for the case A and the case B, respectively.

5.4.1.2 Simulation Results for Mode Selection Algorithm

The simulation results of the MSE for the MS location estimation versus various sampling rates for the first scenario are shown in Figure 5.11 and Figure 5.12, for the case A and case B, respectively. In addition, the simulation results of the MSE for the MS location estimation versus various sampling rates in the second scenario are shown in Figure 5.13 and Figure 5.14, for the case A and case B, respectively. From figures, I observe that the MSE of the advanced TOA trilateration based on the mode selection algorithm is lower than the MSE of that based

on only the line intersection algorithm. Note that the difference between two curves for the first scenario is larger than the difference for the second scenario because the occurrence possibility of the specific case in the first scenario is higher than it in the second scenario.

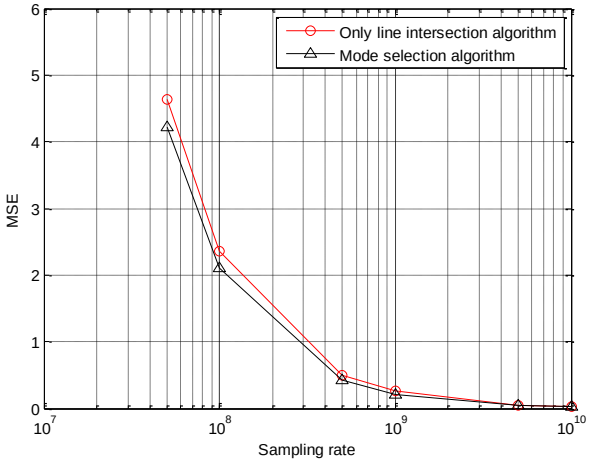

Figure 5.11 Mean squared error curves for the first scenario for the case A

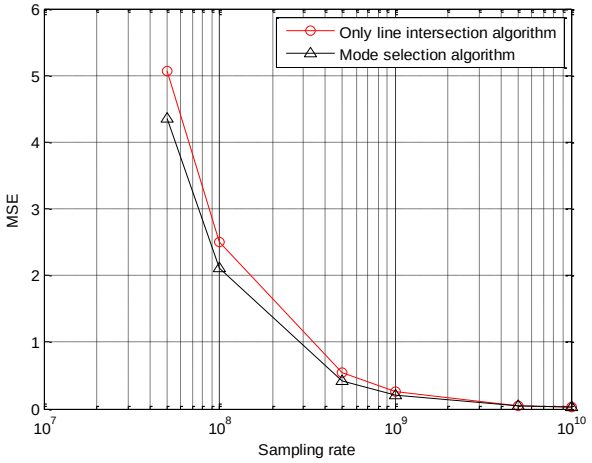

Figure 5.12 Mean squared error curves for the first scenario for the case B

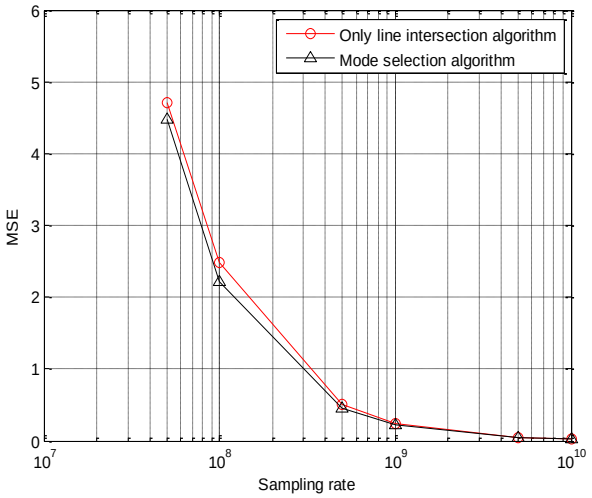

Figure 5.13 Mean squared error curves for the second scenario for the case A

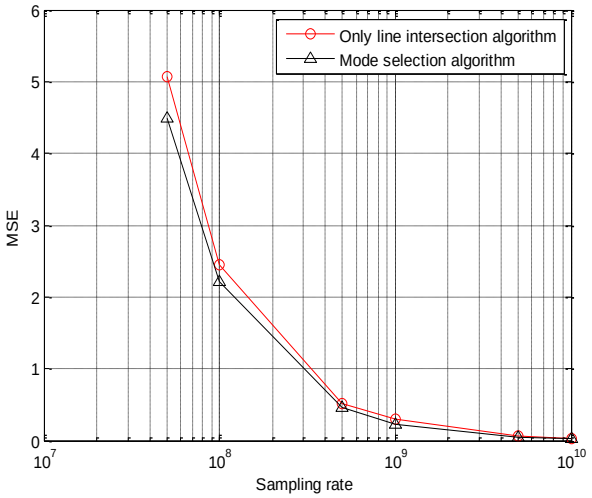

Figure 5.14 Mean squared error curves for the second scenario for the case B

5.5 Hybrid Approach Based on Advanced TOA Algorithms

In this section, we present a hybrid TOA trilateration algorithm based on the line intersection algorithm and the comparison approach on intersection distances.

The line intersection algorithm and the comparison approach of intersection distances have the excellent estimation performances for the general case and the specific case, respectively. For the best performance estimating the MS location, these two methods should be employed with a hybrid form, where it employs the line intersection algorithm for the general case and employs the comparison approach of intersection distances for the specific case. This hybrid TOA trilateration algorithm is summarized in Figure 5.15.

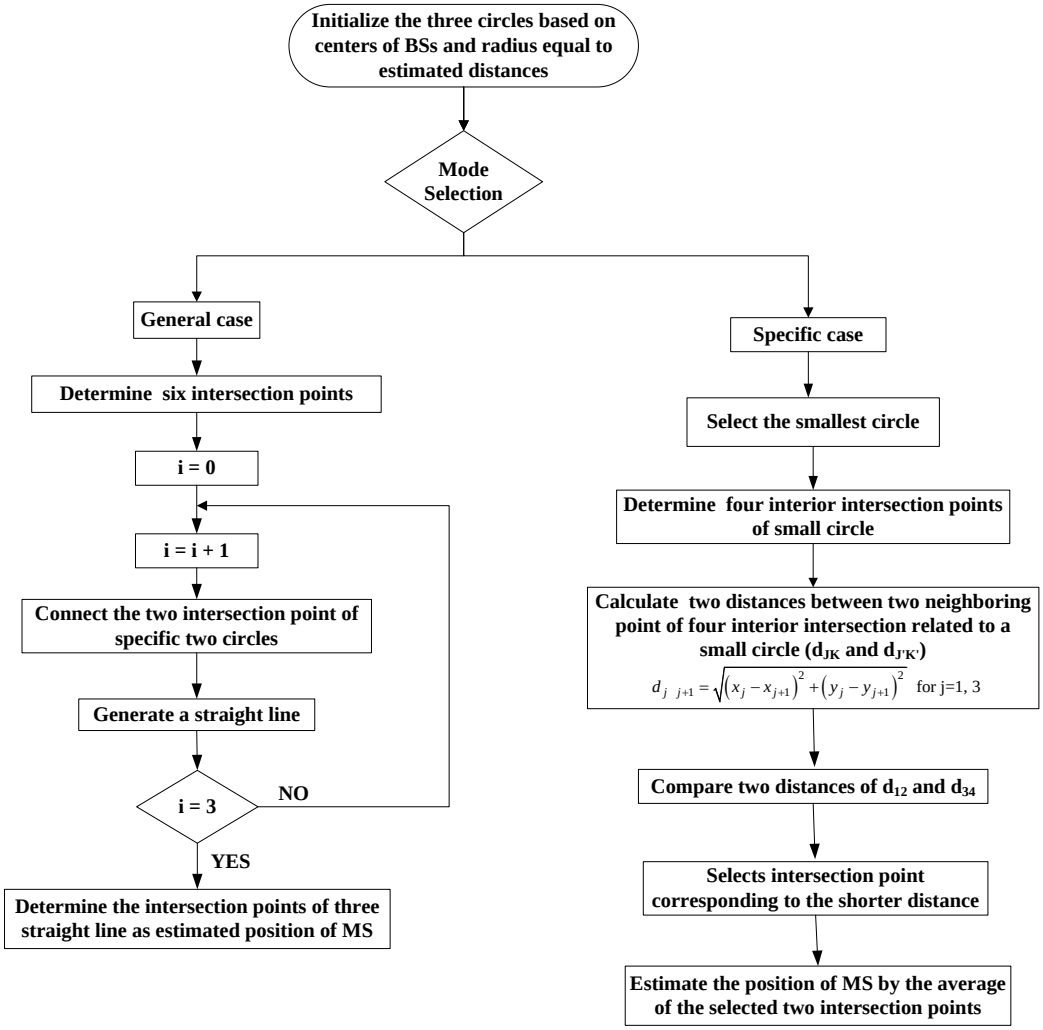

Figure 5.15 Flow chart of the hybrid algorithm based on the line intersection algorithm and the comparison approach of intersection distances

5.5.1 Computer Simulations

In this section, I provide computer simulation scenarios with the simulation results to illustrate the MS location estimation performance for the hybrid algorithm.

5.5.1.1 Simulation Scenario Parameters for Hybrid Algorithm

For the simulation scenario, I consider the three fixed BSs and one movable MS. The two different sets of coordinates of BSs are used to observe and to analyze the difference between conventional, hybrid and only line intersection algorithm. The two different sets of coordinates of BSs for the general case and the specific case are:

1. First set:

   General case: three BSs with coordinates of (-1000, 5000), (6000, -3000), and (-7000, 600).

   Specific case: three BSs with coordinates of (-1000, 4000), (1000, 2000), and (5000, 700).

2. Second set:

   General case: three BSs with coordinates of (-1000, 4500), (6000, -2000), and (-7000, 500).

   Specific case: three BSs with coordinates of (-1000, 5000), (1500, 3000), and (7000, 600).

The coordinates of the MS is randomly chosen within the ranges between -100 and +100 for the case A, -500 and +500 for the case B, and -1000 and +1000 for the case C, respectively. The unit of each coordinate is a meter (m) and I consider the different sampling rate of 10 MHz, 50 MHz, 100 MHz, 500 MHz, and 1 GHz. For two-dimensional (2D) space, I consider three scenarios of occurrence possibility of the general case and the specific case. They are:

1. First scenario: 90% general case and 10% specific case

2. Second scenario: 95% general case and 5% specific case

3. Third scenario: 99% general case and 1% specific case.

For three-dimensional (3D) space, I consider the different scenarios of occurrence possibility of the general case and the specific case that starts from 80% general case and 20% specific case to 100% general case and 0% specific case.

5.5.1.2 Simulation Results for Hybrid Algorithm

5.5.1.2.1 Simulation Results for the First Set

Based on the first set, the simulation result of the MSE of the estimated distance versus sampling rate in 2D space is shown in Figure 5.16, Figure 5.17, and Figure 5.18 for the case A, case B, and case C, respectively. The figures show the performance of the estimated distance based on the higher sampling rate is better than that of the lower sampling rate. The comparisons of MSE curves for estimated locations based on the hybrid algorithm and conventional algorithm of the averaged value of three nearest neighbor intersection points of the three estimated circles are shown in 2D space. The simulation result of the MSE of the MS location estimation versus sampling rate in 2D for the first scenario of occurrence possibility of 90% general case and 10% specific case is shown in Figure 5.19, Figure 5.20, and Figure 5.21, for the case A, case B, and case C, respectively. For the second scenario of occurrence possibility of 95% general case and 5% specific case, the simulation result of the MSE of the MS location estimation versus sampling rate in 2D is shown in Figure 5.22, Figure 5.23, and Figure 5.24, for the case A, case B, and case C, respectively. For the third scenario of occurrence possibility of 99% general case and 1% specific case, the simulation result of the

MSE of the MS location estimation versus sampling rate in 2D is shown in Figure 5.25, Figure 5.26, and Figure 5.27, for the case A, case B, and case C, respectively. The figures show that the hybrid algorithm is better than the conventional algorithm (the averaged value of three nearest neighbor intersection points of the three estimated circles). In addition, the simulation result of the MSE of the MS location estimation comparing between the hybrid algorithm and the only line intersection algorithm in 3D space is shown in Figure 5.28, Figure 5.29, and Figure 5.30, for the case A, case B, and case C, respectively. From figures, I observe that the MSE of the proposed hybrid algorithm is lower than the MSE of that based on only the line intersection algorithm. The difference between the two curves shows that the occurrence possibility of the specific case is higher at 80% than that at 100%.

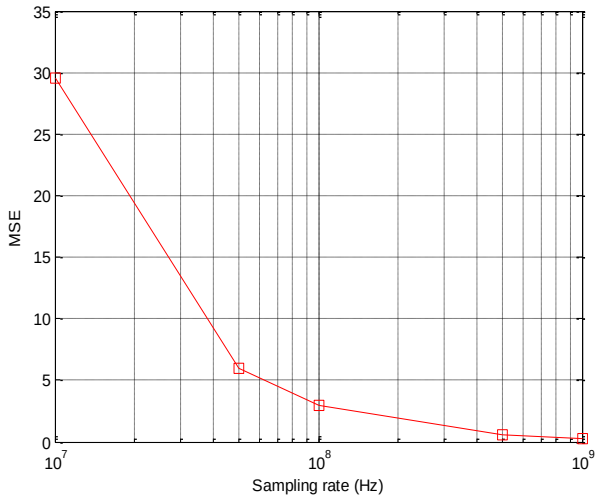

Figure 5.16 For the first set: mean squared error curve of the distance for the case A

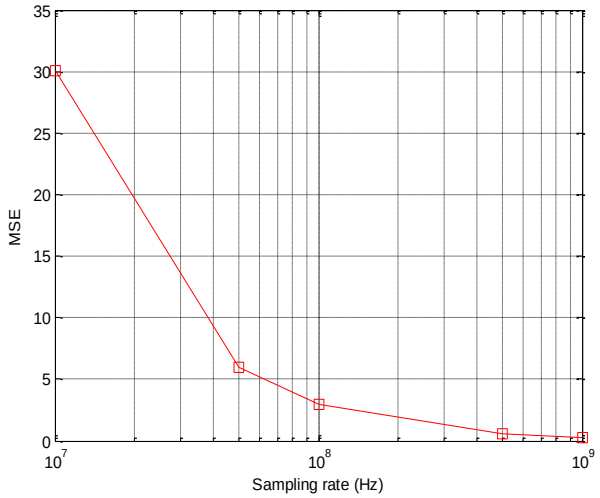

Figure 5.17 For the first set: mean squared error curve of the distance for the case B

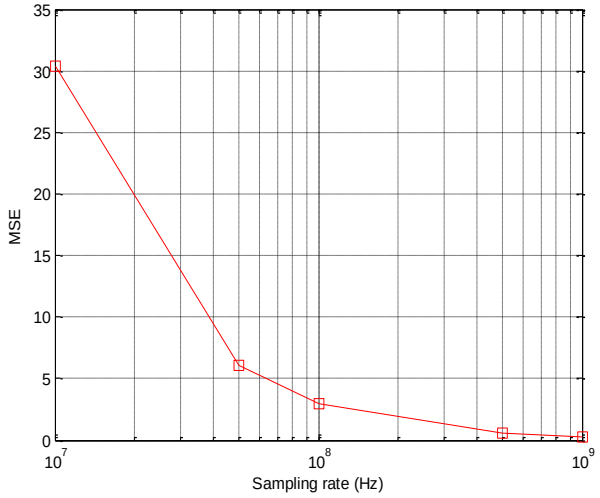

Figure 5.18 For the first set: mean squared error curve of the distance for the case C

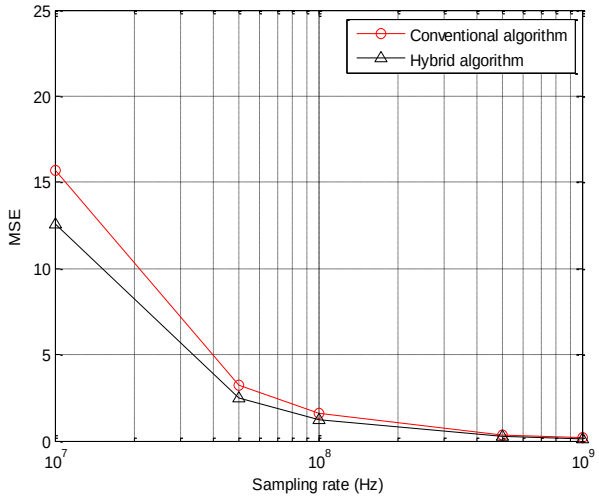

Figure 5.19 For the first set: mean squared error curves of the mobile station position in 2D for the first scenario for the case A

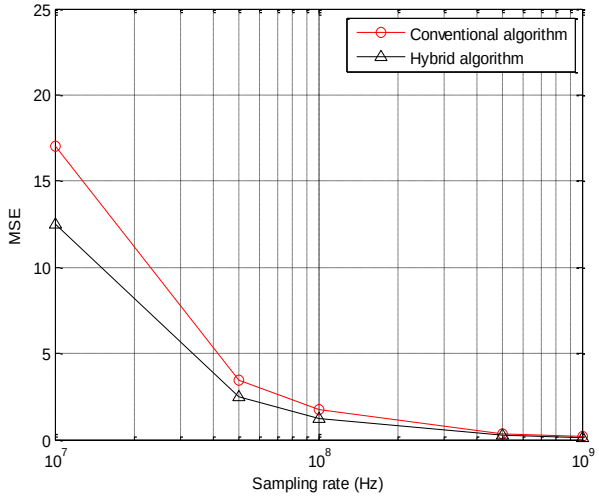

Figure 5.20 For the first set: mean squared error curves of the mobile station position in 2D for the first scenario for the case B

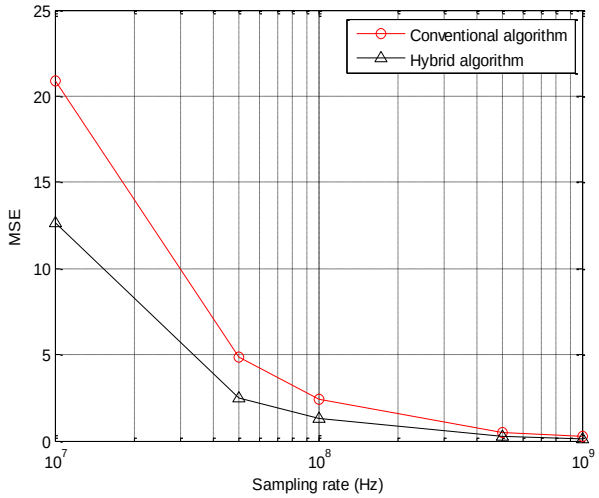

Figure 5.21 For the first set: mean squared error curves of the mobile station position in 2D for the first scenario for the case C

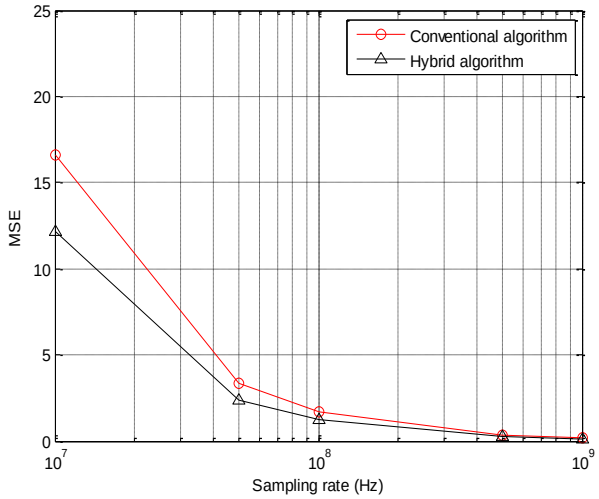

Figure 5.22 For the first set: mean squared error curves of the mobile station position in 2D for the second scenario for the case A

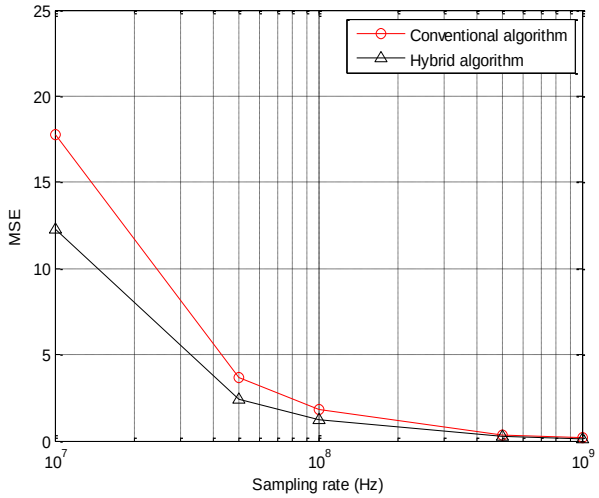

Figure 5.23 For the first set: mean squared error curves of the mobile station position in 2D for the second scenario for the case B

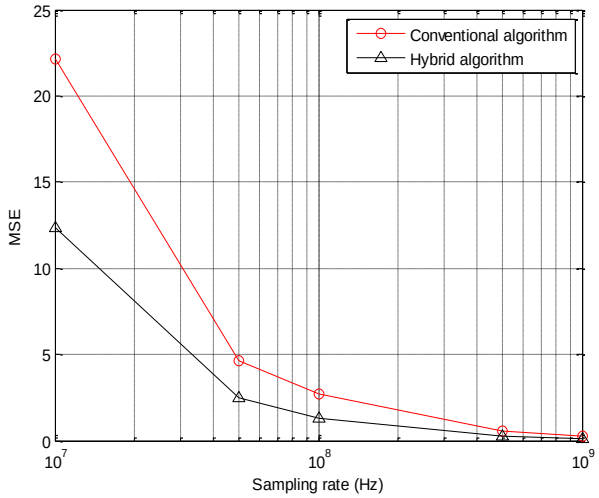

Figure 5.24 For the first set: mean squared error curves of the mobile station position in 2D for the second scenario for the case C

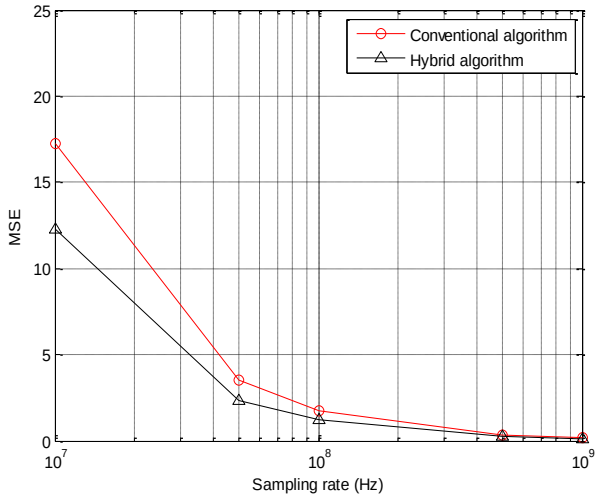

Figure 5.25 For the first set: mean squared error curves of the mobile station in 2D for the third scenario for the case A

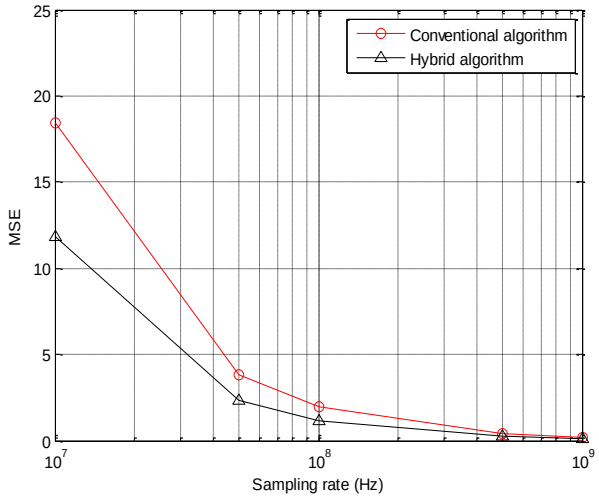

Figure 5.26 For the first set: mean squared error curves of the mobile station in 2D for the third scenario for the case B

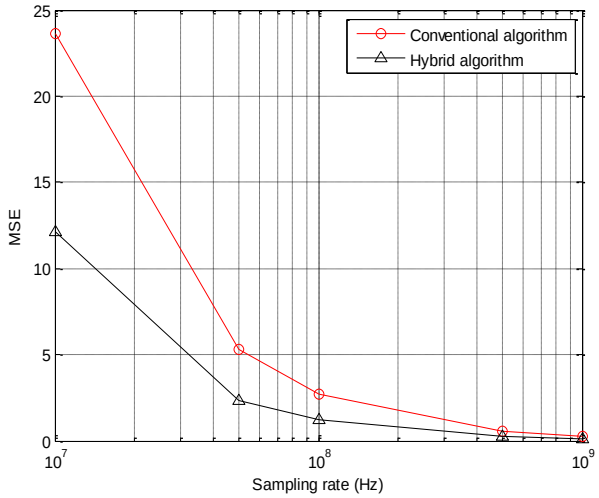

Figure 5.27 For the first set: mean squared error curves of the mobile station in 2D for the third scenario for the case C

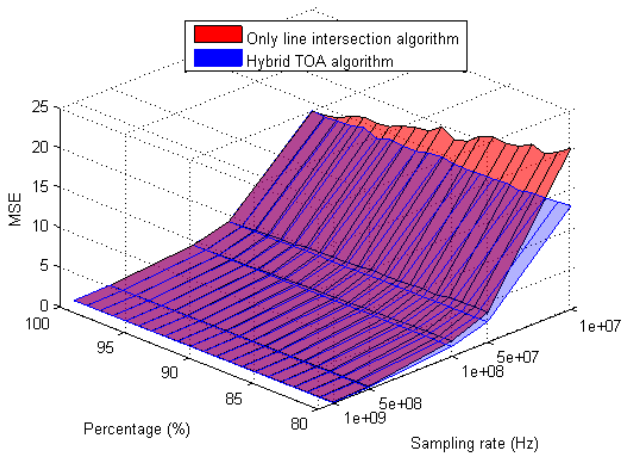

Figure 5.28 For the first set: mean squared error location curves in 3D for the case A

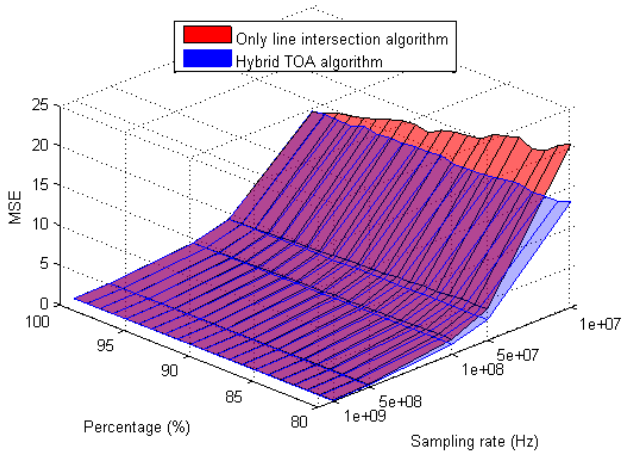

Figure 5.29 For the first set: mean squared error location curves in 3D for the case B

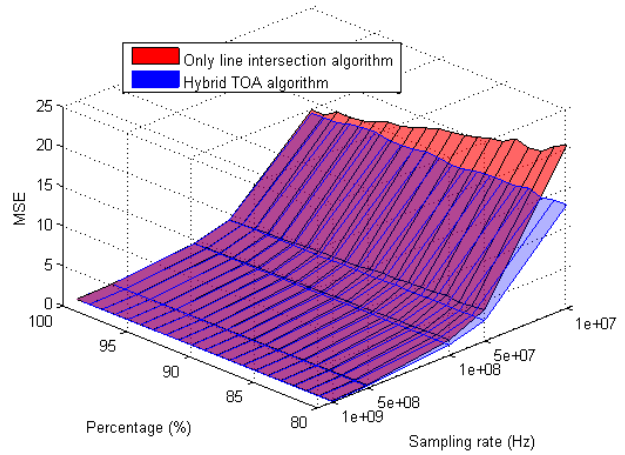

Figure 5.30 For the first set: mean squared error location curves in 3D for the case C

5.5.1.2.2 Simulation Results for the Second Set

Based on the second set, the simulation results of the MSE of the distance in 2D space is shown in Figure 5.31, Figure 5.32, and Figure 5.33, for the case A, case B, and case C, respectively. The figures show the performance of the distance based on the higher sampling

rate is better than that of the lower sampling rate. Similar to the first set, the comparison of MSEs for estimated locations based on the hybrid and conventional (average value of three nearest neighbor intersection points of the three estimated circles) algorithms for the first scenario of occurrence possibility of 90% general case and 10% specific case in 2D is shown in Figure 5.34, Figure 5.35, and Figure 5.36, for the case A, case B and case C, respectively. For the second scenario of occurrence possibility of 95% general case and 5% specific case, the simulation result of the MSE of the MS location estimation versus sampling rate in 2D is shown in Figure 5.37, Figure 5.38, and Figure 5.39, for the case A, case B, and case C, respectively. For the third scenario of occurrence possibility of 99% general case and 1% specific case, the simulation result of the MSE of the MS location estimation versus sampling rate in 2D is shown in Figure 5.40, Figure 5.41, and Figure 5.42, for the case A, case B, and case C, respectively. Figures show that the hybrid algorithm is better than the conventional algorithm, similar to the first set.

In addition, I observe there is a slightly big difference between the conventional and the hybrid algorithms in third cases of the MS ranges at the higher sampling rate comparing to the first set. The simulation result of the MSE of the MS location estimation in 3D space is shown in Figure 5.43, Figure 5.44, and Figure 5.45, for the case A, case B, and case C, respectively. From figures, I observe that the MSE curve of the advanced TOA trilateration based on the proposed hybrid algorithm is lower than the MSE curve based on only the line intersection algorithm, similar to the first set.

Through the simulation results, I observe that the proposed hybrid TOA trilateration algorithm (based on the line intersection algorithm in general case and comparison approach of

intersection distances in the specific case) has a good performance of MS location estimation than that of the conventional algorithm and only line intersection algorithm.

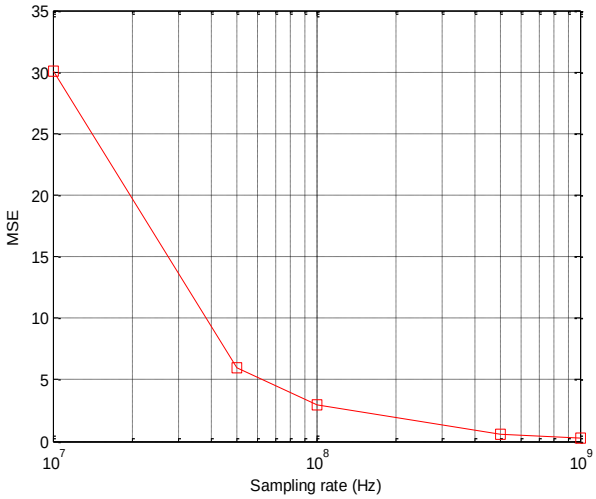

Figure 5.31 For the second set: mean squared error curve of the distance for the case A

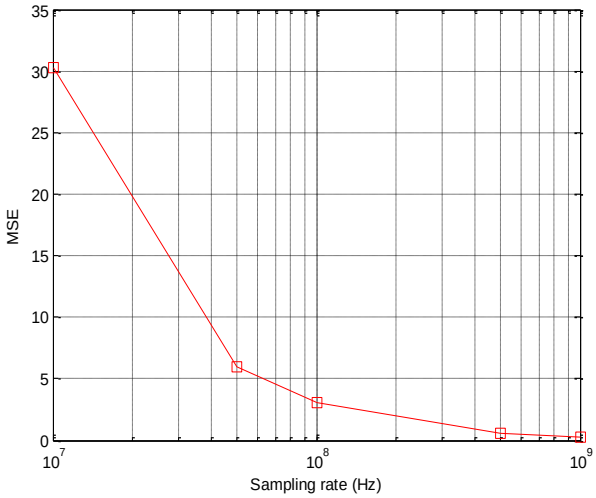

Figure 5.32 For the second set: mean squared error curve of the distance for the case B

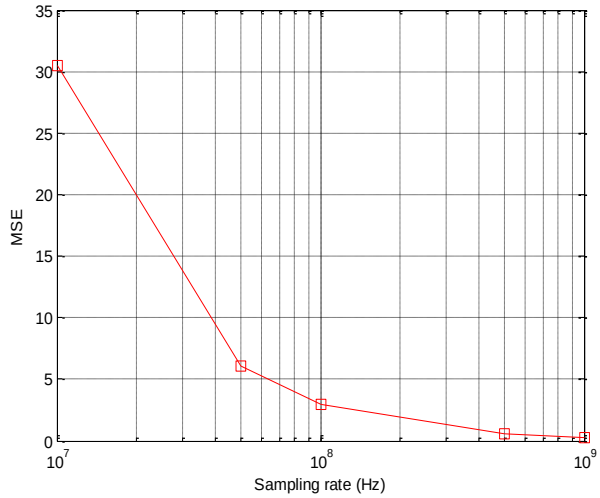

Figure 5.33 For the second set: mean squared error curve of the distance for the case C

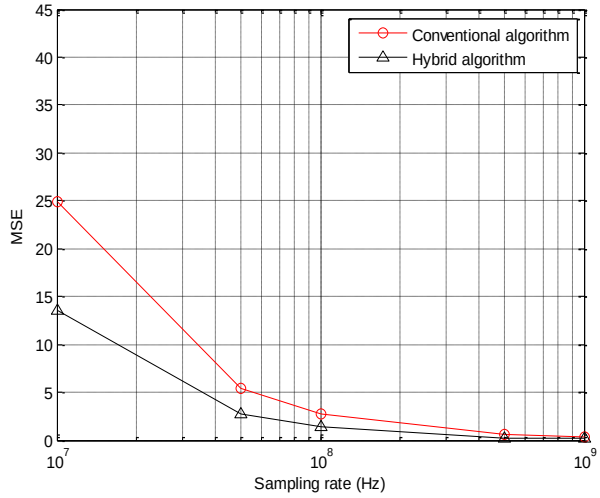

Figure 5.34 For the second set: mean squared error curves of the mobile station position in 2D for the first scenario for the case A

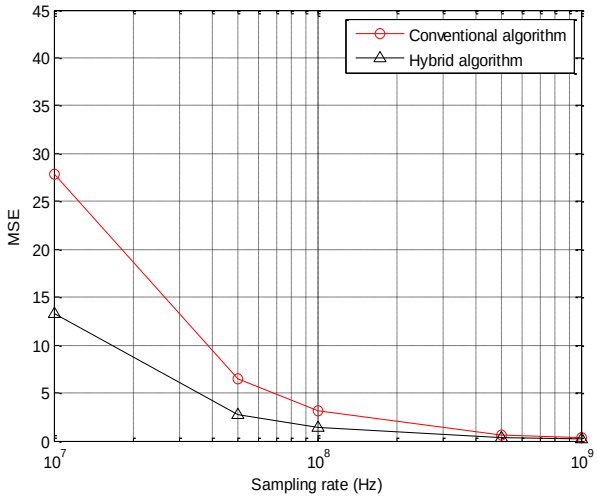

Figure 5.35 For the second set: mean squared error curves of the mobile station position in 2D for the first scenario for the case B

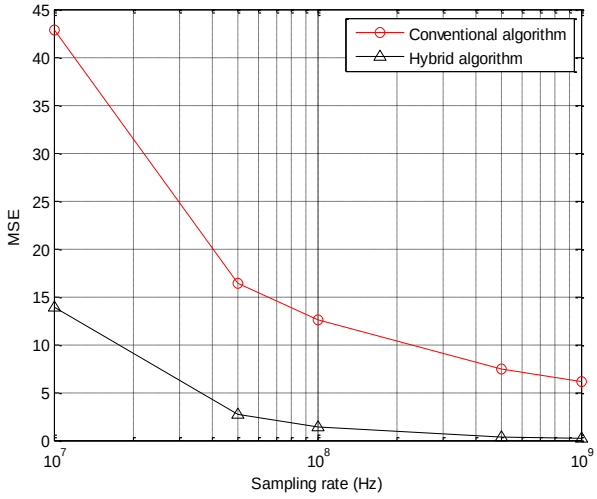

Figure 5.36 For the second set: mean squared error curves of the mobile station position in 2D for the first scenario for the case C

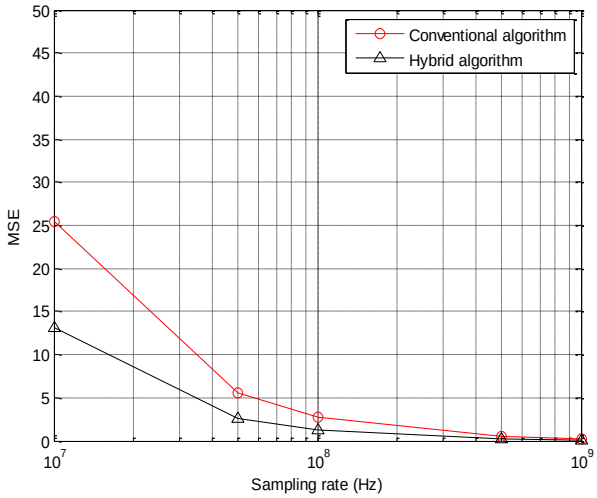

Figure 5.37 For the second set: mean squared error curves of the mobile station position in 2D for the second scenario for the case A

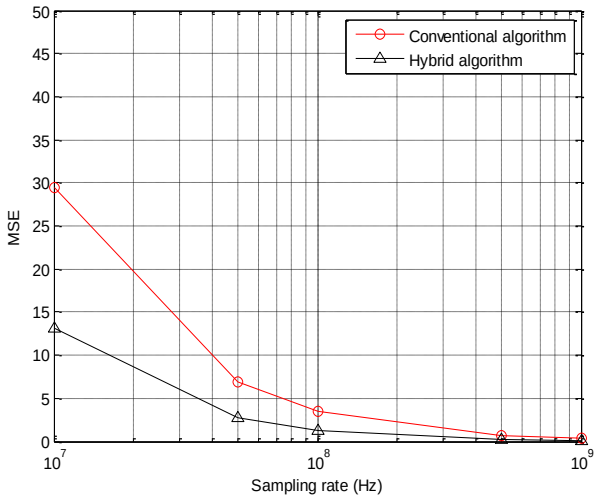

Figure 5.38 For the second set: mean squared error curves of the mobile station position in 2D for the second scenario for the case B

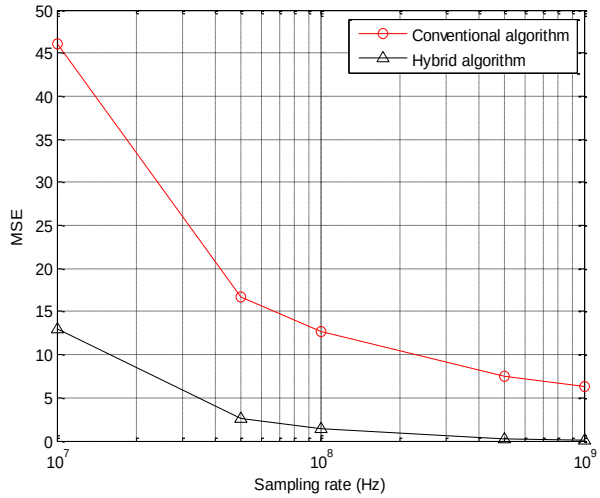

Figure 5.39 For the second set: mean squared error curves of the mobile station position in 2D for the second scenario for the case C

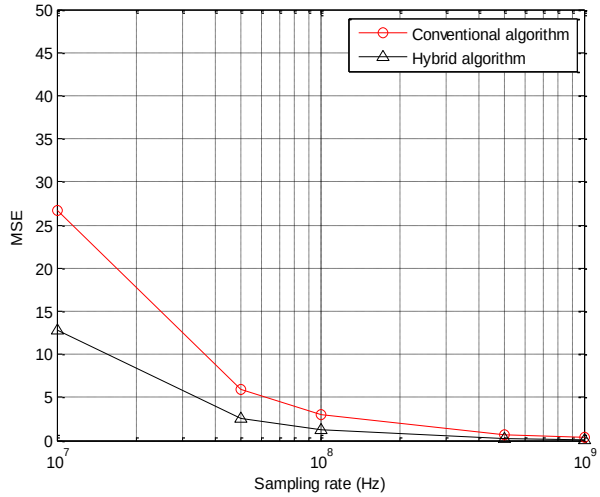

Figure 5.40 For the second set: mean squared error curves of the mobile station position in 2D for the third scenario for the case A

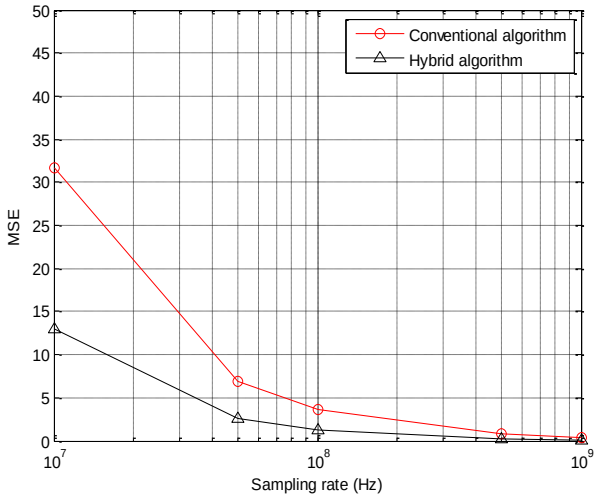

Figure 5.41 For the second set: mean squared error curves of the mobile station position in 2D for the third scenario for the case B

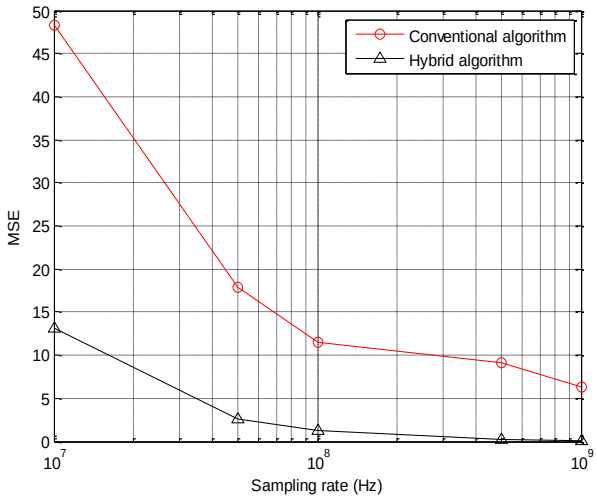

Figure 5.42 For the second set: mean squared error curves of the mobile station position in 2D for the third scenario for the case C

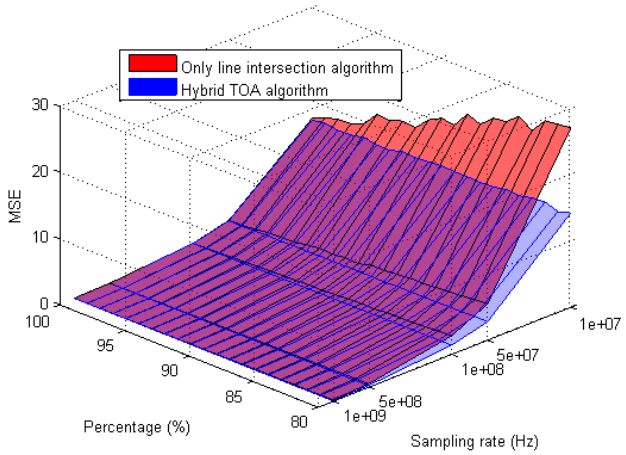

Figure 5.43 For the second set: mean squared error location curves in 3D for the case A

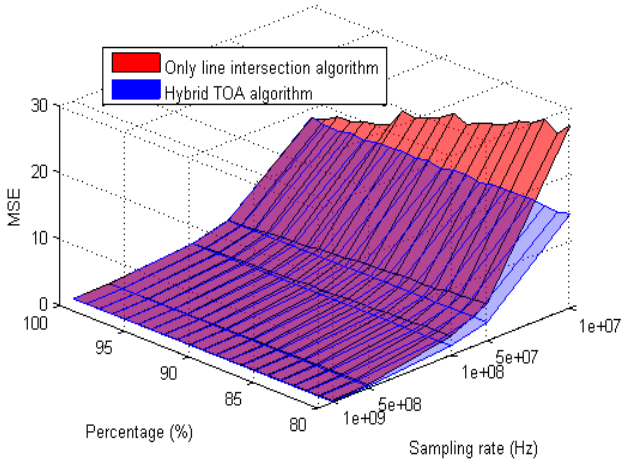

Figure 5.44 For the second set: mean squared error location curves in 3D for the case B

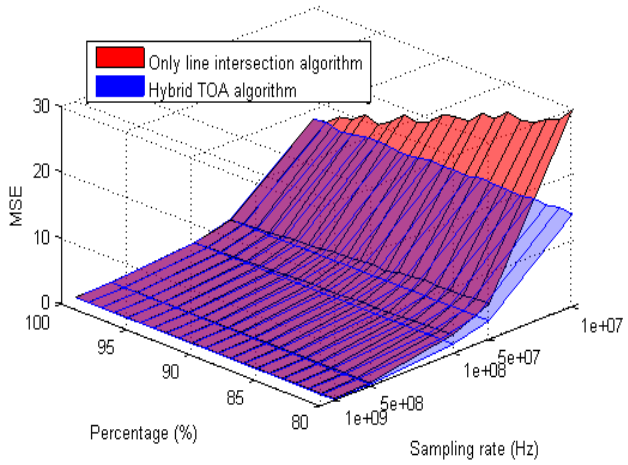

(c)

Figure 5.45 For the second set: mean squared error location curves in 3D for the case C

5.6 Mode Selection Algorithm between Case 3 and Case 4

For the best performance of location estimation, the mode selection algorithm between case 3 and case 4 is proposed to efficiently select case 3 and case 4 modes. It calculates two distances related to the centers of the small circle and two large circles. The center distance between the small circle $C2$ and two large circles, $C1$ and $C3$, is given by,

$$d_{2k} = \sqrt{\left(x_2 - x_K\right)^2 + \left(y_2 - y_K\right)^2} \qquad \text{K=1,3} \tag{5.4}$$

where (x_K, y_K) is the coordinate of large circles, $C1$ and $C3$. It also calculates the absolute value of radius difference between the small circle $C2$ and the two large circles, $C1$ and $C3$, is given by

$$\left(\left|R_2 - R_K\right|\right) \quad \text{for K=1,3.} \tag{5.5}$$

Then center distances, (d_{21}) and (d_{23}), are compared to the absolute value of radius differences, $\left|(R_2 - R_1)\right|$ and $\left|(R_2 - R_3)\right|$. If both center distances are shorter than radius differences, it selects case 4 and determines small circle $C2$ completely lies inside the overlapping area of the two large circles $C1$ and $C3$. And this algorithm employs the closest point algorithm for estimating the location of MS. Otherwise, it selects case 3 and determines small circle $C2$ completely lies inside one of the large circle, but not completely lie inside the other circle, and it employs the small circle intersection approach for estimating the location of MS. The flow chart for the mode selection algorithm between case 3 and case 4 is shown in Figure 5.46 and Table 5.2 summarizes steps of the algorithm.

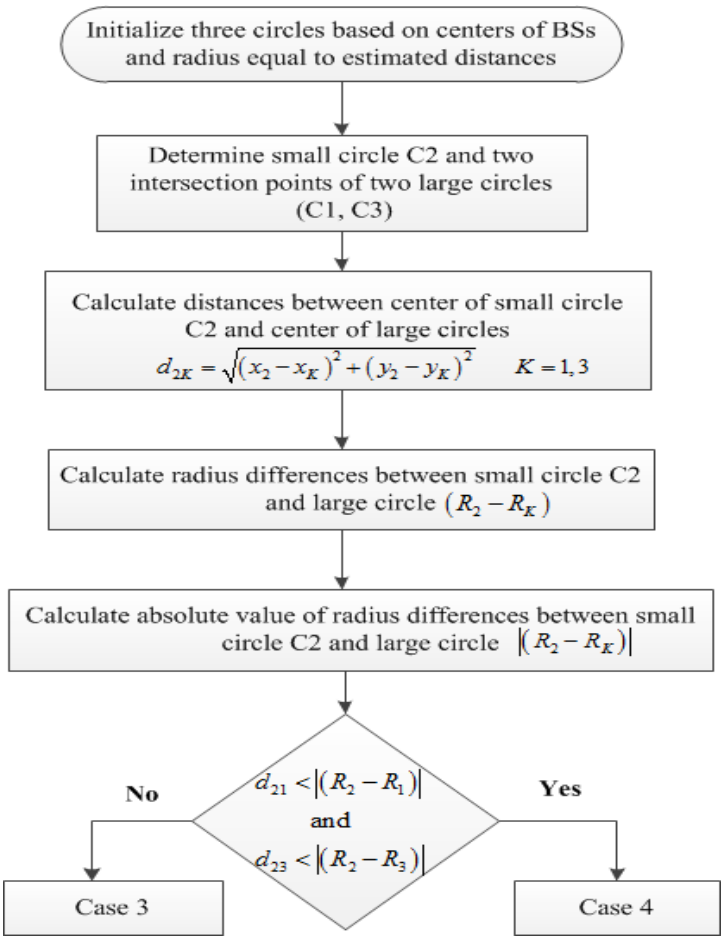

Figure 5.46 Flow chart for mode selection algorithm between case 3 and case 4

Table 5.2 Mode selection algorithm between case 3 and case 4

1. Calculate the distance between the center of the small circle $C2$ and the center of the large circle $C1$

$$d_{21} = \sqrt{(x_2 - x_1)^2 + (y_2 - y_1)^2}.$$

2. Calculate the absolute value of radius differences between the small circle $C2$ and the large circle $C1$

$$|(R_2 - R_1)|.$$

3. Calculate the distance between the center of the small circle $C2$ and the center of the large circles $C3$

$$d_{23} = \sqrt{(x_2 - x_3)^2 + (y_2 - y_3)^2}.$$

4. Calculate the absolute value of radius differences between the small circle $C2$ and the large circle $C3$

$$|(R_2 - R_3)|.$$

5. Compare $|(R_2 - R_1)|$ to d_{21}, and compare $|(R_2 - R_3)|$ to d_{23}.

6. a. If $d_{21} < |(R_2 - R_1)|$, and $d_{23} < |(R_2 - R_3)|$

   ☞ Case 4 (small circle $C2$ completely lies inside the overlapping area of two large circles $C1$ and $C3$).

   b. Otherwise $d_{21} < |(R_2 - R_1)|$, and $d_{23} > |(R_2 - R_3)|$

   ☞ Case 3 (small circle $C2$ completely lies inside the large circle $C1$ but not completely lie inside another circle $C3$).

5.7 Overall Mode Selection Algorithm between All Four Cases

The overall selection mode is based on two equations that compare the absolute value of radii difference to center distances between small circle $C2$ and two large circles $C1$ and $C3$. The two comparing equations are given by

$$d_{21} < |R_2 - R_1|, \tag{5.6}$$

and

$$d_{23} < |R_2 - R_3|. \tag{5.7}$$

The algorithm checks for the possibility of case 3 and 4 based on either (5.6) or (5.7) is true. Then, it again checks if both (5.6) and (5.7) satisfy, it selects case 4 else it selects case 3. And apply the best algorithm according to proper case. Next, the algorithm checks for the possibility of case 1 and 2 based on either (5.6) or (5.7) is false. That means

$$\begin{array}{c} d_{21} > \mathrm{R}_1 > |R_2 - R_1| \\ \text{and} \\ d_{23} > \mathrm{R}_3 > |R_2 - R_3| \end{array}. \tag{5.8}$$

(5.8) is true. It selects the mode selection algorithm between case 1 and case 2, and distinguishes between the general case and the specific case. It applies the line intersection algorithm in case 1 and the comparison approach of intersection distances in case 2. Using (5.6) and (5.7), I can determine mode selection for all four cases and I do not need to determine the

number of intersection points. The flow chart for the overall mode selection algorithm between all four cases is shown in Figure 5.47 and Table 5.3 summarizes the steps of the algorithm.

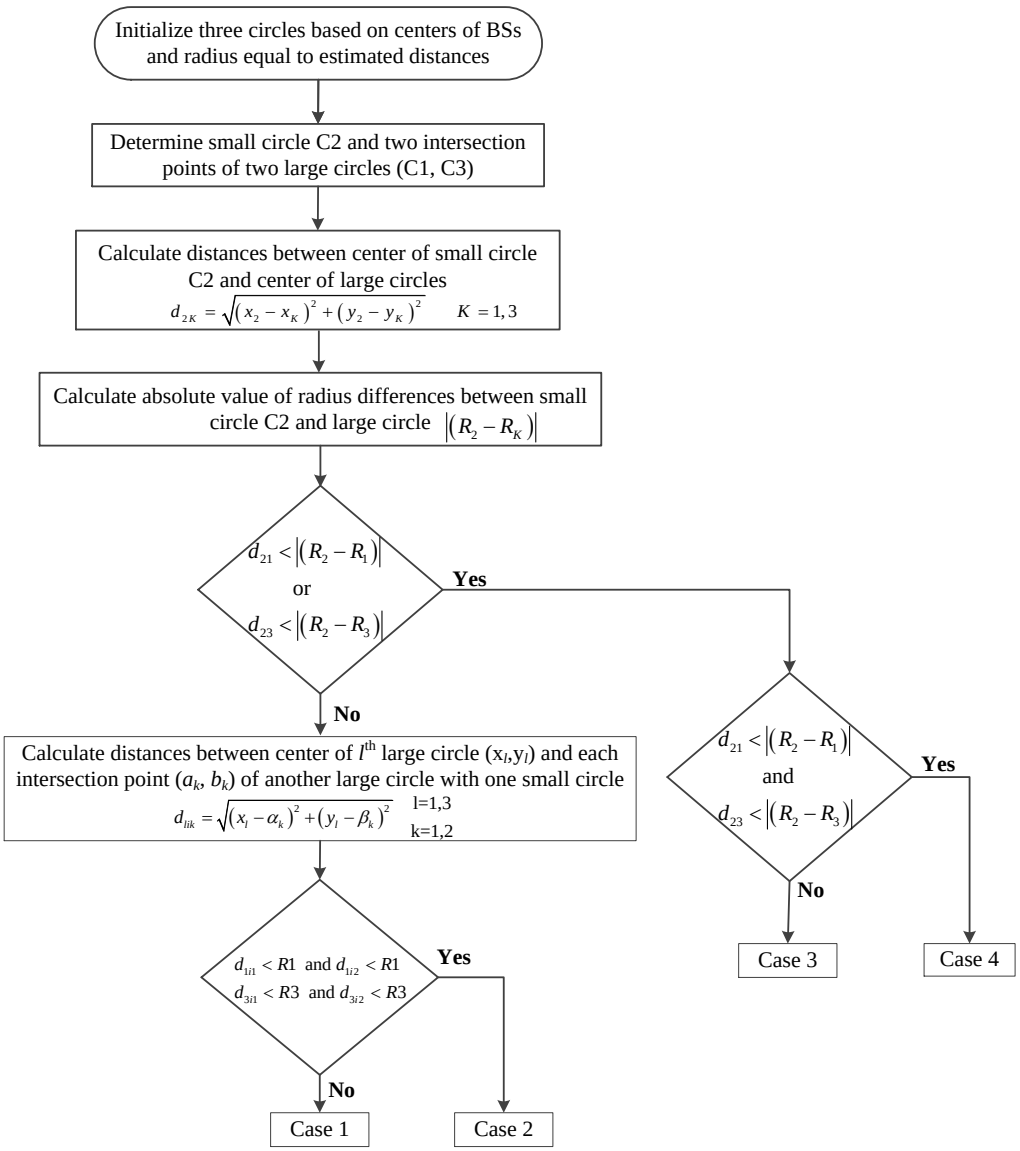

Figure 5.47 Flow chart for overall mode selection algorithm for all four cases

Table 5.3 Overall mode selection algorithm among the four cases

1. Calculate the center distances between small circle $C2$ and large circles $C1$ and $C3$,

$$d_{2K} = \sqrt{(x_2 - x_K)^2 + (y_2 - y_K)^2} \qquad \text{K=1,3}.$$

2. Calculate the absolute values of radius differences between small circle $C2$ and large circle $C1$ and $C3$

$$\left|(R_2 - R_K)\right| \quad \text{where K=1,3}.$$

3. Compare $\left|(R_2 - R_1)\right|$ to d_{21}.

4. Compare $\left|(R_2 - R_3)\right|$ to d_{23}.

5. If $d_{21} < \left|(R_2 - R_1)\right|$, or $d_{23} < \left|(R_2 - R_3)\right|$ satisfy, check

   a. If $d_{21} < \left|(R_2 - R_1)\right|$, and $d_{23} < \left|(R_2 - R_3)\right|$

      ☞ Case 4.

   b. Else, $d_{21} < \left|(R_2 - R_1)\right|$, and $d_{23} > \left|(R_2 - R_3)\right|$

      ☞ Case 3.

6. If $d_{21} < \left|(R_2 - R_1)\right|$, or $d_{23} < \left|(R_2 - R_3)\right|$ does not satisfy, calculate four distances related to the center of one of the large circle and each intersection point (α_k, β_k) of another large circle with one small circle

$$d_{lik} = \sqrt{(x_l - \alpha_k)^2 + (y_l - \beta_k)^2} \quad \begin{matrix} \text{l=1,3} \\ \text{k=1,2} \end{matrix}.$$

7. Compare the radius of $C1$, $R1$, to d_{1i1} and d_{1i2}.

8. Compare the radius of $C3$, $R3$, to d_{3i1} and d_{3i2}.

a. If $d_{1i1} < R1$ and $d_{1i2} < R1$, and $d_{3i1} < R3$ and $d_{3i2} < R3$

☞ Case 2.

b. Otherwise

☞ Case 1.

5.7.1 Computer Simulations

In this section, the computer simulation scenarios are provided to illustrate the MS location estimation performance.

5.7.1.1 Simulation Scenario Parameters

The two different sets are considered.

For first set:

For simulation scenario, three fixed BSs are considered where their coordinates for distinguishing four cases are

Case 1: (-1000, 5000), (6000, -3000), (-7000, 600),

Case 2: (-1000, 4000), (1000, 2000), (5000, 700),

Case 3: (-2000, -3000), (-1300, -1900), (2000, -4000),

Case 4: (-2000, -3000), (-20, -10), (2000, -4000).

For second set:

For simulation scenario, I consider three fixed BSs, where their coordinates for distinguishing four cases are

Case 1: (-1000, 4500), (6000, -2000), (-7000, 500),

Case 2: (-1000, 5000), (1500, 3000), (7000, 600),

Case 3: (-2000, -3000), (-1300, -1900), (2000, -4000),

Case 4: (-2000, -3000), (-20, -10), (2000, -4000).

I assume the three different scenarios of occurrence rates for Case 1, Case 2, Case 3, and Case 4. They are

First Scenario: 60%, 25%, 10%, and 5% for Case 1, Case 2, Case 3, and Case 4,

Second Scenario: 70%, 20%, 10%, and 7% for Case 1, Case 2, Case 3, and Case 4,

Third Scenario: 90%, 7%, 2%, and 1% for Case 1, Case 2, Case 3, and Case 4, respectively. Also, the MS location is randomly selected within ranges between

Case A: -100 ~ +100, Case B: -500 ~ +500

with conditions for each. The unit of coordinates is a meter (m). I consider different sampling rates of 10 MHz, 50 MHz, 100 MHz, 500 MHz, and 1 GHz.

5.7.1.2 Performance Evaluation of Error Model

The performances of the MS location estimation algorithm are evaluated by the root-mean-square error (RMSE). The error between true MS position and estimated MS position is defined by

$$Error_{Position} \triangleq \sqrt{\left(x-\hat{x}\right)^2+\left(y-\hat{y}\right)^2}\,. \tag{5.9}$$

and MSE for estimating the MS position is defined by

$$MSE_{Position} \triangleq E\left[Error_{Position}^{2} \right], \tag{5.10}$$

where $E[\ ]$ is an expectation operator. The RMSE of the estimating MS position is given by

$$RMSE_{Position} = \sqrt{MSE_{Position}}\ . \tag{5.11}$$

5.7.1.3 Simulation Results

5.7.1.3.1 Simulation Results for the First Set

Based on the first set, the simulation results of the root-mean-square error (RMSE) of the estimated distance versus the various sampling rates are shown in Figure 5.48 and Figure 5.49, for the case A and case B, respectively. For the first scenario, Figure 5.50 and Figure 5.51 compare two RMSE curves based on the proposed hybrid algorithm and only line intersection algorithm, for various sampling rates, for the case A and case B, respectively. For the second scenario, the two RMSE curves based on the proposed hybrid algorithm and only line intersection algorithm, for various sampling rates, are shown in Figure 5.52 and Figure 5.53, for the case A and case B, respectively. For the third scenario, the two RMSE curves based on the proposed hybrid algorithm and only line intersection algorithm, for various sampling rates, are shown in Figure 5.54 and Figure 5.55, for the case A and case B, respectively. From figures, I observe that RMSE of the hybrid algorithm is lower than RMSE of only line intersection algorithm, for all cases.

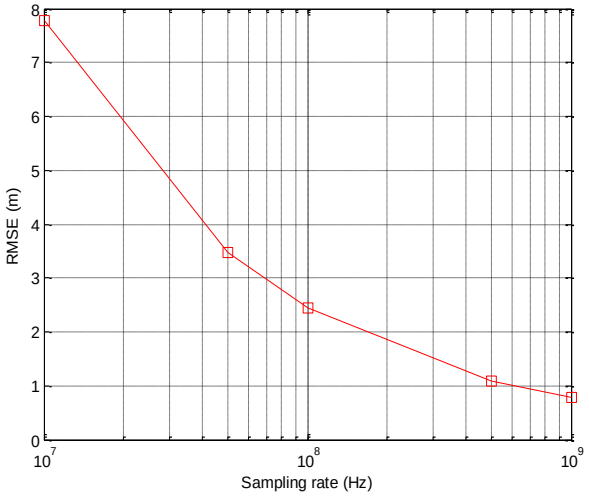

Figure 5.48 For the first set: root-mean-square error curves of distance for the case A

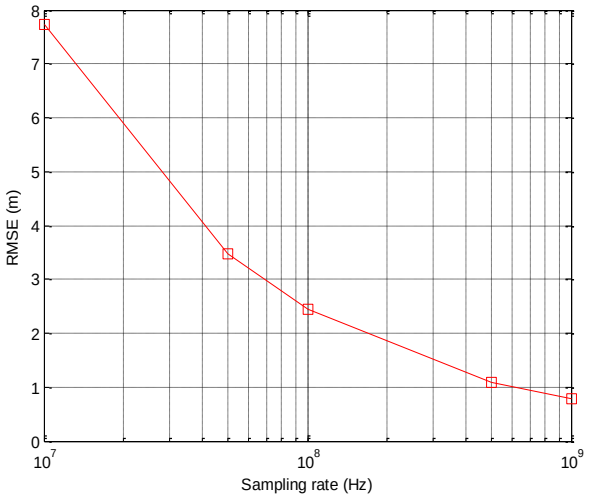

Figure 5.49 For the first set: root-mean-square error curves of distance for the case B

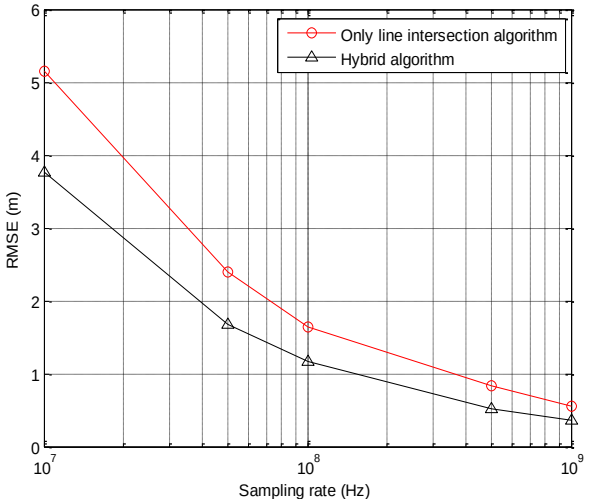

Figure 5.50 For the first set: for the first scenario, root-mean-square error curves of mobile station location for the case A

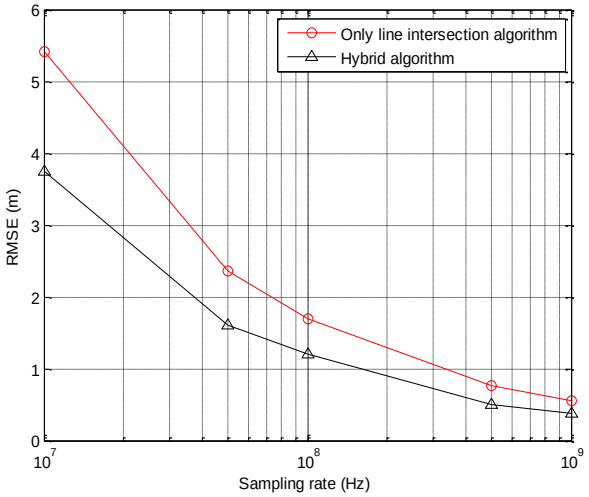

Figure 5.51 For the first set: for the first scenario, root-mean-square error curves of mobile station location for the case B

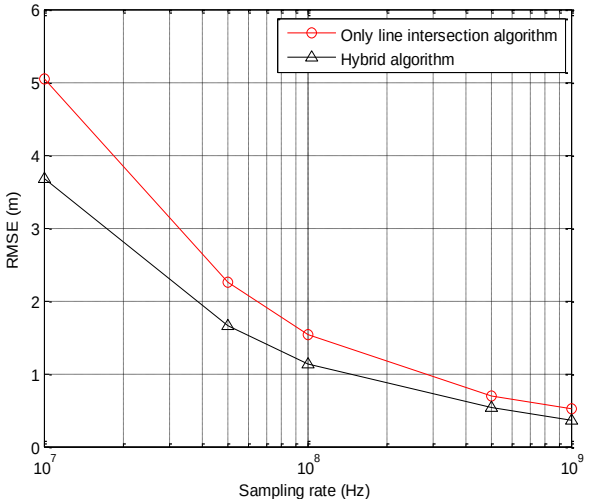

Figure 5.52 For the first set: for the second scenario, root-mean-square error curves of mobile station location for the case A

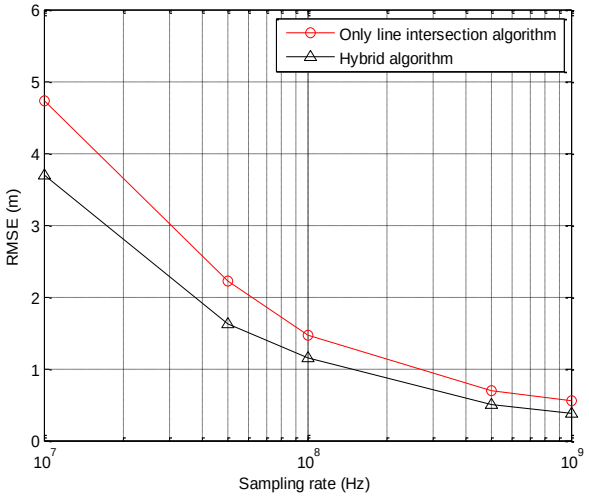

Figure 5.53 For the first set: for the second scenario, root-mean-square error curves of mobile station location for the case B

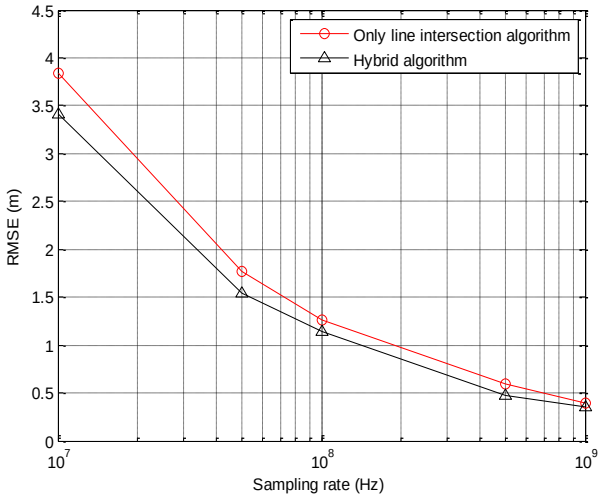

Figure 5.54 For the first set: for the third scenario, root-mean-square error curves of mobile station location for the case A

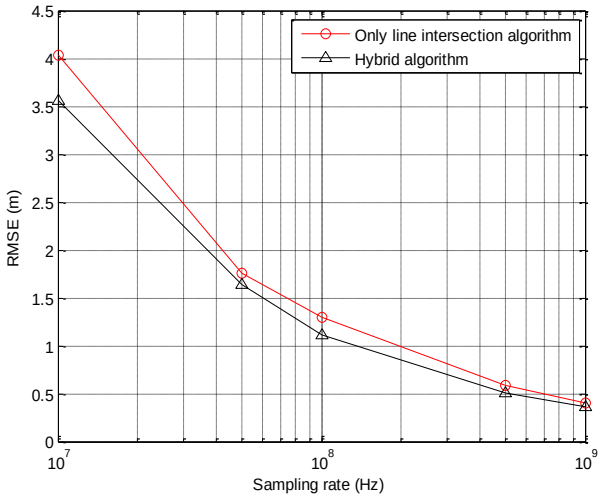

Figure 5.55 For the first set: for the third scenario, root-mean-square error curves of mobile station location for the case B

5.7.1.3.2 Simulation Results for the Second Set

Based on the second set, the simulation results of the root-mean-square error (RMSE) of the estimated distance versus the various sampling rates are shown in Figure 5.56 and Figure 5.57 for the case A and case B, respectively. For the first scenario, Figure 5.58 and Figure 5.59 compare two RMSE curves based on the proposed hybrid algorithm and only line intersection algorithm, for various sampling rates, for the case A and case B, respectively. For the second scenario, the two RMSE curves based on the proposed hybrid algorithm and only line intersection algorithm, for various sampling rates, are shown in Figure 5.60 and Figure 5.61, for the case A and case B, respectively. For the third scenario, the two RMSE curves based on the proposed hybrid algorithm and only line intersection algorithm, for various sampling rates, are shown in Figure 5.62 and Figure 5.63, for the case A and case B, respectively. From figures, I observe that RMSE of the hybrid algorithm is lower than RMSE of only line intersection algorithm, for all cases.

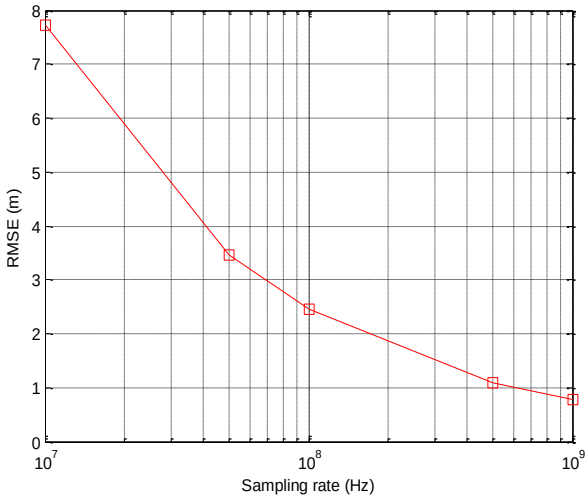

Figure 5.56 For the second set: root-mean-square error curves of distance for the case A

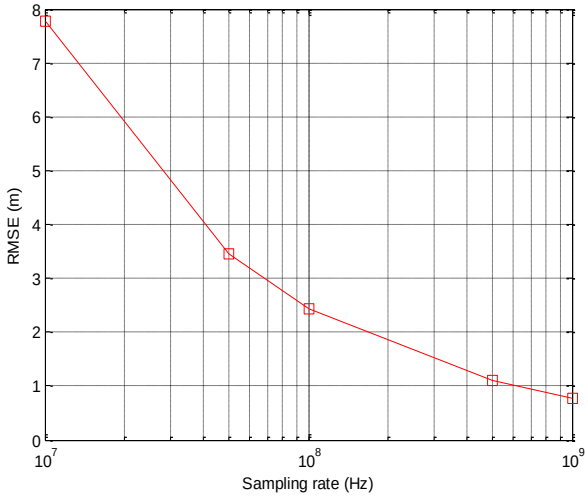

Figure 5.57 For the second set: root-mean-square error curves of distance for the case B

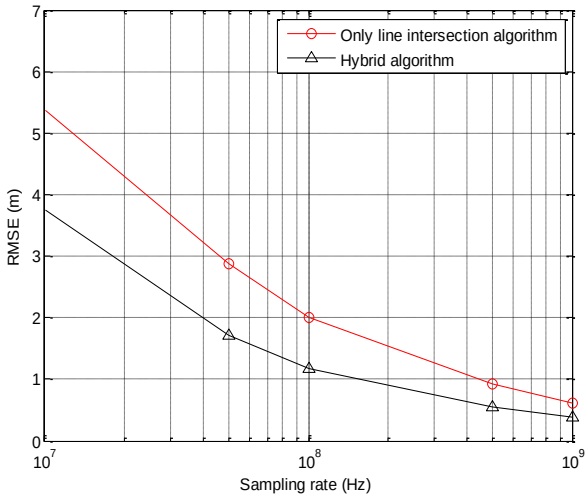

Figure 5.58 For the second set: for the first scenario, root-mean-square error curves of the mobile station location for the case A

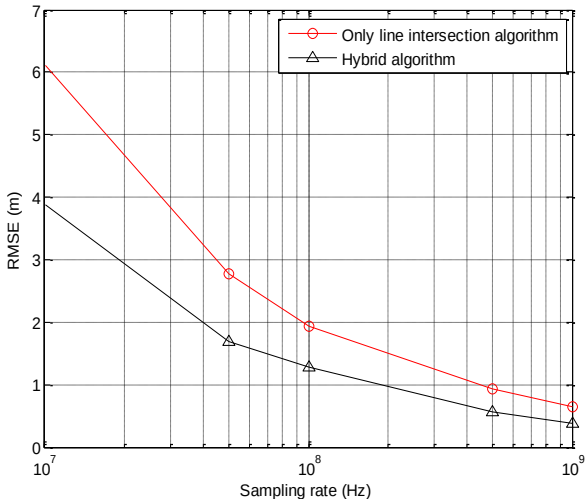

Figure 5.59 For the second set: for the first scenario, root-mean-square error curves of the mobile station location for the case B

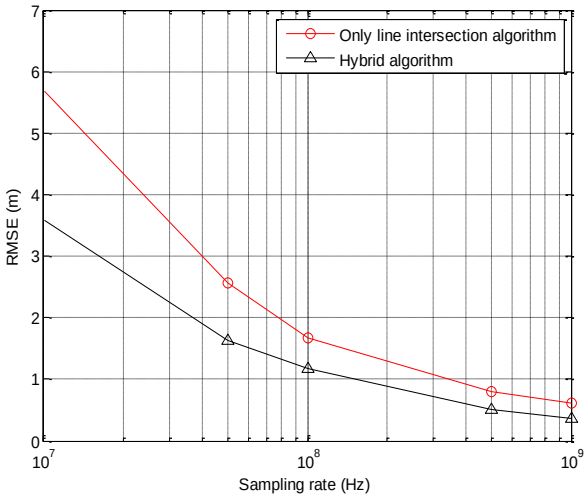

Figure 5.60 For the second set: for the second scenario, root-mean-square error curves of the mobile station location for the case A

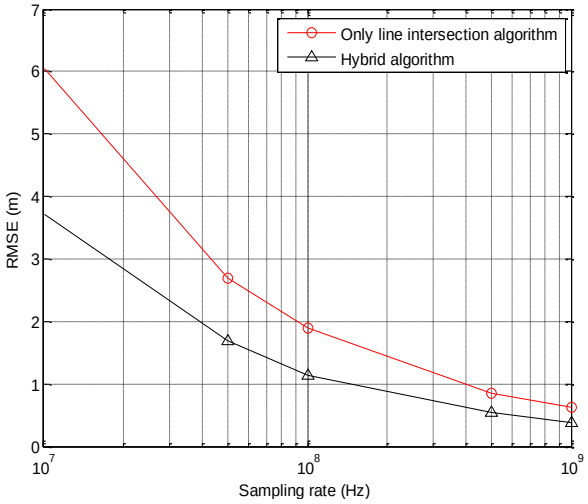

Figure 5.61 For the second set: for the second scenario, root-mean-square error curves of the mobile station location for the case B

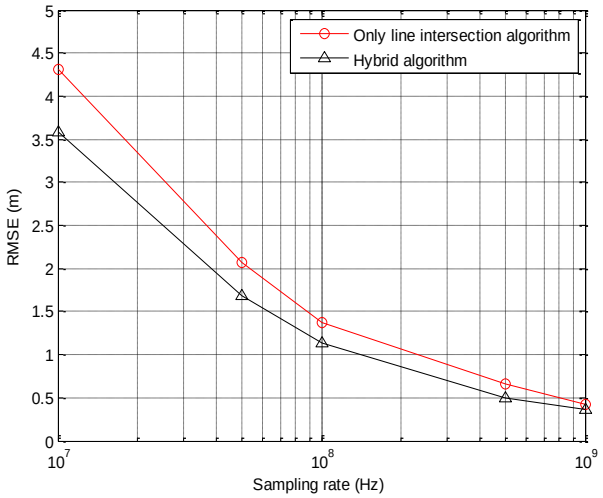

Figure 5.62 For the second set: for the third scenario, root-mean-square error curves of the mobile station location for the case A

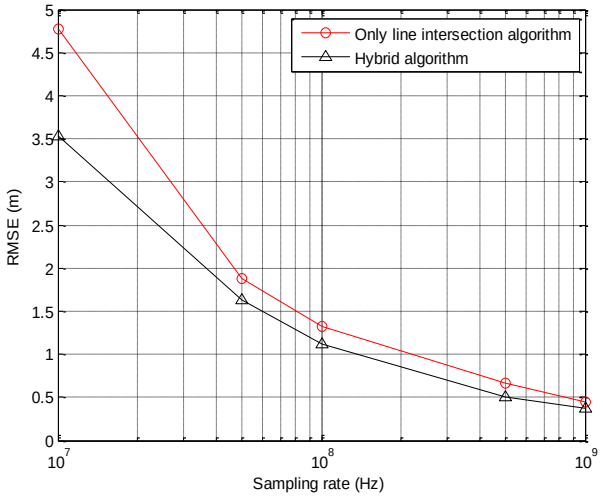

Figure 5.63 For the second set: for the third scenario, root-mean-square error curves of the mobile station location for the case B

5.8 Concluding Remarks

The TOA trilateration algorithm determines the location of the MS at an intersection point of three circles based on distances between the MS and BSs, and center being the coordinates of BSs. The distance between the MS and BS is usually estimated by counting the number of delay samples, the three circles may not meet at a single point, causing the location estimation error of the MS. In order to solve the MS location problem, I propose the hybrid algorithm based on the line intersection algorithm for the general case and comparison approach of intersection distances for the specific case. Although the line intersection algorithm, which has good performance in the general case, it may have a high estimation error in the specific case. The comparison approach of intersection distances has worse performance for estimating the MS location compared to the line intersection algorithm in the general case, but the comparison approach of intersection distances has good performance in the specific case. Also, in order to alternately use both algorithms according to the proper mode case, I provide the mode selection algorithm. The mode selection algorithm compares the distances between the intersection points of the small circle and one large circle to the radius of another large circle. If all distances are shorter than the corresponding radii, it selects the specific case mode and employs the comparison algorithm of intersection distances. Otherwise, it selects the general case and employs the line intersection algorithm. The simulation results of the proposed algorithm were illustrated through computer simulations that show the proposed hybrid algorithm has better MS location performance than that of the conventional and only line intersection algorithms.

Also, I provide overall selection mode algorithm of all four different cases. To get the best MS location estimation, I employ the line intersection algorithm or comparison approach of intersection distances or small circle intersection approach or closest point algorithm, according

to the proper case. The selection procedure for four cases is based on two equations that compare radii differences to center distances between the smallest circle and two large circles. For the best localization performance, the proposed four algorithms should be employed with a hybrid form.

6 Conclusions

In this dissertation, some of advanced TOA trilateration algorithms proposed to estimate the location of MS. I summarized those algorithms in the order to be appeared in the thesis.

The TOA trilateration algorithm determined the location of the MS at the intersection point of three circles based on distances between the MS and BSs, and center being the coordinates of BSs. The three circles might not meet at a single point because the distance between the MS and BS was usually estimated by counting the number of delay samples, which it must be an integer although it was not originally integer. Therefore, the distance was slightly increased; three circles based on the estimated distance did not meet at a point causing the serious estimation location error of the MS in four different cases. In order to solve the location problem, the advanced TOA trilateration algorithms had been proposed. They were the shortest distance algorithm and the line intersection algorithm in the general case (case 1), and comparison approach of intersection distances in the specific case (case 2), the small circle intersection approach in the case 3 and the closest point algorithm in the case 4, respectively. For the best performance of the location estimation, the proposed four algorithms should be employed with a hybrid form. For this purpose, a mode selection algorithm had been proposed to efficiently select the proper case, and a hybrid TOA trilateration algorithm based on four algorithms was proposed.

In this study, all possible cases for occurring the location estimation error had been considered and I verified that the proposed algorithm had lower error comparing to the

conventional TOA algorithm. This advanced hybrid TOA trilateration algorithm is expected to be mainly employed in various fields requiring excellent location estimation performance.

References

[1] S. Spiekermann, "General Aspects of Location-based services," in *Location-based services*, ed: Elsevier, 2004, pp. 9-26.

[2] D. H. Stojanovic and S. J. Djordjevic-Kajan, "Developing location-based services from a GIS perspective," in *5th International Conference on Telecommunications in Modern Satellite, Cable and Broadcasting Service. TELSIKS 2001. Proceedings of Papers (Cat. No.01EX517)*, Nis, Yugoslavia, Yugoslavia, 2001, pp. 459-462

[3] O. Mohareri and A. B. Rad, "A Vision-Based Location Positioning System Via Augmented Reality: An Application in Humanoid Robot Navigation," *International Journal of Humanoid Robotics*, vol. 10, no. 3, p. 1350019, Sep. 2013.

[4] R. Rahdar, J. T. Stracener, and E. V. Olinick, "A Systems Engineering Approach to Improving the Accuracy of Mobile Station Location Estimation," *IEEE Systems Journal*, vol. 8, no. 1, pp. 14-22, 2014.

[5] A. Aljadhai and T. F. Znati, "Predictive mobility support for QoS provisioning in mobile wireless environments," *IEEE Journal on Selected Areas in Communications*, vol. 19, no. 10, pp. 1915-1930, 2001.

[6] S. Ahonen and P. Eskelinen, "Mobile terminal location for UMTS," *IEEE Aerospace and Electronic Systems Magazine*, vol. 18, no. 2, pp. 23-27, 2003.

[7] A. H. Sayed, A. Tarighat, and N. Khajehnouri, "Network-based wireless location: challenges faced in developing techniques for accurate wireless location information," *IEEE Signal Processing Magazine*, vol. 22, no. 4, pp. 24-40, 2005.

[8] C. Chen, S. Su, and C. Lu, "Geometrical positioning approached for mobile location estimation," in *2010 2nd IEEE International Conference on Information Management and Engineering*, Chengdu, China, 2010, pp. 268-272.

[9] C. Jung-Chieh, W. Yeong-Cheng, M. Ching-Shyang, and C. Jiunn-Tsair, "Network-side mobile position location using factor graphs," *IEEE Transactions on Wireless Communications*, vol. 5, no. 10, pp. 2696-2704, 2006.

[10] M. Zaidi, R. Tourki, and R. Ouni, "A new geometric approach to mobile position in wireless LAN reducing complex computations," in *5th International Conference on Design & Technology of Integrated Systems in Nanoscale Era*, 2010, pp. 1-7.

[11] G. M. Djuknic and R. E. Richton, "Geolocation and assisted GPS," *Computer*, 2, pp. 123-125, 2001.

[12] P. K. Enge, "The global positioning system: Signals, measurements, and performance," *International Journal of Wireless Information Networks*, vol. 1, no. 2, pp. 83-105, 1994.

[13] J. J. Caffery, *Wireless location in CDMA cellular radio systems*. Boston: Kluwer Academic, 2000.

[14] C. L. Yang, Y. K. Chang, Y. T. Chen, C. P. Chu, and C. C. Chen, "A Self-Adaptable Indoor Localization Scheme for Wireless Sensor Networks," *International Journal of Software Engineering and Knowledge Engineering*, vol. 21, no. 1, pp. 33-54, Feb 2011.

[15] S. Go and J. W. Chong, "Improved TOA-Based Localization Method with BS Selection Scheme for Wireless Sensor Networks," *Etri Journal*, vol. 37, no. 4, pp. 707-716, 2015.

[16] I. Guvenc and C.-C. Chong, "A survey on TOA based wireless localization and NLOS mitigation techniques," *IEEE Communications Surveys & Tutorials*, vol. 11, no. 3, 2009.

[17] J. Saloranta and G. Abreu, "Solving the fast moving vehicle localization problem via TDOA algorithms," in *Positioning Navigation and Communication (WPNC), 2011 8th Workshop on*, 2011, pp. 127-130.

[18] M. Dakkak, A. Nakib, B. Daachi, P. Siarry, and J. Lemoine, "Indoor localization method based on RTT and AOA using coordinates clustering," *Computer Networks*, vol. 55, no. 8, pp. 1794-1803, 2011.

[19] M. Fewell, "Area of common overlap of three circles," 2006.

[20] *Revision of the Commissions Rules to Insure Compatibility with Enhanced 911 Emergency Calling Systems*, F. C. Commission FCC Docket No. 94-102, July 1996.

[21] J. J. Caffery and G. L. Stuber, "Overview of radiolocation in CDMA cellular systems," *IEEE Communications Magazine*, vol. 36, no. 4, pp. 38-45, Apr. 1998.

[22] C. Drane, M. Macnaughtan, and C. Scott, "Positioning GSM telephones," *IEEE Communications Magazine*, vol. 36, no. 4, pp. 46-54, 59, Apr. 1998.

[23] J. M. Zagami, S. A. Parl, J. J. Bussgang, and K. D. Melillo, "Providing universal location services using a wireless E911 location network," *IEEE Communications Magazine*, vol. 36, no. 4, pp. 66-71, Apr. 1998.

[24] S. Tekinay, E. Chao, and R. Richton, "Performance benchmarking for wireless location systems," *IEEE Communications Magazine*, vol. 36, no. 4, pp. 72-76, Apr. 1998.

[25] J. H. Reed, K. J. Krizman, B. D. Woerner, and T. S. Rappaport, "An overview of the challenges and progress in meeting the E-911 requirement for location service," *IEEE Communications Magazine*, vol. 36, no. 4, pp. 30-37, Apr. 1998.

[26] H. Yilin Zhao, "Standardization of mobile phone positioning for 3G systems," *IEEE Communications Magazine*, vol. 40, no. 7, pp. 108-116, 2002.

[27] J. Figueiras, "Accuracy Enhancements for Positioning of Mobile Devices in Wireless Communication Networks," Ph.D., Department of Electronic Systems, Aalborg University, Aalborg, 2008.

[28] M. P. Wylie-Green and S. S. Wang, "Observed time difference (OTD) estimation for mobile positioning in IS-136 in the presence of BTS clock drift," in *IEEE 54th Vehicular Technology Conference. VTC Fall 2001. Proceedings (Cat. No.01CH37211)*, 2001, pp. 2677-2681 vol.4.

[29] M. Pent, M. A. Spirito, and E. Turco, "Method for positioning GSM mobile stations using absolute time delay measurements," *Electronics Letters*, vol. 33, no. 24, pp. 2019-2020, 1997.

[30] E. D. Kaplan, *Understanding GPS: principles and applications*. MA, USA: Artech House, 1996.

[31] A. Roxin, J. Gaber, M. Wack, and A. Nait-Sidi-Moh, "Survey of Wireless Geolocation Techniques," in *2007 IEEE Globecom Workshops*, 2007, pp. 1-9.

[32] M. Ali, "The system applications of novel methods of location and tracking of cellular mobiles," in *IEE Colloquium on Novel Methods of Location and Tracking of Cellular Mobiles and Their System Applications (Ref. No. 1999/046)*, 1999, pp. 6/1-6/4.

[33] I. K. Adusei, K. Kyamakya, and K. Jobmann, "Mobile positioning technologies in cellular networks: an evaluation of their performance metrics," in *MILCOM*, 2002, pp. 1239-1244.

[34] C.-S. Chen, "Artificial neural network for location estimation in wireless communication systems," *Sensors*, vol. 12, no. 3, pp. 2798-2817, 2012.

[35] C.-S. Chen and J.-M. Lin, "Applying Rprop neural network for the prediction of the mobile station location," *Sensors*, vol. 11, no. 4, pp. 4207-4230, 2011.

[36] J. J. Caffery and G. L. Stuber, "Radio location in urban CDMA microcells," in *Personal, Indoor and Mobile Radio Communications, 1995. PIMRC'95. Wireless: Merging onto the Information Superhighway., Sixth IEEE International Symposium on*, 1995, pp. 858-862.

[37] A. Borsodi and M. Fattouche, "Super resolution of discrete arrivals in a position location cellular system," in *Wireless*, 1995, pp. 727-39.

[38] R. W. Klukas, *A superresolution based cellular positioning system using GPS time synchronization*: University of Calgary, 1997.

[39] Z. Abu-Shaban, X. Zhou, and T. D. Abhayapala, "A Novel TOA-Based Mobile Localization Technique Under Mixed LOS/NLOS Conditions for Cellular Networks," *IEEE Transactions on Vehicular Technology*, vol. 65, no. 11, pp. 8841-8853, 2016.

[40] I. Jami, M. Ali, and R. Ormondroyd, "Comparison of methods of locating and tracking cellular mobiles," 1999.

[41] M. A. Spirito, S. Poykko, and O. Knuuttila, "Experimental performance of methods to estimate the location of legacy handsets in GSM," in *Vehicular Technology Conference, 2001. VTC 2001 Fall. IEEE VTS 54th*, 2001, pp. 2716-2720.

[42] C.-D. Wann and Y.-M. Chen, "Position tracking and velocity estimation for mobile positioning systems," in *Wireless Personal Multimedia Communications, 2002. The 5th International Symposium on*, 2002, pp. 310-314.

[43] S.-B. Lee and J.-D. Kim, "A Design and Implementation of BIS Linked LBS Based Alarm System," *The Korea Institute of Electronic Communication Sciences, The Conference of KIECS*, vol. 4, no. 2, pp. 115-117, Nov. 2010.

[44] S.-W. Baek; and H.-J. Kim, "Development of a Location Tracking System for Operation Management of Public Garbage Trucks," *The Korea Institute of Electronic Communication*

Sciences, The Journal of The Korea Institute of Electronic Communication Sciences, vol. 6, no. 6, pp. 909-914, Dec. 2011.

[45] J.-H. Lee, "Hierarchical Clustering-Based Cloaking Algorithm for Location-Based Services," *The Korea Institute of Electronic Communication Sciences, The Journal of The Korea Institute of Electronic Communication Sciences,* vol. 8, no. 8, pp. 155-1160, Aug. 2013.

[46] M. Prasad. (2002). *Location Based Services*. Available: http://www.GISdevelopment.net, http://www.pelagis.net/gis_con/paper/Location%20based%20services.pdf

[47] D. Mohapatra and S. B. Suma, "Survey of location based wireless services," presented at the 2005 IEEE International Conference on Personal Wireless Communications, ICPWC 2005, New Delhi, India, 23-25 Jan, 2005.

[48] I. K. Adusei, K. Kyamakya, and F. Erbas, "Location-based services: advances and challenges," in *Canadian Conference on Electrical and Computer Engineering 2004 (IEEE Cat. No.04CH37513)*, 2004, pp. 1-7 Vol.1.

[49] A. Küpper, *Location-based services: fundamentals and operation*: John Wiley & Sons, 2005.

[50] T. S. Rappaport, J. H. Reed, and B. D. Woerner, "Position location using wireless communications on highways of the future," *IEEE Communications Magazine,* vol. 34, no. 10, pp. 33-41, 1996.

[51] M. F. Mokbel, "Privacy in Location-Based Services: State-of-the-Art and Research Directions," presented at the Proceedings of the 2007 International Conference on Mobile Data Management, 2007.

[52] L. Barkhuus and A. K. Dey, "Location-Based Services for Mobile Telephony: a Study of Users' Privacy Concerns," in *Interact*, Zurich, Switzerland, 2003, pp. 702-712.

[53] R. Zekavat and R. M. Buehrer, *Handbook of Position Location: Theory, Practice and Advances*: Wiley-IEEE Press, 2011.

[54] C. Gentile, N. Alsindi, R. Raulefs, and C. Teolis, *Geolocation techniques: principles and applications*: Springer Science & Business Media, 2012.

[55] P. Prasithsangaree, P. Krishnamurthy, and P. K. Chrysanthis, "On indoor position location with wireless LANs," in *PImRc*, Pavilhao Atlantico, Lisboa, Portugal, 2002, pp. 720-724.

[56] H. Liu, H. Darabi, P. Banerjee, and J. Liu, "Survey of wireless indoor positioning techniques and systems," *IEEE Transactions on Systems, Man, and Cybernetics, Part C (Applications and Reviews)*, vol. 37, no. 6, pp. 1067-1080, 2007.

[57] Y. Zhang, W. Fu, D. Wei, J. Jiang, and B. Yang, "Moving target localization in indoor wireless sensor networks mixed with LOS/NLOS situations," *EURASIP Journal on Wireless Communications and Networking*, vol. 2013, no. 1, p. 291, 2013.

[58] P. Misra and P. Enge, "Special issue on global positioning system," *Proceedings of the IEEE*, vol. 87, no. 1, pp. 3-15, 1999.

[59] H. Koshima and J. Hoshen, "Personal locator services emerge," *IEEE Spectrum*, vol. 37, no. 2, pp. 41-48, 2000.

[60] J. Y. Koh, I. Nevat, D. Leong, and W. Wong, "Geo-Spatial Location Spoofing Detection for Internet of Things," *IEEE Internet of Things Journal*, vol. 3, no. 6, pp. 971-978, 2016.

[61] A. Whitmore, A. Agarwal, and L. Da Xu, "The Internet of Things—A survey of topics and trends," *Information Systems Frontiers*, vol. 17, no. 2, pp. 261-274, 2015/04/01 2015.

[62] N. Deligiannis, S. Louvros, and S. Kotsopoulos, "Mobile Positioning Technology," in *Encyclopedia of Information Science and Technology, Second Edition*, ed: IGI Global, 2009, pp. 2595-2603.

[63] M. Porretta, P. Nepa, G. Manara, and F. Giannetti, "Location, Location, Location," *IEEE Vehicular Technology Magazine*, vol. 3, no. 2, pp. 20-29, 2008.

[64] S. K. C. Chan, K. K. H. Kan, and J. K.-Y. Ng, "A Dual-Channel System for Providing Location Estimation in Mobile Computing," *Journal of Interconnection Networks*, vol. 04, no. 03, pp. 271-290, 2003.

[65] Y. Kuniyoshi, R. Fukano, T. Otani, T. Kobayashi, and N. Otsu, "Haptic Detection of Object Affordances by a Multi-Fingered Robot Hand," *International Journal of Humanoid Robotics*, vol. 02, no. 04, pp. 415-435, 2005.

[66] M. Porretta, P. Nepa, G. Manara, F. Giannetti, M. Dohler, B. Allen, *et al.*, "A novel single base station location technique for microcellular wireless networks: description and validation by a deterministic propagation model," *IEEE Transactions on Vehicular Technology*, vol. 53, no. 5, pp. 1502-1514, 2004.

[67] M. Porretta, P. Nepa, G. Manara, F. Giannetti, M. Dohler, B. Allen, *et al.*, "User positioning technique for microcellular wireless networks," *Electronics Letters*, vol. 39, no. 9, pp. 745-747, 2003.

[68] A. Amar and A. J. Weiss, "Advances in direct position determination," in *Processing Workshop Proceedings, 2004 Sensor Array and Multichannel Signal*, 2004, pp. 584-588.

[69] Y. Wang, "Linear least squares localization in sensor networks," *Eurasip journal on wireless communications and networking*, vol. 2015, no. 1, p. 51, 2015.

[70] J. J. Caffery, "A new approach to the geometry of TOA location," in *Vehicular Technology Conference Fall 2000. IEEE VTS Fall VTC2000. 52nd Vehicular Technology Conference (Cat. No.00CH37152)*, 2000, pp. 1943-1949 vol.4.

[71] R. Henniges, "Current approaches of Wifi Positioning," presented at the Service-Centric Networking- Seminar WS2011/2012, TU-Berlin, 2012.

[72] M. A. Hallak, M. S. Safadi, and R. Kouatly, "Mobile Positioning Technique using Signal Strength Measurement method with the aid of Passive Mobile Listener Grid," in *2006 2nd International Conference on Information & Communication Technologies*, 2006, pp. 105-110.

[73] C. Li and Z. Weihua, "Hybrid TDOA/AOA mobile user location for wideband CDMA cellular systems," *IEEE Transactions on Wireless Communications*, vol. 1, no. 3, pp. 439-447, Jul. 2002.

[74] G. Kbar and W. Mansoor, "Mobile station location based on hybrid of signal strength and time of arrival," in *International Conference on Mobile Business, ICMB 2015*, Sydney, NSW, Australia, 2005, pp. 585-591.

[75] S.-H. Jeong and H.-S. Shin, "A Study for Location Determination Technology over Mobile Network," *The Korea Institute of Electronic Communication Sciences, The Conference of KIECS*, vol. 4, no. 1, pp. 119-123, May 2010.

[76] F. Thomas and L. Ros, "Revisiting trilateration for robot localization," *IEEE Transactions on Robotics*, vol. 21, no. 1, pp. 93-101, 2005.

[77] D. E. Manolakis, "Efficient solution and performance analysis of 3-D position estimation by trilateration," *IEEE Transactions on Aerospace and Electronic Systems*, vol. 32, no. 4, pp. 1239-1248, 1996.

[78] F. Izquierdo, M. Ciurana, F. Barcelo, J. Paradells, and E. Zola, "Performance evaluation of a TOA-based trilateration method to locate terminals in WLAN," in *2006 1st International Symposium on Wireless Pervasive Computing*, 2006, pp. 1-6.

[79] E. Doukhnitch, M. Salamah, and E. Ozen, "An efficient approach for trilateration in 3D positioning," *Computer Communications*, vol. 31, no. 17, pp. 4124-4129, Nov 20 2008.

[80] S. Gezici, "A survey on wireless position estimation," *Wireless Personal Communications*, vol. 44, no. 3, pp. 263-282, Feb 2008.

[81] D. Munoz, F. B. Lara, C. Vargas, and R. Enriquez-Caldera, *Position Location Techniques and Applications*: Academic Press, 2009.

[82] J. Uren and W. F. Price, *Surveying for engineers*: Macmillan International Higher Education, 1994.

[83] R. G. Brown and P. Y. Hwang, *Introduction to random signals and applied Kalman filtering* vol. 3: Wiley New York, 1992.

[84] A. De Gante and M. Siller, "A survey of hybrid schemes for location estimation in wireless sensor networks," *Procedia Technology*, vol. 7, no. pp. 377-383, 2013.

[85] A. Günther and C. Hoene, "Measuring round trip times to determine the distance between WLAN nodes," in *International conference on research in networking*, 2005, pp. 768-779.

[86] K. W. Cheung and H. C. So, "A multidimensional scaling framework for mobile location using time-of-arrival measurements," *IEEE Transactions on Signal Processing*, vol. 53, no. 2, pp. 460-470, 2005.

[87] M. McGuire, K. N. Plataniotis, and A. N. Venetsanopoulos, "Location of mobile terminals using time measurements and survey points," *IEEE Transactions on Vehicular Technology*, vol. 52, no. 4, pp. 999-1011, 2003.

[88] N. Patwari, J. N. Ash, S. Kyperountas, A. O. Hero, R. L. Moses, and N. S. Correal, "Locating the nodes: cooperative localization in wireless sensor networks," *IEEE Signal processing magazine*, vol. 22, no. 4, pp. 54-69, 2005.

[89] S. Sand, A. Dammann, and C. Mensing, "Position Estimation," in *Positioning in Wireless Communications Systems*, ed, 21 February 2014

[90] L. Ying, Y.-C. Liang, and S.-X. Wang, "Location parameters estimation in mobile communication systems," in *Communication Technology Proceedings, 2000. WCC-ICCT 2000. International Conference on*, 2000, pp. 261-268.

[91] J. Shen, A. F. Molisch, and J. Salmi, "Accurate passive location estimation using TOA measurements," *IEEE Transactions on Wireless Communications*, vol. 11, no. 6, pp. 2182-2192, 2012.

[92] S. A. Hussain, M. Emran, M. Salman, U. Shakeel, M. Naeem, S. Ahmed, *et al.*, "Positioning a Mobile Subscriber in a Cellular Network System based on Signal Strength," *IAENG International Journal of Computer Science*, vol. 34, no. 2, 2007.

[93] P. Kim and S. Chang, "Intelligent Positioning and Optimal Diversity Schemes for Mobile Agents in Ubiquitous Networks," *International Journal of Software Engineering and Knowledge Engineering*, vol. 18, no. 5, pp. 637-650, 2008.

[94] F. Santini, R. Nambisan, and M. Rucci, "Active 3D Vision through Gaze Relocation in a Humanoid Robot," *International Journal of Humanoid Robotics*, vol. 6, no. 3, pp. 481-503, Sep 2009.

[95] G. Sun, J. Chen, W. Guo, and K. R. Liu, "Signal processing techniques in network-aided positioning: a survey of state-of-the-art positioning designs," *IEEE Signal Processing Magazine*, vol. 22, no. 4, pp. 12-23, 2005.

[96] M. Vossiek, L. Wiebking, P. Gulden, J. Wieghardt, C. Hoffmann, and P. Heide, "Wireless local positioning," *IEEE microwave magazine*, vol. 4, no. 4, pp. 77-86, 2003.

[97] W. Singh and J. Sengupta, "An Efficient Algorithm for Optimizing Base Station Site Selection to Cover a Convex Square Region in Cell Planning," *Wireless Personal Communications*, vol. 72, no. 2, pp. 823-841, Sep 2013.

[98] B. Bhowmik, P. Sarkar, P. Shekhar, and N. Thakur, "Received Signal Strength Based Effective Call Scheduling in Wireless Mobile Network," *International Journal of Advancements in Technology*, vol. 2, no. 2, pp. 292-305, 2011.

[99] T. Jin, "Position Estimation of Mobile Robots using Multiple Active Sensors with Network," *International Journal of Fuzzy Logic and Intelligent Systems*, vol. 11, no. 4, 2011.

[100] T. Jin, K. Morioka, and H. Hashimoto, "Appearance Based Object Identification for Mobile Robot Localization in Intelligent Space with Distributed Vision Sensors," *International Journal of Fuzzy Logic and Intelligent Systems*, vol. 4, no. 2, 2004.

[101] S. Pradhan and S.-S. Hwang, "A TOA Shortest Distance Algorithm for Estimating Mobile Location," *The Journal of the Korea Institute of Electronic Communication Sciences*, vol. 8, no. 12, pp. 1883-1890, 2013.

[102] S. Pradhan, G. Khadka, and S. S. Hwang, "Mobile Location Estimation Based on the TOA Geometry," presented at the Conference of the Korean Institute of Communications and Information Sciences, Naju, Korea, May 10, 2013.

[103] S. Pradhan and S.-S. Hwang, "Mathematical analysis of line intersection algorithm for TOA trilateration method," presented at the Joint 7th International Conference on Soft Computing and Intelligent Systems and 15th International Symposium on Advanced Intelligent Systems (SCIS & ISIS), Kitakyushu, Japan, 2014.

[104] S. Pradhan, J.-Y. Pyun, G.-R. Kwon, S. Shin, and S.-S. Hwang, "Enhanced location detection algorithms based on time of arrival trilateration," presented at the 48th Asilomar Conference on Signals, Systems and Computers, Pacific Grove, CA, 2014.

[105] S. Pradhan and S. S. Hwang, "Location Estimation Algorithms for the Enhanced TOA Trilateration," presented at the Asia-Pacific Conference on Computer Aided System Engineering (APCASE 2014), Bali, Indonesia, 10-12 February 2014, 2014.

[106] X. Wen, A. B. Baggeroer, and C. D. Richmond, "Bayesian bounds for matched-field parameter estimation," *IEEE Transactions on Signal Processing*, vol. 52, no. 12, pp. 3293-3305, 2004.

[107] H. L. Van Trees, *Optimum Array Processing: Part IV of Detection, Estimation, and Modulation Theory*: Wiley, 2004.

[108] A. B. Baggeroer, W. A. Kuperman, and H. Schmidt, "Matched field processing: Source localization in correlated noise as an optimum parameter estimation problem," *The Journal of the Acoustical Society of America*, vol. 83, no. 2, pp. 571-587, 1988.

[109] Y. I. Abramovich and N. K. Spencer, "DOA estimation performance breakdown: A new approach to prediction and cure," in *2002 11th European Signal Processing Conference*, 2002, pp. 1-4.

[110] S. Pradhan, G. Khadka, and S. S. Hwang, "TOA Trilateration Method Based on Line Intersection Algorithm," presented at the The 14th International Symposium on Advanced Intelligent System (ISIS 2013), Daejeon, Korea, November 13-16, 2013.

[111] S. Pradhan, S.-S. Hwang, H.-R. Cha, and Y.-C. Bae, "Line Intersection Algorithm for the Enhanced TOA Trilateration Technique," *International Journal of Humanoid Robotics*, vol. 11, no. 4, p. 1442003, 2014.

[112] S. Pradhan and S. S. Hwang, "TOA Trilateration Algorithm Based on Comparison of Intersection Distances," presented at the ISIS 2015 The 16th International Symposium on Advanced Intelligent Systems, Mokpo, South Korea, November 4-7, 2015.

[113] F. Gustafsson and F. Gunnarsson, "Mobile positioning using wireless networks: possibilities and fundamental limitations based on available wireless network measurements," *IEEE Signal Processing Magazine*, vol. 22, no. 4, pp. 41-53, 2005.

[114] S. Pradhan; and S. S. Hwang, "Mode Selection Algorithm for Advanced TOA Trilateration Techniques," presented at the Eighth International Conference on Advances in Satellite and Space Communications (SPACOMM 2016), Lisbon, Portugal, February 21-25, 2016.

[115] S.-S. Hwang and S. Pradhan, "Comparison Approach of Intersection Distances for Advanced TOA Trilateration," *International Journal of Humanoid Robotics*, vol. 14, no. 03, p. 1750019, 2017.

[116] S. Pradhan, S. Shin, G. R. Kwon, J. Y. Pyun, and S. S. Hwang, "The advanced TOA trilateration algorithms with performance analysis," in *2016 50th Asilomar Conference on Signals, Systems and Computers*, Pacific Grove, CA, USA, 2016, pp. 923-928.

Appendix A: Representative Publications

1. Following are the representative journal publications based on the contributions of this dissertation:

S. Pradhan, S.-S. Hwang, "A TOA Shortest Distance Algorithm for Estimating Mobile Location," The Journal of the Korea Institute of Electronic Communication Science, Volume 8, Issue 12, 2013, pp. 1883-1890.

S. Pradhan, S.-S. Hwang, H.-R. Cha, and Y.-C. Bae, "Line Intersection Algorithm for the Enhanced TOA Trilateration Technique," International Journal of Humanoid Robotics, vol. 11, no. 04, p. 1442003, Dec. 2014.

S.-S. Hwang and S. Pradhan, "Comparison Approach of Intersection Distances for Advanced TOA Trilateration," International Journal of Humanoid Robotics, vol. 14, no. 03, p. 1750019, Sep. 2017.

S. Pradhan, Y. C. Bae, J. Y. Pyun, N. Y. Ko and S. S. Hwang, "Mathematical Analysis for Enhanced TOA Trilateration Localization Algorithm" (Submitted)

S. Pradhan and S. S. Hwang, "Hybrid TOA Trilateration Algorithm based on Line Intersection and Comparison Approach of Intersection Distances" (Submitted)

S. Pradhan and S. S. Hwang, "Mode Selection of Advanced TOA Trilateration Algorithm for Estimating Mobile Location" (Submitted)

2. Following are the representative conference publications based on the contributions of this dissertation:

S. Pradhan, G. Khadka, S. S. Hwang, "Mobile Location Estimation Based on TOA Geometry," The Korea Information and Communication Society, Spring Conference (2013), Naju, Korea, May 10, 2013, pp. 40-43.

S. Pradhan, G. Khadka, S. S. Hwang, "TOA Trilateration Method Based on Line Intersection Algorithm," The 14th International Symposium on Advanced Intelligent System (ISIS 2013), Daejeon, Korea, November 13-16, 2013.

S. Pradhan, S. S. Hwang, "Location Estimation Algorithms for the Enhanced TOA Trilateration," Asia-Pacific Conference on Computer Aided System Engineering (APCASE 2014), Bali, Indonesia, 10-12 February 2014, Page 65 of 236.

S. Pradhan, J. Y. Pyun, G. R. Kwon, S. Shin, and S. S. Hwang, "Enhanced location detection algorithms based on time of arrival trilateration," 2014 48th Asilomar Conference on Signals, Systems and Computers, Pacific Grove, CA, 2014, pp. 1179-1183.

S. Pradhan and S. S. Hwang, "Mathematical analysis of line intersection algorithm for TOA trilateration method," 2014 Joint 7th International Conference on Soft Computing and Intelligent Systems (SCIS) and 15th International Symposium on Advanced Intelligent Systems (ISIS), Kitakyushu, Japan, December 3-6, 2014, pp. 1219-1223.

S. Pradhan and S. S. Hwang, "TOA Trilateration Algorithm Based on Comparison of Intersection Distances," ISIS 2015 The 16th International Symposium on Advanced Intelligent Systems, Mokpo, South Korea, November 4-7, 2015.

S. Pradhan and S. S. Hwang, "Mode Selection Algorithm for Advanced TOA Trilateration Techniques," The Eighth International Conference on Advances in Satellite and Space Communications (SPACOMM 2016), Lisbon, Portugal, February 21-25, 2016.

S. Pradhan, S. Shin, G. R. Kwon, J. Y. Pyun and S. S. Hwang, "The advanced TOA trilateration algorithms with performance analysis," 2016 50th Asilomar Conference on Signals, Systems and Computers, Pacific Grove, CA, 2016, pp. 923-928.

S. Pradhan and S. S. Hwang, "Selection Mode Related to Advanced TOA Trilateration Algorithms" (Submitted)

Acknowledgment

The completion of this thesis owes a great deal to the people around me in various aspects. First and foremost, I would like to express my deepest gratefulness and sincere gratitude to my advisor, Prof. Suk-seung Hwang for giving his invaluable support, encouragement, supervision, motivation, personal guidance, and some very useful suggestions throughout the course of my research. His friendly behavior and teaching methodology really motivate me to move ahead in my research work. I would heartily appreciate his endless effort and guidance for improving my research work, writing skill as well as presentation skills.

I would sincerely like to thank my dissertation committee members Prof. Chung Ghiu Lee, Prof. Dong-Gi Lee, Prof. Yung-Tae Yoo, and Prof. Bong Seok Park, Kongju National University, for their detailed and constructive comments, suggestions, recommendations, and expertise feedback during the preparation of this dissertation. Likewise, I would like to thank all reviewers at different leading international symposium, conferences and reputed journals for their efforts and time that they spend in giving valuable feedback for the betterment of the manuscripts that I have submitted for possible publication. Their suggestions have certainly raised the quality of manuscripts, which I had submitted and those are the building block of this dissertation.

Likewise, I would like to thank all the lab members of Adaptive Signal Processing and to all friends in South Korea for their continuous support and kind cooperation.

My parents have been a constant source of inspiration and guidance. I would like to deeply thank my parents for their unconditional love and support in every moment of my life and their understanding during my study. They have never failed to believe in me.

The financial support by Smart Green Construction technology project, National Research Foundation of Korea, and Chosun University is greatly acknowledged.

Sajina Pradhan